Workspaces of continuous robotic manipulators

D i s s e r t a t i o n

zur Erlangung des akademischen Grades

Dr. rer. nat.

eingereicht bei der Fakultät für Mathematik und Naturwissenschaften
der Technischen Universität Ilmenau

vorgelegt von Dipl.-Math. Boris Thomaschewski

Gutachter: Privatdozent Dr. H. Abeßer, TU Ilmenau
              Prof. Dr. A. Hofmann, TU Ilmenau
              Prof. Dr. Ch. Großmann, TU Dresden

eingereicht am 13. September 2001

verteidigt am 12. August 2002

Preface

This thesis was the result of a $4\frac{1}{2}$ year stay with the Analysis Group at the Institute for Mathematics of the Technische Universität Ilmenau.

The motivation to this subject is due to Professor J. Steigenberger and Dozent H. Abeßer, who patiently supervised and enriched my work throughout the years. Very useful hints also came from Dr. H. Huijberts, in particular during my one week stay with him in London. Thank you very much!

In this context I also wish to thank all my colleagues of the Analysis Group who always helped my ideas with encouraging discussions and precious comments. And, last but not least, they made my stay in Ilmenau a great experience also in private life.

ii

Contents

Chapter 1

Introduction

Manipulators (manually controlled devices that transmit movements of the human hand to objects that cannot be reached directly or which are too dangerous or poisonous to be touched) and industrial robots (freely programmable, with grippers or other tools equipped machines with at least three degrees of freedom for various industrial applications) play a very important role in many areas as mass production and high precision production at chain belts (microchips cannot be built without robots anymore), construction (cranes and further tools that help to construct roads, buildings, etc.) and medicine (devices as endoscopes), to name but a few. We will call both manipulators and industrial robots *robotic manipulators* in the sequel.

Typically, the degree of freedom of robotic manipulators is not very high and they consist of only few links with translatory and/or rotatory joints. Some of the advantages of a low number of links are low production cost, relatively easy control (programmed or online), robustness and high accuracy even after thousands of repetitions. The most important disadvantage is that sometimes the operation area of the robotic manipulator is not free of obstacles. In production, this might not be the problem in most of the cases, but in medical surgery doctors definitely do not want to get rid of all the obstacles (which are part of the human body) when operating on interior organs. Thus there is an enormous need of research on more flexible robotic manipulators.

A milestone was Hirose's introduction of the Active Cord Mechanism (ACM) in 1976 [18] (see Figure 1.1) when the investigation of snake-like or hyper-redundant (due to the very high or even infinite degree of kinematic redundancy) robots was born. Since then this topic has become increasingly interesting. Two types are of major interest, namely snake-like vehicles as in Figure 1.1 (which we will not treat here) and elephant-trunk-like robotic manipulators. Many ideas in this research area are adopted from biology (e.g., movements of snakes and elephant-trunks as in Figure 1.2) and thus these robots are commonly called biologically inspired robots. Even though building and controlling hyper-redundant robots is very difficult, complex and expensive, their ability to locomote effectively over different
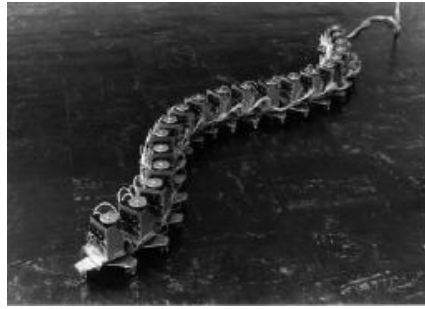
Figure 1.1: Hirose's Active Cord Mechanism

Figure 1.2: Snake and elephant-trunk

surfaces or to avoid obstacles due to their flexibility is very often worth the effort. These robots are already used in a vast area of applications as minimally invasive surgery, power plant maintainance, detection of earthquake victims or as mani-
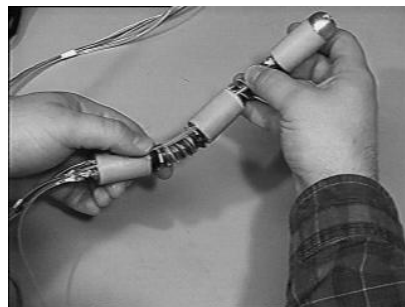
Figure 1.3: Caltech prototype of a robotic endoscope

pulators on the international space station ISS, to name but a few. Therefore, companies like NASA, Hughes Aircraft, JPL and NEC already built such robots. Additionally, theoretical and practical progress has been achieved by the German National Research Center for Information Technology [23] [25], the Copernicus

Project at the University of Metz, France [27], Burdick and Chirikjian (now at John Hopkins University) and their coworkers [5] [8] [9] [10] [11] [12] at Caltech, USA, and the Hirsose group in Japan, see also [19] for a survey in detail and further references.

Though many papers on discrete robots of that kind have been published, not very much can be found yet on continuous robots (seminal work appeared in [12] and [13]). One might object that all 'real' robots are discrete, but this is, even today, not necessarily the case (e.g., piezo-electric elements are continuously deformable). On the other hand, a continuous model can also be viewed as a good approximation of a robot with many links, see [14], [15] and Figure 1.4), and it
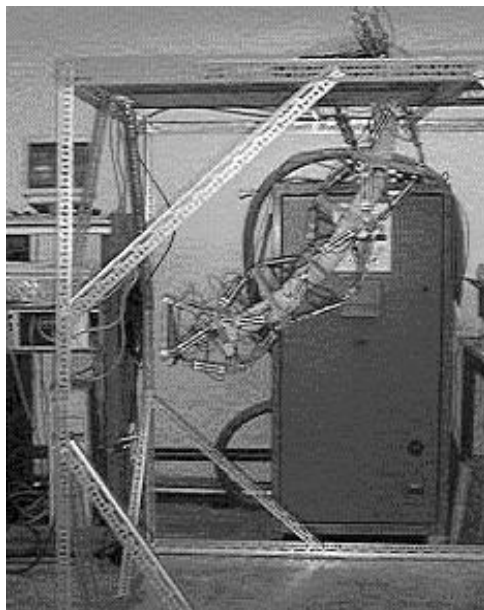
Figure 1.4: Binary manipulator introduced by Chirikjian

may simplify computations.

In this context we will investigate continuous planar and 3D robotic manipulators that are fixed at one end and controlled by distributed bending moments. Therefore, as a first step, the workspaces of a simple model of a planar manipulator with uniformly bounded curvature ($|\kappa| \leq M$) and free terminal direction will be determined for various values of M. The main idea is to describe the boundary of the workspace with optimal control techniques. The problem of determining the workspace is exactly the same as looking for the reachability set at time T of a particle moving in the plane with constant speed $v = 1$ object to the same curvature constraint. This has already been treated in [16]. We will get the same result more transparently using optimal control and extend the result to the case when the terminal direction is prescribed which might be very helpful or even necessary in many applications. Afterwards we will apply similar techniques in

order to describe workspaces of 3D continuous robotic manipulators.

A very interesting fact is that the equations of motion used here are the same as in *Dubins' problem* which is finding the shortest path of a simple mobile robot (the so-called unicycle) with prescribed initial and terminal point and orientation of the principal axis. This is treated in Chapter 2 including a brief historical overview of this problem. In this context we completely solve *Dubins' problem* for free terminal direction since we need these results to determine the 2D workspaces. At the end of the chapter we give a new, relatively short proof of Dubins' theorem.

Finally, we investigate workspaces of 3D manipulators with similar techniques as in the 2D case. The fact, that 3D motions are only achieved when at least two controls (e.g., curvature and torsion) are used, complicates the situation extremely. Unfortunately, due to this difficulty, we are not able to completely solve this problem. Nevertheless, we can present quite a few results which give an idea of the complexity of this problem in 3D but also how these workspaces can possibly be described.

In the following sections we will shortly summarize the contents of the present work and present the mathematical preliminaries and notation used throughout this thesis.

1.1   Organization of the thesis

In Chapter 2 we investigate a slight modification of *Dubins' problem* which we call *Dubins' problem* for free terminal direction. We will show how this problem is connected to the workspaces of continuous robotic manipulators. After the mathematical formulation of the time-optimal problem, we derive a few necessary conditions via optimal control techniques, mainly Pontryagin's Maximum Principle. With further geometric considerations we will solve this problem. The result extends the facts already known on shortest paths of this particular type of mobile robot, see [37] for an overview. Furthermore, we present a new short proof of Dubins' theorem using a mixture of Dubins' ideas and optimal control.

In Chapter 3 we determine the workspaces of 2D continuous robotic manipulators which are fixed at one end assuming an arbitrary but fixed curvature constraint. This is pursued for two cases, namely with and without prescription of the terminal orientation. At first, we describe the (simple) mathematical model of such a manipulator and, in both cases, we present a few basic properties of its workspace, e.g., that it is compact. In order to determine the workspaces we consider a two-parameter family of optimal control problems that will enable us to get a description of the boundaries of the workspaces. The results are very similar to those of the solution of *Dubins' problem* treated in Chapter 2.

In Chapter 4 we investigate the workspaces of 3D continuous robotic manipulators with free terminal orientation. We introduce a (simple) mathematical model

which is also used to describe elastic rods, see e.g., [22]. Since for motions of the manipulator in $\mathbb{R}^3$ at least two controls are necessary, the situation is a lot more complicated as in Chapter 3. Nevertheless, we can prove some properties as in the 2D case, e.g., that the workspace is compact again. Introducing the adequate three-parameter family of optimal control problems gives further insight on how the boundaries of the 3D workspaces look like. Unfortunately, the determination of the workspaces is far too difficult at this stage. Anyhow, we present a few ideas how they could look like in a certain simplified situation.

1.2 Mathematical preliminaries

We assume basic knowledge on linear and nonlinear control theory (see e.g., [35], [21] and [29]), optimal control (see e.g., [6], [22] and [2]) and differential geometry (see e.g., [30]). Many books on (optimal) control theory include introductions to differential geometry as [22] and [29]. Here we only want to repeat the standard approach to the solution of optimal control problems and the basic terms and notation of differential geometry.

1.2.1 Optimal control

Since the solution of the problems considered is achieved via optimal control, we want to describe the standard procedure how the solution to these problems is generally attacked.

We introduce the basic notation not in the most general way and adapt it to our needs appropiately from [6].

Definition 1.2.1 *Let $f : \mathbb{R}^n \times \mathbb{R}^m \to \mathbb{R}^n$ be a familiy of smooth vector fields, $U \subset \mathbb{R}^m$ closed and $\mathcal{U} := \{u : \mathbb{R}_0^+ \to U, \ u \ measurable\}$. Then*

$$\dot{x} = f(x, u), \quad 0 \le t \le T, \quad x(0) = x_0 \in \mathbb{R}^n, \quad u \in \mathcal{U} \tag{1.1}$$

is called a control system *with* control space *U. Let $T > 0$, $B \subset \mathbb{R} \times \mathbb{R}^n$, $g : \mathbb{R} \times \mathbb{R}^n \to \mathbb{R}$ and $(T, x(T)) \in B$. Then a (particular)* Mayer problem *of optimal control is seeking the minimum (or maximum) of*

$$I[x, u] = g(T, x(T))$$

with control system (1.1) and boundary condition

$$e[x] := (T, x(T)) \in B. \tag{1.2}$$

All pairs $(x(\cdot), u(\cdot))$ such that x is absolutely continuous, $u \in U$ and x and u satisfy the differential equation (1.1) and the boundary condition (1.2) are called admissible solutions.

Usually, the solution of such an optimal control problem is attacked as follows.

(1) Proof of existence of admissible solutions.

(2) Proof of existence of an optimal solution (not necessarily unique).

(3) Reduce the number of admissible solutions to solutions that satisfy various necessary conditions for optimality.

(4) Find sufficient conditions for optimality and describe the solution(s).

Condition (1) is equivalent to the concept of reachability of a system, i.e., there exists a solution such that the terminal point (set) can be reached.

Definition 1.2.2 *Consider control system (1.1). Then $x_1 \in \mathbb{R}^n$ is* reachable *from x_0 if there exists a $u_1 \in \mathcal{U}$ and a $T \geq 0$ such that $x(T) = x_1$ when u_1 is plugged in the control system above. The system (1.1) is* (completely) reachable *from x_0 if every $x_1 \in \mathbb{R}^n$ is reachable from x_0.*
If furthermore $h : \mathbb{R}^n \to \mathbb{R}^p$ is a smooth function and the output *of the system is given by $y = h(x)$, then $y_1 \in \mathbb{R}^p$ is* output reachable *from $y_0 = h(x_0)$ if there exists a $u_1 \in \mathcal{U}$ and a $T \geq 0$ such that $y(T) = y_1$ when u_1 is plugged in the system. The system is* (completely) output reachable *from $y_0 = h(x_0)$ if every $y_1 \in \mathbb{R}^p$ is* output reachable *from $y_0 = h(x_0)$.*
The (output) reachable set at time T *is the set of all (output) reachable points from x_0 (y_0) in time T and denoted by R_T. The* (output) reachable set *is the set of all (output) reachable points from x_0 (y_0) and denoted by R.*

Obvoiusly $R = \cup_{T \geq 0} R_T$ and the system is completely (output) reachable from x_0 if and only if $R = \mathbb{R}^n$ ($R = \mathbb{R}^p$). Thus there exist admissible solutions if $B \subset R$ (or $B \subset R_T$ if T is fixed).
Condition (2) can usually be shown by the Arzelá-Ascoli theorem or Filippov's Existence Theorem and variations of it.
Condition (3) is usually treated by the use of Pontryagin's Maximum Principle (PMP) and further higher order conditions if applicable.
For Condition (4) sometimes Boltyansky's suffcent condition or similar techniques apply. But mostly this is the most difficult part and purely geometrical techniques are used to determine further properties. Very often this part cannot be carried out completely.
Since we will not need PMP in its full generality and all the other theorems in detail here we refer the reader to the standard optimal control literature, e.g., [2] and [6]. The concepts above can also be introduced for control systems on manifolds, see e.g., [22].

1.2.2 Differential geometry

Of course, we cannot give a complete introduction to differential geometry here (see e.g., [30] for a more comprehensive survey on that topic), but we will introduce the basic terms that will be needed in Chapter 4. We will follow [20], where also plenty further references concerning differential geometry needed for control systems can be found, e.g., [29].

Definition 1.2.3 *A set M is called a* manifold *of dimension n if there exists an index set I, a family of relatively open subets $(U_i)_{i \in I} \subset M$, a family of open subsets $(V_i)_{i \in I} \subset \mathbb{R}^n$ and diffeomorphisms $\phi_i : U_i \mapsto V_i$, $i \in I$, such that $\cup_{i \in I} U_i = M$ and the mappings $\phi_{ji} : \phi_i(U_i \cap U_j) \to \phi_j(U_i \cap U_j)$, $y \mapsto \phi_{ji}(y) := \phi_j \circ \phi_i^{-1}(y)$ (whenever $U_i \cap U_j \neq \emptyset$) are diffeomorphisms. For every $i \in I$, the pair (U_i, ϕ_i) is called a* local coordinate chart *on M, and $\mathcal{A} := \{(U_i, \phi_i), i \in I\}$ is called an* atlas *on M. If $N \subset M$ is itself a manifold, then N is called a* submanifold *of M.*
For $x \in \mathbb{R}^n$ the at x is denoted by $T_x \mathbb{R}^n$ (which is a copy of $\mathbb{R}^n$) and its natural basis by $\{\frac{\partial}{\partial x_1}|_x, \ldots, \frac{\partial}{\partial x_n}|_x\}$. Let M be an n-dimensional manifold, $m \in M$ and (U, ϕ) a local coordinate chart around m. For $\tau \in T_{\phi(m)} \mathbb{R}^n$, define $\phi^*(m)\tau := \frac{\partial \phi^{-1}}{\partial x}(\phi(m))\tau$. Then the basis of the tangent space $T_m M$ *of M at m is defined by $\frac{\partial}{\partial \phi_k}|_m := \phi^*(m)\frac{\partial}{\partial x_k}|_{\phi(m)}$, $k = 1, \ldots, n$ and $T_m M$ is the linear span of the basis vectors. The set $TM := \{(m, \tau) : m \in M, \tau \in T_m M\}$ is called* tangent bundle *of M.*
A vector field *on M is a mapping τ assigning each $m \in M$ a vector $\tau(m) \in T_m M$. τ is called* smooth *if for each $m \in M$ there exists a local coordinate chart (U, ϕ) around m and functions $\tau_1, \ldots, \tau_n \in \mathcal{C}^\infty(U)$ such that for all $\overline{m} \in U$ we have $\tau(\overline{m}) = \sum_{i=1}^n \tau_i(\overline{m})\frac{\partial}{\partial \phi_i}|_{\overline{m}}$. The set of all smooth vector fields on M is denoted by $V(M)$.*
The cotangent space *at $m \in M$, denoted by $T_m^* M$, is the dual space of $T_m M$, i.e., the space of linear mappings $\omega : T_m M \to \mathbb{R}$. If $\omega \in T_m^* M$ then the value of ω at $\tau \in T_m M$ is denoted by $\omega(\tau)$ or $\langle \omega, \tau \rangle$. If $\tau_1, \ldots, \tau_n$ is a basis of $T_m M$, then there exists a unique basis $\omega_1, \ldots, \omega_n$ of $T_m^* M$ such that $\langle \omega_i, \tau_j \rangle = \delta_{ij}$. This basis is called the* dual basis *of $T_m^* M$ with respect to $\tau_1, \ldots, \tau_n$. Given a coordinate chart (U, ϕ) around m, the dual basis with respect to $\frac{\partial}{\partial \phi_1}|_m, \ldots, \frac{\partial}{\partial \phi_n}|_m$ is denoted by $d\phi_1|_m, \ldots, d\phi_n|_m$. The set $T^* M := \{(m, \omega) : m \in M, \omega \in T_m^* M\}$ is called* cotangent bundle *of M.*
A covector field *(or* one-form*) on M is a mapping ω assigning each $m \in M$ a covector $\omega(m) \in T_m^* M$. ω is called* smooth *if for each $m \in M$ there exists a local coordinate chart (U, ϕ) around m and functions $\omega_1, \ldots, \omega_n \in \mathcal{C}^\infty(U)$ such that for all $\overline{m} \in U$ we have $\omega(\overline{m}) = \sum_{i=1}^n \omega_i(\overline{m})d\phi_i|_{\overline{m}}$.*

Definition 1.2.4 *Let M be a manifold. Then for any two $\sigma, \tau \in V(M)$, in local coordinates given by $\sigma(x) = (\sigma_1(x), \ldots, \sigma_n(x))$ and $\tau(x) = (\tau_1(x), \ldots, \tau_n(x))$, the*

Lie bracket *is defined (in local coordinates) by*

$$[\sigma, \tau] := \frac{\partial \sigma}{\partial x}\tau - \frac{\partial \tau}{\partial x}\sigma.$$

Remark 1.2.5 It can be shown that the definition of the Lie bracket is well-defined, i.e., it is independent on the particular choice of local coordinates. Since the Lie bracket is bilinear (over $\mathbb{R}$), skew-symmetric and it satisfies the Jacobi-identity

$$[\sigma, [\tau, \nu]] + [\tau, [\nu, \sigma]] + [\nu, [\sigma, \tau]] = 0,$$

the pair $(V(M), [\cdot, \cdot])$ is a *Lie algebra.*   □

Example 1.2.6 Let $M = \mathbb{R}^n$ and consider the linear vector fields Ax and Bx. Then

$$[A, B](x) = (AB - BA)(x),$$

which is the well-know matrix commutator.   □

Definition 1.2.7 *Any group G that is an analytic manifold and that satisfies the property that the operations*

$$(g, h) \mapsto g \cdot h \quad and \quad g \mapsto g^{-1},$$

$g, h \in G$, are analytic is called a Lie group.

Definition 1.2.8 *Let G be a Lie group with group identity e and $g \in G$. The mapping $L_g : G \to G$, $L_g(x) = gx$ is called* left-translation *on G. A vector field X on G is called* left-invariant *if $(L_g)_* X(e) = X(g)$.*

Note that the tangent map $(L_g)_*$ takes $T_e G$ onto $T_g G$ since $L_g(e) = g$.

Lemma 1.2.9 *For left-invariant vector fields X on a Lie group G the following hold.*

a) *The vector field is uniquely determined by the value at the group identity $X(e)$.*

a) *If G is a subgroup of $GL_n(\mathbb{R})$, then the left-translation is given by matrix multplication from the left, $X(g) = gX(e)$.*

For left-invariant vector fields the following holds.

Lemma 1.2.10 *Let X and Y be left invariant vector fileds on a Lie group G. Then $[X, Y]$ is again a left invariant vector field on G and the following holds for every $g \in G$: $[X(g), Y(g)] = [gX(e), gY(e)] = g[X(e), Y(e)]$.*

Proof This is a well-known fact and can be found in the standard literature, e.g., [22]. ∎

Definition 1.2.11 *A* Poisson bracket *(or* Poisson structure*) on M is a bilinear map $\{\cdot, \cdot\} : \mathcal{C}^\infty(M) \times \mathcal{C}^\infty(M) \to \mathcal{C}^\infty(M)$, $(F, G) \mapsto \{F, G\}$, such that for all $F, G, H \in \mathcal{C}^\infty(M)$ the following hold:*

   i) $\{F, G\} = -\{G, F\}$ *(skew-symmetry),*

   ii) $\{F, \{G, H\}\} + \{G, \{H, F\}\} + \{H, \{F, G\}\} = 0$ *(Jacobi-identity),*

   iii) $\{F, GH\} = \{F, G\}H + G\{F, H\}$ *(Leibnitz-rule).*

M together with a Poisson bracket is called a Poisson manifold.

Lemma 1.2.12 *Let M be an r-dimensional Poisson manifold with local coordinates $x_1, \ldots, x_r$. Then*

   i) there locally exist smooth function $w_{ij} : M \to \mathbb{R}$, $1 \leq i, j \leq r$, such that the Poisson bracket is locally given as

$$\{F, G\}(x) = \sum_{i,j=1}^{r} w_{ij}(x) \frac{\partial F}{\partial x_i}(x) \frac{\partial G}{\partial x_j}(x),$$

   ii) the functions w_{ij} determined in (i) are determined by $w_{ij}(x) = \{x_i, x_j\}(x)$, $1 \leq i, j \leq r$, and satisfy $w_{ij}(x) = -w_{ji}(x)$ and

$$\sum_{l=1}^{r} \left(w_{lj} \frac{\partial w_{ik}}{\partial x_l} + w_{li} \frac{\partial w_{kj}}{\partial x_l} + w_{lk} \frac{\partial w_{ji}}{\partial x_l} \right) = 0$$

   for all $1 \leq i, j, k \leq r$.

Definition 1.2.13 *The matrix $W(x)$ with entries $w_{ij}(x)$, $1 \leq i, j \leq r$, is called the* structure matrix *of the Poisson structure. The* rank *of the Poisson bracket in every $x \in M$ is defined as the rank of $W(x)$. A Poisson bracket is said to be* non-degenerate *if $\operatorname{rank} W(x) = \dim M$ for every $x \in M$.*

Example 1.2.14 *Let $(x_1, \ldots, x_{2n}) = (q_1, \ldots, q_n, p_1, \ldots, p_n) \in M = \mathbb{R}^{2n}$. Then*

$$\{F, G\}(q, p) := \sum_{i=1}^{n} \left(\frac{\partial F}{\partial q_i} \frac{\partial G}{\partial p_i} - \frac{\partial F}{\partial p_i} \frac{\partial G}{\partial q_i} \right)(q, p)$$

defines a non-degenerate Poisson bracket on M since $\{q_i, q_j\} = \{p_i, p_j\} = 0$ and $\{q_i, p_j\} = \delta_{ij}$, hence the structure matrix is given by

$$W(x) = \begin{pmatrix} 0 & I_n \\ -I_n & 0 \end{pmatrix}.$$

This bracket is called the standard Poisson bracket *on $\mathbb{R}^{2n}$.* □

It can be shown that for a $2n$-dimensional manifold M with non-degenerate Poisson bracket there exist locally around any point $x_0 \in M$ coordinates $(q,p) = (q_1, \ldots, q_n, p_1, \ldots, p_n)$, called *canonical coordinates*, such that the Poisson bracket writes as in Example 1.2.14 (Darboux-Theorem).

Definition 1.2.15 *Let M be a Poisson manifold and $F \in \mathcal{C}^\infty(M)$. For arbitrary $x \in M$ define $X_F(x) : \mathcal{C}^\infty(M) \to \mathbb{R}$ by $X_F(x)G := \{F, G\}(x)$. Since it can be shown that $X_F(x) \in T_x M$ for any $x \in M$ it follows that X_F is a smooth vector field on M satisfying*

$$X_F(G) = \{F, G\} \quad \text{for any } G \in \mathcal{C}^\infty(M).$$

X_F is called the Hamiltonian vector field *corresponding to the* Hamiltonian function *F and the Poisson bracket on M.*

Definition 1.2.16 *Let M be a manifold with non-degenerate Poisson bracket. The bilinear map $\omega_x : T_x M \times T_x M \to \mathbb{R}$ is defined by*

$$\omega_x(X_F(x), X_G(x)) := \{F, G\}(x).$$

For varying x we obtain a differential two-form ω *called* symplectic form *on M. M togehter with the symplectic form ω is called a* symplectic manifold.

Lemma 1.2.17 *Let M be a symplectic manifold and $F, G, H \in \mathcal{C}^\infty(M)$ with corresponding Hamiltonian vector fields X_F, X_G and X_H. Then*

  i) $w_x(X_H(x), Z) = dH(x)(Z) \quad$ for any $Z \in T_x M$, $x \in M$,

  ii) $[X_F, X_G] = X_{\{F,G\}}$,

  iii) there exists a double contravariant tensor Ω such that $\Omega(\cdot, dH) = H$ and thus $\{F, G\} = \Omega(F, G)$.

Remark 1.2.18   i) In local coordinates, we have

$$\{F, G\}(x) = dF(x)W(x)dG(x)^T \quad \text{and} \quad X_F(x) = (dF(x)W(x))^T.$$

  ii) The tensor Ω corresponding to the standard Poisson bracket of Example 1.2.14 is denoted by

$$\Omega = \frac{\partial}{\partial q_{(i)}} \wedge \frac{\partial}{\partial p_{(i)}}.$$

<div align="right">□</div>

Remark 1.2.19 Let Q be an n-dimensional manifold with cotangent bundle T^*Q. On T^*Q there is a naturally defined Poisson bracket defined in local coordinates as follows. Let $q_0 \in Q$ and $q_1, \ldots, q_n$ local coordinates for Q around q_0. Then there exist natural coordinates $(q_1, \ldots, q_n, p_1, \ldots, p_n)$ for T^*Q. For any two $F, G \in \mathcal{C}^\infty(T^*Q)$ their Poisson bracket is defined as

$$\{F, G\}(q, p) := \sum_{i=1}^{n} \left(\frac{\partial F}{\partial q_i} \frac{\partial G}{\partial p_i} - \frac{\partial F}{\partial p_i} \frac{\partial G}{\partial q_i} \right)(q, p).$$

It can be shown that this bracket is well-defined, i.e., it does not depend on the particular choice of coordinates. $\qquad\square$

At this point we introduce some of the notation used throughout the thesis.

1.3 Notation

We want to introduce some notation that will be used throughout the thesis. Let $k \in \mathbb{N}$, $T > 0$ and $M > 0$. Then

$$
\begin{aligned}
\mathcal{C}[0, T] &:= \{f : [0, T] \to \mathbb{R} \mid f \text{ is continuous}\} \\
\mathcal{C}^k[0, T] &:= \{f : [0, T] \to \mathbb{R} \mid f \text{ is } k \text{ times continuously differentiable}\} \\
\mathrm{Lip}_M[0, T] &:= \{f \in \mathcal{C}[0, T] : |f(s) - f(t)| \leq M|s - t| \, \forall \, s, t \in [0, T]\} \\
A[0, T] &:= \{f : [0, T] \to \mathbb{R} : f \text{ is absolutely continuous}\} \\
\mathcal{U}_M &:= \{u : [0, T] \to \mathbb{R} \text{ measurable}, |u(s)| \leq M \text{ for every } s \in [0, T]\} \\
\mathcal{U} &:= \{u : [0, T] \to \mathbb{R}^3, u_i \in \mathcal{U}_1\}
\end{aligned}
$$

L	straight line segment
C	arc of a circle of maximal curvature
C$^+$	C turning anti-clockwise
C$^-$	C turning clockwise
CL	$\mathcal{C}^1$-concatenation of first C and then L
CC	$\mathcal{C}^1$-concatenation of C and C
CC locus	all terminal points $(x(T), y(T))$ of manipulators of type CC
CL locus	all terminal points $(x(T), y(T))$ of manipulators of type CL

Chapter 2

Dubins' Problem for free terminal direction

In this chapter, which is practically self-contained, *Dubins' problem* will be investigated and the connection to workspaces of robotic manipulators will be demonstrated.

2.1 Introduction

This problem probably goes back to Markov [26], who posed the following in 1889:

> Find the shortest continuously differentiable curve between an initial and a terminal point in the plane with prescribed initial and terminal tangent direction and the curvature constraint $|\kappa| \leq 1$ almost everywhere.

Almost 70 years later, in 1957, Dubins [17] analyzed this problem (commonly called *Dubins' problem* today) in detail, which is the same as finding the shortest path of a particle or a very simple mobile robot with no side-slip (the well-known unicycle) moving in the plane with the speed being unity and the same curvature constraint. From now on, we call this Dubins' car. Using geometric methods he showed that the shortest paths are concatenations of at most three parts, each of which is either a straight line segment or an arc of a circle of radius 1.

In 1975, Cockayne and Hall [16] determined the reachable set at given time T of Dubins' car with arbitrary terminal direction. In 1990, Reeds and Shepp [33] investigated optimal paths for Dubins' car moving forward and backward using purely geometric techniques.

When the curvature κ is viewed as control, then *Dubins' problem* is a time-optimal control problem. This approach was first pursued by Sussmann and Tang [40] and simultanously by Laumond, Souères and coworkers [1][4][24][36][38] who completely solved Dubins' as well as Reeds' and Shepp's problem. The results are

summarized in [37].

In this chapter we solve *Dubins' problem* without prescribing the terminal direction (from now on we call this problem *Dubins' problem* for free terminal direction) using optimal control and geometric techniques. We will also describe the optimal control synthesis for all terminal points. This result is of interest for motion planning of mobile robots. Furthermore, we like to stress that the optimal control approach used here seems to be the appropriate approach for many similar problems such as workspaces of continuous robotic manipulators. We will see in Chapter 3 that the equations of motion of Dubins' car are the same as the equations decribing the shape of a continuous 2D robotic manipulator. Thus applying Pontryagin's Maximum Principle delivers very similar necessary conditions in both problems (only the functionals to be minimized are different). Moreover, the results of this chapter will help us to determine the workspaces of the manipulators in Chapter 3. Finally, we illustrate how to solve Dubins' classical result (including a new proof that concatenations of four or more circular arcs cannot be optimal) employing the techniques of the present work.

2.2 Model of Dubins' car and classification of optimal paths

Consider the x-y-plane and let θ denote the angle between the x-axis and the moving direction of Dubins' car (tangent to the path). Assume, without loss of generality, that the initial point is $(x_0, y_0) = (0,0)$ and the initial direction is $\theta_0 = 0$. Then, taking the no side-slip condition

$$\dot{y}\cos\theta - \dot{x}\sin\theta = 0$$

into account, the kinematics of Dubins' car is described, for all $t \geq 0$, by

$$\begin{array}{llll}
\dot{x}(t) & = & \cos\theta(t), & x(0) & = & 0, \\
\dot{y}(t) & = & \sin\theta(t), & y(0) & = & 0, \\
\dot{\theta}(t) & = & u(t), & \theta(0) & = & 0,
\end{array} \qquad (2.1)$$

with $u \in \mathcal{U}_1$ (thus $\theta(\cdot)$, $\dot{x}(\cdot)$ and $\dot{y}(\cdot)$ are continuous). A possible path followed by Dubins' car is visualized in Figure 2.1. Since the coordinates $(x(\cdot), y(\cdot))$ of (2.1) describe a planar $\mathcal{C}^1$-curve parametrized by arc length t, the control of the system can be viewed (almost everywhere) as the curvature of the path followed by Dubins' car. We assume that the absolute value of the curvature is uniformly bounded by 1 ($u \in \mathcal{U}_1$).

For any fixed $(x_T, y_T) \in \mathbb{R}^2$ we seek the minimal arc length $T \geq 0$ such that the terminal point of $(x(\cdot), y(\cdot))$ is $(x(T), y(T)) = (x_T, y_T)$ and $\theta(T)$ is arbitrary. Formally, we pose the following time-optimal control problem:

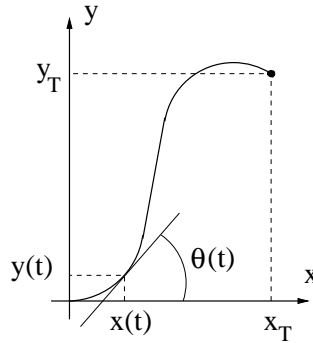 Minimize $T \geq 0$ subject to (2.1), $(x(T), y(T)) = (x_T, y_T)$, $u \in \mathcal{U}_1$.   (2.2)

Figure 2.1: Model of Dubins' car

2.2.1 Well-posedness of the problem

The following lemma shows that the system (2.1) is output reachable (with output $(x(\cdot), y(\cdot))$). In other words, the union of all terminal points $(x(T), y(T))$ of solutions to (2.1) over all times $T \geq 0$ is equal to $\mathbb{R}^2$. Moreover, the optimal control problem (2.2) has a solution for every terminal point.

Lemma 2.2.1 *The following hold:*

(i) $\{(x(T), y(T)) \,|\, T \geq 0, \, (x(\cdot), y(\cdot), \theta(\cdot)) \text{ solves (2.1)}, \, u \in \mathcal{U}_1\} = \mathbb{R}^2.$

(ii) *For any* $(x_T, y_T) \in \mathbb{R}^2$ *there exisits a solution to (2.2).*

Proof (i) Let $\phi \in [0, 2\pi)$, $T \geq \phi$ and define

$$u(t) := \begin{cases} 1 & \text{for all} \quad t \in [0, \phi] \\ 0 & \text{for all} \quad t \in (\phi, T] \end{cases}$$

Then $(x(\cdot), y(\cdot))|_{[0,\phi]}$ is an arc of C_1 of length ϕ and is followed by a straight line $(x(\cdot), y(\cdot))|_{(\phi, T]}$ of length $T - \phi$ being tangent to the previous arc, see Figure 2.2. It is obvious that with this $u(\cdot)$ and varying ϕ and arc length T, in particular any point $(x_T, y_T) \in \mathbb{R} \times \mathbb{R}_0^-$ can be reached. Replacing $u(\cdot)$ by $-u(\cdot)$, by analogous arguments, any point $(x_T, y_T) \in \mathbb{R} \times \mathbb{R}_0^+$ in the upper half plane can be reached. This completes the proof of (i).

(ii) This part of the proof is shown analogously to the proof of Theorem 7 on page 22 in [40]. Instead of the point $(x_T, y_T, \theta_T) \in \mathbb{R}^3$ the compact manifold $(x_T, y_T) \times S^1$ can also be reached in minimal time.

∎

Remark 2.2.2 The ouput reachability of system (2.1) is an immediate consequence of the reachability of the system of *Dubins' problem*, the proof above was just given for illustration. □
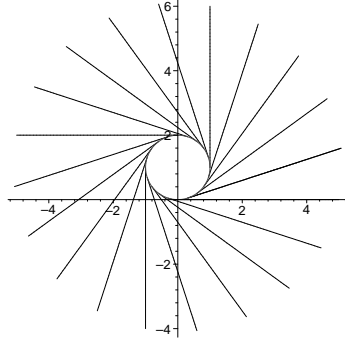
Figure 2.2: Set of reachable points for the C$^+$L strategy

2.2.2   Necessary conditions for optimality

Now we state a version of Pontryagin's Maximum Principle, which can be found in the standard literature as [6] or the original work [32], tailored for the needs of our analysis.

Theorem 2.2.3 (Pontryagin's Minimum Principle (optimal time)) *If the control $u(\cdot) \in \mathcal{U}_1$ is an optimal control to problem (2.2) with corresponding state function $(x(\cdot), y(\cdot), \theta(\cdot))$, then*

(i) *there exists an absolutely continuous vector function $\lambda : [0, T] \to \mathbb{R}^3 \backslash \{0\}$ satisfying the adjoint equations*

$$
\begin{aligned}
\dot{\lambda}_1(t) &= -\tfrac{\partial}{\partial x} H((x(t), y(t), \theta(t)), (\lambda_1(t), \lambda_2(t), \lambda_3(t)), u(t)), \\
\dot{\lambda}_2(t) &= -\tfrac{\partial}{\partial y} H((x(t), y(t), \theta(t)), (\lambda_1(t), \lambda_2(t), \lambda_3(t)), u(t)), \qquad (2.3) \\
\dot{\lambda}_3(t) &= -\tfrac{\partial}{\partial \theta} H((x(t), y(t), \theta(t)), (\lambda_1(t), \lambda_2(t), \lambda_3(t)), u(t)),
\end{aligned}
$$

for almost every $t \in [0, T]$ where the Hamiltonian *of (2.2) is given by*

$$
H : \mathbb{R}^3 \times \mathbb{R}^3 \times [-1, 1] \to \mathbb{R}, \quad ((x, y, \theta), \lambda, u) \mapsto \lambda_1 \cos \theta + \lambda_2 \sin \theta + \lambda_3 u,
$$

(ii) *there exists a constant $\lambda_0 \in \{0, 1\}$ such that*

$$
H((x(t), y(t), \theta(t)), \lambda(t), u(t)) = \min_{v \in \mathcal{U}_1} H((x(t), y(t), \theta(t)), \lambda(t), v(t)) = -\lambda_0
$$

for almost every $t \in [0, T]$,

(iii) *the following transversality condition holds*

$$
\lambda_3(T) = 0. \qquad (2.4)
$$

Essential properties of the optimal control problem (2.2) are collected in the following lemma.

Lemma 2.2.4 *Suppose $(x(\cdot), y(\cdot), \theta(\cdot)) : [0, T] \to \mathbb{R}^3$ is an optimal solution to (2.2) with the corresponding optimal control $u(\cdot) \in \mathcal{U}_1$, $\lambda : [0, T] \to \mathbb{R}^3 \backslash \{0\}$ as in Theorem 2.2.3 and $I \subset [0, T]$ an open interval. Then there exists a $\lambda_0 \in \{0, 1\}$ such that*

(i) $-\lambda_0 = (\lambda_1(t) \cos \theta(t) + \lambda_2(t) \sin \theta(t) + \lambda_3(t) u(t))$ *for almost every $t \in [0, T]$.*

(i) $u(t) = -\text{sign}\, \lambda_3(t)$, *if $\lambda_3(t) \neq 0$.*

(iii) $\lambda_3(\cdot) \in \mathcal{C}^1[0, T]$ *and, if there are no switching times in I, then $\lambda_3(\cdot)|_I \in \mathcal{C}^2$.*

(iv) $(x(\cdot), y(\cdot))|_I$ *is of type C, if $\lambda_3(t) \neq 0$ for all $t \in I$.*

(v) $\dot{\lambda}_1(\cdot)_{[0,T]} \equiv \dot{\lambda}_2(\cdot)_{[0,T]} \equiv 0$ *and $\ddot{\lambda}_3(t) = -\lambda_3(t) - \lambda_0 u(t)$, if $\lambda_3(t) \neq 0$ for all $t \in I$.*

(vi) $(x(\cdot), y(\cdot))|_I$ *is of type L, if $\lambda_3(\cdot)_I \equiv 0$.*

(vii) $\lambda_3(T) = 0$.

Proof The corresponding Hamiltonian is as in PMP

$$H : \mathbb{R}^3 \times \mathbb{R}^3 \times [-1, 1] \to \mathbb{R}, \quad ((x, y, \theta), (\lambda_1, \lambda_2, \lambda_3), u) \mapsto \lambda_1 \cos \theta + \lambda_2 \sin \theta + \lambda_3 u.$$

By Theorem 2.2.3 we have for almost every $t \in [0, T]$

$$
\begin{aligned}
\dot{\lambda}_1(t) &= -H_x((x(t), y(t), \theta(t)), (\lambda_1(t), \lambda_2(t), \lambda_3(t), u(t)) = 0, \\
\dot{\lambda}_2(t) &= -H_y((x(t), y(t), \theta(t)), (\lambda_1(t), \lambda_2(t), \lambda_3(t)), u(t)) = 0, \\
\dot{\lambda}_3(t) &= -H_\theta((x(t), y(t), \theta(t)), (\lambda_1(t), \lambda_2(t), \lambda_3(t)), u(t)) = \\
&= \lambda_1(t) \sin \theta(t) - \lambda_2(t) \cos \theta(t).
\end{aligned}
\tag{2.5}
$$

(i) and (ii) follow directly from the Hamiltonian being constant to λ_0, (iii) follows from (2.5). From (ii) it follows that $u(\cdot)|_I = 1$ or $u(\cdot)|_I = -1$, thus the curvature is equal to ± 1 and hence (iv) follows. The first claim of (v) follows immediately from (2.5). Together with (2.1), (i) and (iii) this yields

$$\ddot{\lambda}_3(t) = (\lambda_1(t) \cos \theta(t) + \lambda_2(t) \sin \theta(t)) u(t) = -\lambda_3(t) - \lambda_0 u(t) \quad \text{for all } t \in I,$$

(see also Figure 2.3), and this proves the second part of (v). Substituting $\dot{\lambda}_3(\cdot)|_I \equiv 0$ into (2.5) yields that $\theta(\cdot)|_I$ has to be constant and thus $u(\cdot)|_I \equiv 0$ and (vi) is shown. Finally, (vii) is eaual to the transversality condition in Theorem 2.2.3. ∎
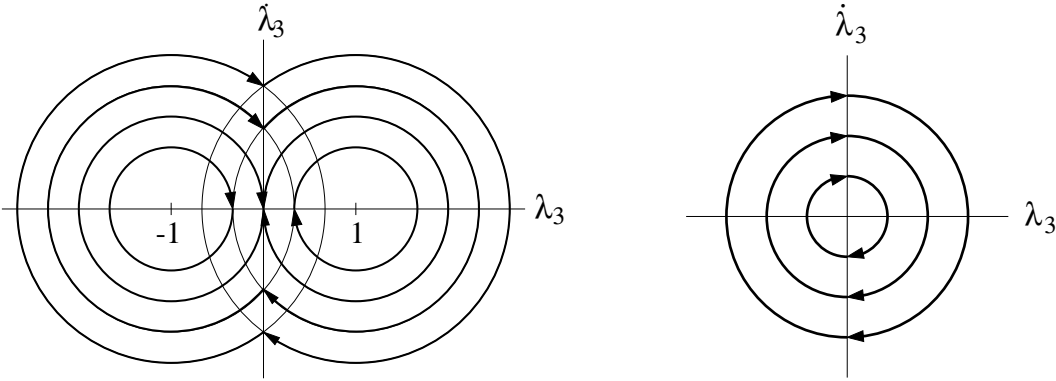
Figure 2.3: $\lambda_3 - \dot{\lambda}_3$ - phase portrait; normal and abnormal case

Definition 2.2.5 *The function* $\lambda_3 : [0, T] \rightarrow \mathbb{R}$ *is called* switching function *(since changes of sign imply changes of control strategy). If* $\lambda_3(t_0) = 0$ *for some* $t_0 \in [0, T]$ *and* $\lambda_3 \not\equiv 0$ *on every neighbourhood of* t_0, *then* t_0 *is called* switching parameter *or* switching time; *the corresponding* $(x(t_0), y(t_0), \theta(s_0))$ *is called* switching point. *An optimal solution is called* abnormal *if* $\lambda_0 = 0$ *and* normal *otherwise.*

Now we are in a position to classify the optimal solution to (2.2) in terms of different types of paths.

Proposition 2.2.6   *(i) The optimal solution to (2.2) is necessarily a finite concatenation of C and L parts.*

  (ii) If the optimal solution is a concatenation of only circular arcs C, then the arcs between two consecutive switching points and the last arc (between the last switching point and the terminal point are all of the same length. The length of all these arcs is greater than or equal to π and not smaller than the length of the first arc.

 (iii) There are no switchings between L parts, i.e., straight line segments with different angles with respect to the x-axis.

Proof   In order to prove (i) we follow the ideas of [40]. We need to show that there are only finitely many switching points. By Lemma 2.2.4 (iii) $\lambda_3(\cdot)_{[0,T]}$ is continuous and thus the set $F := \{s \in [0,1] : \lambda_3(s) \neq 0\}$ is a union of open intervals. We will show that their number is finite. In F there are at most two intervals with 0 or T as endpoints. Let $I = (t_1, t_2) \subset F$ such that $t_1, t_2 \notin F$. Then $\lambda_3(t_1) = \lambda_3(t_2) = 0$ (interior interval) and we assume that there are infinitely many interior intervals. On each interior interval I the function $\lambda_3(\cdot)$ has to satisfy the differential equation in Lemma 2.2.4 (v). Then $t_2 - t_1 \geq \pi$

(see Figure 2.3) and this cannot be true for infinitely many intervals in $[0, 1]$ and we arrive at the desired contradiction. From Lemma 2.2.4 (iv) and (vi) the claim (i) follows.

Claim (ii) follows from Lemma 2.2.4 (iii), (v) and (viii). A good illustration are the phase curves in Figure 2.3 which are symmetric to the axis $\lambda_3 = 0$ which implies the first part of the claim (regard $\lambda_3(t) = 0$). It can also be seen that there are at least half circles between two intersections with the axis $\lambda_3 = 0$ and thus the distance between two switching times is at least π.

Claim (iii) is obvious, since the path $(x(\cdot), y(\cdot))_{[0,T]}$ is a $\mathcal{C}^1$-curve and thus there cannot be any edges at concatenations of L parts. ∎

Proposition 2.2.7 *Consider an optimal path with respect to problem (2.2). Then the following hold.*

(i) If a part of the optimal path is of type L, then the path is necessarily of type CL or type L.

(ii) If no part of the optimal path is of type L, then the path is necessarily of type CC or C. In the CC case the first arc is not longer than the second arc which is not shorter than π.

Proof   (i) Let $0 \leq t_0 \leq t_1 < t_2 \leq t_3 \leq T$ and suppose

$$\lambda_3(t) \begin{cases} \neq 0 & , \quad \text{for all } t \in (t_0, t_1) \\ = 0 & , \quad \text{for all } t \in [t_1, t_2] \\ \neq 0 & , \quad \text{for all } t \in (t_2, t_3), \end{cases}$$

and let $\lambda_3(t_3) = 0$ (this is possible since $\lambda_3(T) = 0$ because of Lemma 2.2.4 (vii)). Then by Lemma 2.2.4 (vi), $(x(\cdot), y(\cdot))|_{[t_1,t_2]}$ is of type L. We show that if $\lambda_0 = 0$ then $t_0 = t_1 = 0$, $t_2 = t_3 = T$ and $(x(\cdot), y(\cdot))|_{[0,T]}$ is of type L and if $\lambda_0 = 1$ then $t_1 < 2\pi$, $t_2 = t_3 = T$ and $(x(\cdot), y(\cdot))|_{[0,T]}$ is of type CL.

In the abnormal case ($\lambda_0 = 0$), by assumption $\lambda_3(t_1) = \dot{\lambda}_3(t_1) = \lambda_3(t_2) = \dot{\lambda}_3(t_2) = 0$. Thus, by Lemma 2.2.4 (iii) and (v), we get $\lambda_3(\cdot)|_{(t_0,t_1)} \equiv \lambda_3(\cdot)|_{(t_2,t_3)} \equiv 0$, see also Figure 2.3. Therefore, both intervals (t_0, t_1) and (t_2, t_3) have to be empty and we have proved the claim in the abnormal case.

Now consider the normal case ($\lambda_0 = 1$). First assume that $t_2 < T$. On the interval (t_2, t_3), the solution of the differential equation in Lemma 2.2.4 (v) is given by $\lambda_3(t) = A \sin(t + \varphi) + 1$ or $\lambda_3(t) = A \sin(t + \varphi) - 1$ for some suitable constants A and φ. From $\lambda_3(t_2) = \dot{\lambda}_3(t_2) = 0 = \lambda_3(t_3)$ and the special form of the solution it follows that $\dot{\lambda}_3(t_3) = 0$ and $t_3 - t_2 = 2\pi$, see also Figure 2.3. Therefore, the path $(x(\cdot), y(\cdot))|_{[t_2,t_3]}$ is a full circle which obviously cannot be optimal on a shortest path, and thus $t_2 = t_3 = T$. On the other hand, by analogous arguments, it can be shown that $\lambda_3(\cdot)|_{[0,t_1)} \neq 0$ thus $t_1 < 2\pi$ and the claim follows.

(ii) We show that if the path is a finite concatenation of C parts, then the path $(x(\cdot), y(\cdot))|_{[0,T]}$ is of the form CC and the second arc is not shorter than π and at least as long as the first.

Assume that there is an optimal path with $n \geq 3$ switching times $t_1 < \cdots < t_n < T$. Then $t_{i+1} - t_i = d$, $i = 1, \ldots, n-1$, by Proposition 2.2.6 and $T - t_n = d$ since $\lambda_3(T) = 0$ by Lemma 2.2.4 (vii). Furthermore, on any interval of length d $\lambda_3(\cdot)$ has exactly one zero. Therefore, the distance between 0 and the first switching is at most d and the first arc is the shortest. This means that all switching points and the terminal point lie on a straight line s. Obviously, since the second arc intersects s in two points,
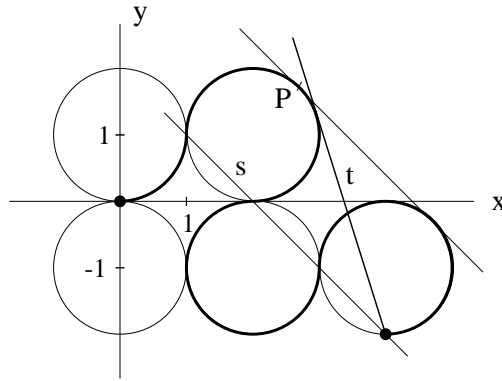

Figure 2.4: A CCCC path cannot be optimal

there exists a point P on the second arc where the tangent to it is parallel to the straight line s, see also Figure 2.4. To any point Q on the remainder of the path exists a tangent to the second arc between P and the second switching point containing Q. In particular, there exists a tangent t to the second arc reaching the terminal point and this is a shorter path of the type CCL and we have a contradiction to our assumption. This proves the claim.

∎

2.2.3   Sufficient conditions for optimality

The main result of this section is to determine the subsets of terminal points in $\mathbb{R}^2$ that are reached by the the same type of optimal paths. This is illustrated in Figure 2.5.

Theorem 2.2.8 *The solution to (2.2) is given by one of the following strategies, where all circular arcs are shorter than 2π:*

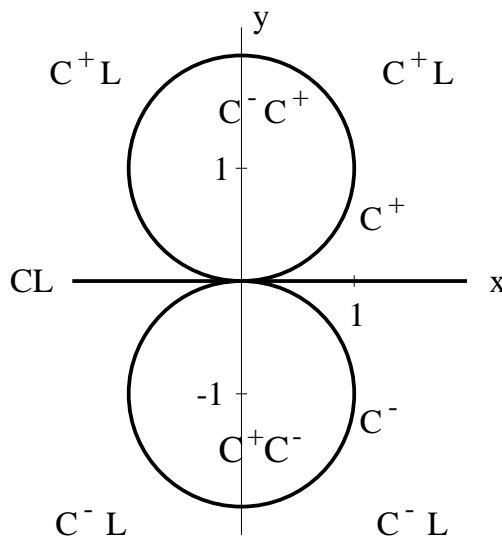|	location of the terminal point	strategy
(a)	in $\mathbb{R}_0^+ \times \{0\}$	L
(b)	on C_1	C^+
	on C_2	C^-
(c)	outside C_1 in $\mathbb{R} \times \mathbb{R}^+$	C^+L
	outside C_2 in $\mathbb{R} \times \mathbb{R}^-$	C^-L
	in $\mathbb{R}^- \times \{0\}$	C^+L or C^-L
(d)	inside C_1	C^-C^+
	inside C_2	C^+C^-

The result of Theorem 2.2.8 is depicted in Figure 2.5.

Figure 2.5: The synthesis of the optimal paths

Remark 2.2.9 The shortest path to a terminal point inside $C_1 \cup C_2$ is not shorter than π by Proposition 2.2.7 and to each abnormal optimal strategy there exists a normal strategy which solves the problem in the same time. $\quad\square$

For the proof of Theorem 2.2.8 the following lemmas are needed.

Lemma 2.2.10 *Let $M_1, M_2 \subset \mathbb{R}^2$ be two convex compact sets with $M_1 \subset M_2$. Then the arclength of the boundary of M_1 is not greater than the arclength of the boundary of M_2.*

Proof See e.g. [42]. $\quad\blacksquare$

Lemma 2.2.11 *Let (x, y) be a point in the lower half plane outside C_2. Then there exists exactly one C^+L path and one C^-L path to (x, y) such that the lengths of the C parts are shorter than 2π. Furthermore, the C^-L path is shorter than the C^+L path.*

Proof It is obvious that there exists exactly one C^+L path and one C^-L path
to (x, y) with the lengths of the C parts being shorter than 2π. Denote by a and
b the lengths of the L parts of the C^+L path and the C^-L path, respectively, and
by c and d the distances between (x, y) and $(0, 1)$ and $(0, -1)$, see also Figure
2.6, first picture.

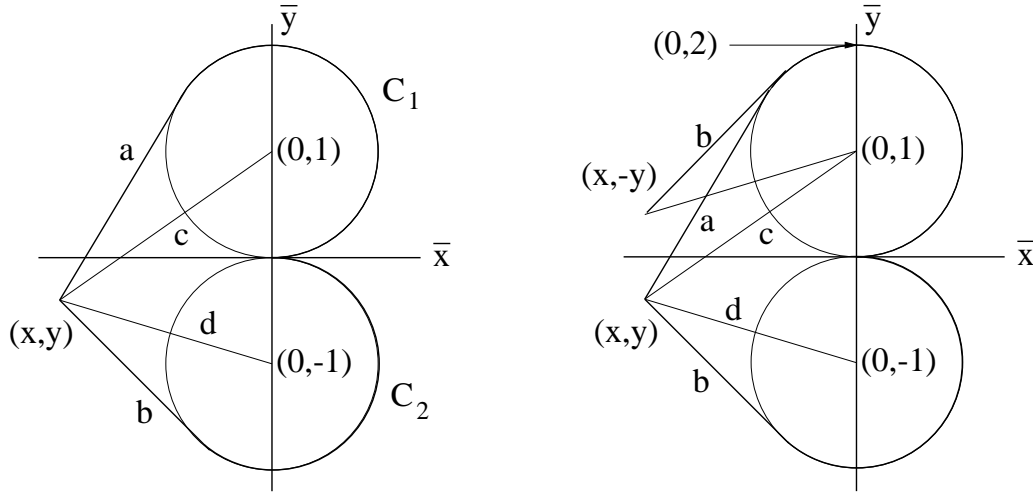 Now assume that there exists a C^+L path to (x, y) in the lower half plane which

Figure 2.6: CL paths to (x, y) and reflection of the lower half plane about the
$\overline{x}$-axis

is shorter than the C^-L path reaching (x, y). We have $c^2 = a^2 + 1$, $d^2 = b^2 + 1$
and $a^2 - b^2 = c^2 - d^2 = -4y > 0$. The lengths of the C parts of the C^+L and the
C^-L path are $\pi + \alpha$ and $\pi + \beta$ for some $0 < \alpha < \beta < \pi$. From that we see that
we only need to consider points (x, y) with $x < 0$ and $-2 < y < 0$ outside C_2.
We distinguish three cases, namely $x \leq -1$, $-1 < x < 0$ and $-1 < y < 0$ and
finally $-1 < x < 0$ and $-2 < y < -1$.
At first consider $x \leq -1$. Reflect C_2 and the C^-L path about the $\overline{x}$-axis, see
also Figure 2.6, second picture. Consider the C^+L path between (x, y) and $(0, 2)$
as a function $f_1 : [x, 0] \to \mathbb{R}$ with $f_1(x) = y$, $f_1(0) = 2$, and the reflected C^-L
path between $(x, -y)$ and $(0, 2)$ as a function $f_2 : [x, 0] \to \mathbb{R}$ with $f_2(x) = -y$,
$f_2(0) = 2$. Then $f_1'(s) \geq f_2'(s)$ for all $s \in [x, 0]$ and thus the C^+L path is longer
than the C^-L path.
Defining and comparing similar functions as above, the C^+L path is longer than
the C^-L path if $-1 < x < 0$ and $-1 < y < 0$.
Now let $-1 < x < 0$ and $-2 < y < -1$. Then the length of the C^-L path is
smaller than $\frac{3\pi}{2} + 1$ and the length of the C^+L path is greater than $\frac{3\pi}{2} + 1$ and
we have the claim.   ∎

Finally, we have all tools at hand in order to prove Theorem 2.2.8.

Proof [Theorem 2.2.8] The only possible optimal strategies are the four strategies CL,CC,C and L listed in Proposition 2.2.7. We only need to consider circular arcs of length shorter than 2π, since otherwise we could reduce the length of the path by 2π by leaving out a complete circle. Because of the symmetry of system (2.1), that is $(x(\cdot), y(\cdot), \theta(\cdot), u(\cdot))$ solves (2.1) if and only if $(x(\cdot), -y(\cdot), -\theta(\cdot), -u(\cdot))$ solves (2.1), we restrict our attention to the closed lower half plane in case of (b) and (c) and to the upper half plane in case (d).

(a) Obviously, a straight line (strategy L) is the shortest path between two points in the plane and any point $(x_T, 0) \in \mathbb{R}_0^+ \times \{0\}$ can be reached this way.

(c) Terminal points in the lower half plane outside C_2 can only be reached by the CC or the CL strategy and we will show that no CC strategy is optimal. By Lemma 2.2.11 the C^+L strategy is longer than the C^-L strategy here and we have the claim.
Assume that g is an optimal CC path with switching time $t_0 > 0$ and terminal point in the lower half plane outside C_2.
We only need to consider C^+C^- paths with $t_0 < \frac{\pi}{2}$. This can be seen as follows. Suppose g is of the C^-C^+ type. Then there exists a straight line through the terminal point which is tangent to the first arc (see Figure 2.7, first picture). This CL path $\tilde{g}$ is obviously shorter and we arrive at a contradiction. If $t_0 \geq \frac{\pi}{2}$ then the second arc of the C^+C^- path cannot be shorter than the first by Proposition 2.2.7 and the endpoint lies in the upper half plane and we arrive at a contradiction again.
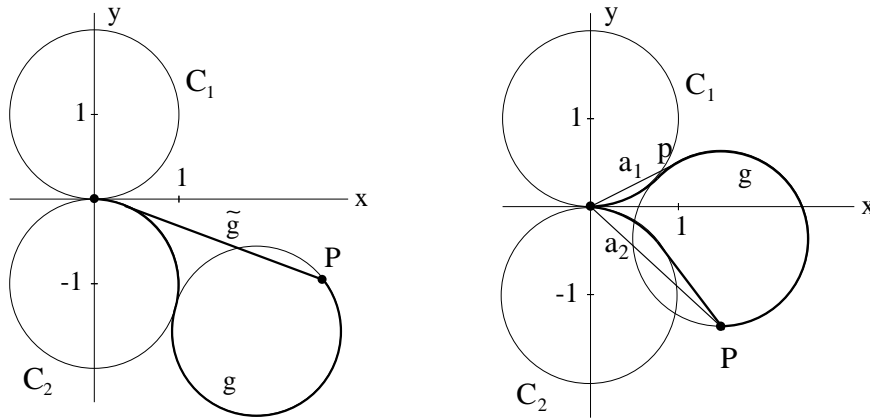 Now we consider a C^-L path and a C^+C^- path to the same terminal point

Figure 2.7: Two cases of possible CC and CL paths to the same endpoint

(Figure 2.7, second picture). Denote the straight line segment between $(0,0)$ and the terminal point by a_2 and the straight line segment through

the origin tangent to the second arc of the CC path by a_1 (if there are two such tangents then take the one the touches the second arc at the smaller switching time). Obviously, the path consisting of a_1 and the remainder of the second arc is shorter than the CC path. The set bounded by a_2 and the C^-L path is convex and contained in the convex set bounded by a_2 and the path just constructed. Therefore, by Lemma 2.2.10, the C^-L path is shorter than the path above which is again shorter than the C^+C^- path and we arrive at a contradiction.

Thus the shortest path to a point in the lower half plane outside C_2 is of type C^-L. If the terminal point lies on the negative x-axis, both strategies C^-L and C^+L reach the point in the same time and we have proved (c).

(d) Now we show that inside C_1 the C^-C^+ strategy is optimal.

Reaching a terminal point inside C_1 is only possible with C^-L or C^-C^+ paths. Note again that due to the parametrization by arc length switching times coincide with angles of circular arcs C.

The switching time $\varphi < 2\pi$ for the C^-L path is well defined by the terminal point and $\frac{3\pi}{2} < \varphi$ holds. It is possible to reach the same terminal point with two C^-C^+ paths with switching times $\delta < \frac{\pi}{2}$ and $\gamma > \frac{3\pi}{2}$, see Figure 2.8. But the second arc of the C^-C^+ path with switching time γ is shorter than
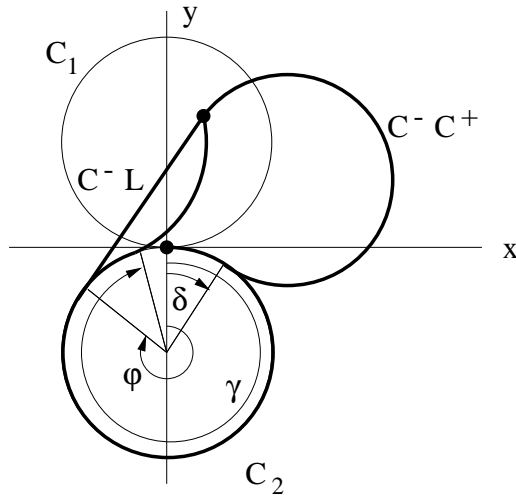
Figure 2.8: The possible strategies for endpoints inside C_1

π and thus shorter than the first arc which is impossible on an optimal path by Proposition 2.2.7. Therefore, we consider the C^-C^+ path with switching time δ and the C^-L path with switching time φ only.

We denote with l_{CC} and l_{CL} the lengths of the considered C^-C^+ and C^-L path, respectively. Both paths are the same on C_2 until they reach the switching point of the C^-C^+ path at angle (and time) δ, see Figure 2.9.
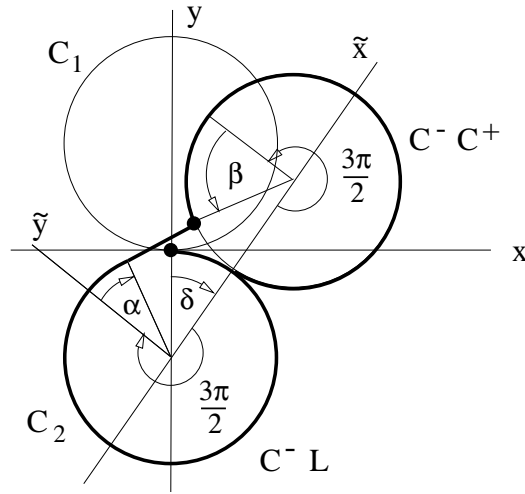
Figure 2.9: The CL and the CC path to a final point inside C_1

Then they turn into opposite directions for $\frac{3\pi}{2}$ (if the C^-C^+ path should reach the final point earlier, then the C^-L path is definitely longer). Note that $\varphi = \delta + \frac{3\pi}{2} + \alpha$ with $0 \le \alpha \le \frac{\pi}{2}$ since otherwise the C^-L path could not intersect the second arc of the C^-C^+ path and would not reach the terminal point.

For lengths greater than $\delta + \frac{3\pi}{2}$ we introduce a new coordinate saystem. The $\tilde{x}$-axis is the straight line through the center of C_2 and the center of the second arc of the C^-C^+ path. The $\tilde{y}$-axis is the straight line throught the center of C_2 orthogonal to the $\tilde{x}$-axis, also look at Figure 2.10. We denote

Figure 2.10: A rotation of figure 2.9 by the angle $\pi - \delta$

with β' the angle between the $\tilde{y}$-axis and the line through the center of C_2

and the terminal point. Obviously $\beta' > \beta$ and thus we get

$$
\begin{aligned}
l_{CC} &= \delta + \frac{3\pi}{2} + \beta \\
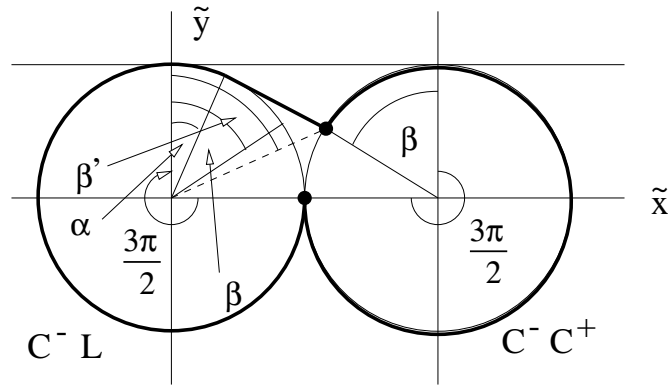l_{CL} &= \delta + \frac{3\pi}{2} + \alpha + \tan(\beta' - \alpha) \geq \delta + \frac{3\pi}{2} + \alpha + \tan(\beta - \alpha) \\
&\geq \delta + \frac{3\pi}{2} + \alpha + (\beta - \alpha) = \delta + \frac{3\pi}{2} + \beta = l_{CC}
\end{aligned}
$$

and therefore the C^-C^+ path is the shortest in case (d).

(b) Now suppose the terminal point is on C_1 or C_2. Applying the poof of (c) with length of the L part being 0, the CC strategy is not better than the C strategy. Applying the proof of (d) with $\delta = 0$, the CL strategy is not better either and we have claim (b).

$\blacksquare$

2.3   A new short proof of Dubins' result

In this section we use the approach of the previous section to present a proof of Dubins' result [17] on shortest paths with *prescribed* terminal direction. We present a new way to show that concatenations of four or more circular arcs cannot be optimal. We do not give a result corresponding to Theorem 2.2.8 since this can be found in [37].

Theorem 2.3.1 (Dubins) *Let $\theta_T \in [0, 2\pi)$ and consider the optimization problem (2.2) with the additional terminal point condition $\theta(T) = \theta_T \bmod 2\pi$. The optimal path is of type CLC or CCC (the middle arc is of length greater than π) or a subtype CL, LC, CC, L or C.*

Proof   The conditions (i)-(vi) in Lemma 2.2.4 are valid again, just the transversality condition (vii) does not hold. Proposition 2.2.6 and Proposition 2.2.7 (i) also hold here and optimal paths are finite C-L-concatenations. If a straight line segment is part of an optimal path, it can be shown analogously to Proposition 2.2.7 (ii) that the path is of type CLC or subtypes. Otherwise we have concatenations of finitely many circular arcs and it remains to show is that there are at most three.

Suppose we have an optimal path consisting of a concatenation of n circular arcs, $n > 3$. Since the 2nd up to the (n-1)st arc are of the same length l_2 with $\pi \leq l_2 < 2\pi$ by Proposition 2.2.6, all switching points lie on one straight line l. Furthermore, if $n \geq 5$, there exist exactly one parallel to l touching the 2nd and 4th arc, we call it p, and this gives a shorter path, see also Figure 2.11. Therefore, at most four circular arcs can be optimal.
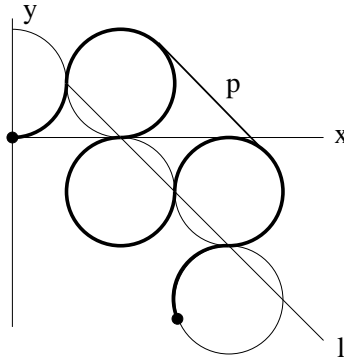
Figure 2.11: Concatenation of 5 circular arcs (not optimal)

Now we show that even concatenations of four circular arcs cannot be optimal. We consider a path p_1 consisting of four circular arcs of length $l_i, i = 1, \ldots, 4$, respectively, fulfilling the necessary conditions for optimality (i)-(vi) of Lemma 2.2.4. Then $l_2 = l_3 \geq \pi$ due to Proposition 2.2.6. Without loss of generality we may assume that the first and third arc are followed clockwise, the second and fourth anti-clockwise. Denote the centers of the four arcs with M_i, $i = 1, \ldots, 4$ and the switching points with S_i, $i = 1, 2, 3$, respectively. Since $l_2 = l_3$, the
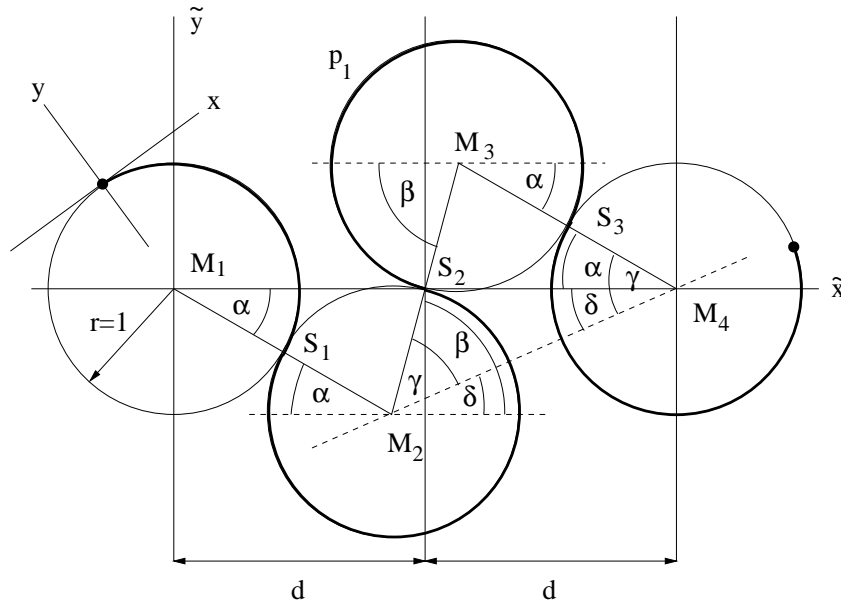
Figure 2.12: New coordinate system for a CCCC path

midpoint between M_1 and M_4 is S_2 as well as the midpoint between M_2 and M_3. We introduce a new coordinate system by $M_1 = (0,0)$, $S_2 = (d,0)$ and the following notation:

α angle between the $\tilde{x}$-axis and the straight line through M_1 and M_2
β angle between the $\tilde{x}$-axis and the straight line through M_2 and M_3
γ angle between the straight line through M_2 and M_4 and
      the straight line through M_2 and M_3
δ angle between the $\tilde{x}$-axis and the straight line through M_2 and M_4

Then $M_4 = (2d, 0)$, $M_2 = (2\cos\alpha, -2\sin\alpha)$ and $M_3 = (2d - 2\cos\alpha, 2\sin\alpha)$ with $\cos\alpha = \frac{d^2+3}{4d}$, consider triangle $M_1M_2S_2$ in Figure 2.12 (necessarily $M_2 \in \mathbb{R} \times \mathbb{R}_0^-$). In the setup above the first and the last circle cannot intersect and therefore $1 \leq d \leq 3$. The length of p_1 is

$$l_{p_1} = l_1 + \alpha + \pi + 2\beta + \pi + \alpha + l_4 = l_1 + l_4 + 2\pi + 2(\alpha + \beta).$$

Now we have the necessary setup and will consider the cases $d = 1$, $1 < d < 3$ and $d = 3$. In each case we will show that there exists a shorter path than p_1, thus concatenations of four circular arcs cannot be optimal.

If $d = 1$, then $M_2 = M_4$, $M_1 = M_3$ and $l_2 = l_3 = 2\pi$. Leaving out the second and the third arc would save a path of length 4π and the CC strategy would be shorter.

If $1 < d < 3$, we compare the path p_1 with an alternative path p_2 which follows the same first circle for the time (angle) $l_1 - \epsilon$ with a sufficiently small $\epsilon > 0$. Then the appropiate second circle is well defined as well as the new third circle touching the new second circle and the fourth circle. We denote the centers of the new circles with M_2' and M_3', see Figure 2.13. The length of the new path p_2 is

$$\begin{aligned} l_{p_2} &= l_1 - \epsilon + \alpha' + \pi + 2\beta' + \pi + \alpha'' + \alpha'' - \alpha + l_4 = \\ &= l_1 + l_4 + 2\pi + 2(\alpha'' + \beta') - 2\epsilon \end{aligned}$$

since $\alpha' = \alpha - \epsilon$. We now show that $\alpha'' + \beta' < \alpha + \beta + \epsilon$ and therefore path p_2 is shorter than path p_1. At first it is obvious that $\alpha + \beta = \gamma - \delta + \gamma + \delta = 2\gamma$ and $\alpha'' + \beta' = 2\gamma'$. The distances between the centers of the second and fourth circle are $2\sqrt{d^2 - 2d\cos\alpha + 1}$ and $2\sqrt{d^2 - 2d\cos(\alpha - \epsilon) + 1}$, respectively. Therefore, considering the triangles $M_3M_2M_4$ and $M_3'M_2'M_4$, we have

$$\gamma = \arccos\frac{\sqrt{d^2 - 2d\cos\alpha + 1}}{2}, \quad \gamma' = \arccos\frac{\sqrt{d^2 - 2d\cos(\alpha - \epsilon) + 1}}{2}.$$

Introducing $f(\epsilon) = 2\gamma' - 2\gamma - \epsilon$, we need to show that $f(\epsilon) < 0$ for small $\epsilon > 0$. With $\cos\alpha = \frac{d^2+3}{4d}$ we get, after an easy but lengthy calculation, $f(0) = f'(0) = 0$ and

$$f''(0) = \frac{\sqrt{(9 - d^2)(d^2 - 1)}}{d^2 - 9} < 0 \quad \text{for } 1 < d < 3$$

and we have $f(\epsilon) < 0$ and our claim for small $\epsilon > 0$.

If $d = 3$ we just reduce l_1 by a small ϵ, 'glue' a new second circle to the new
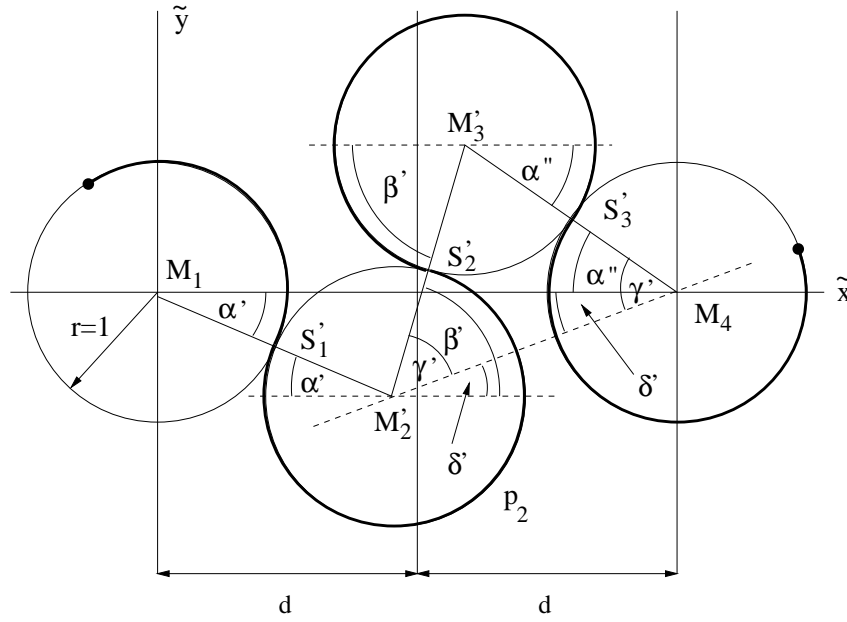
Figure 2.13: Alternative CCCC path if $1 < d < 3$
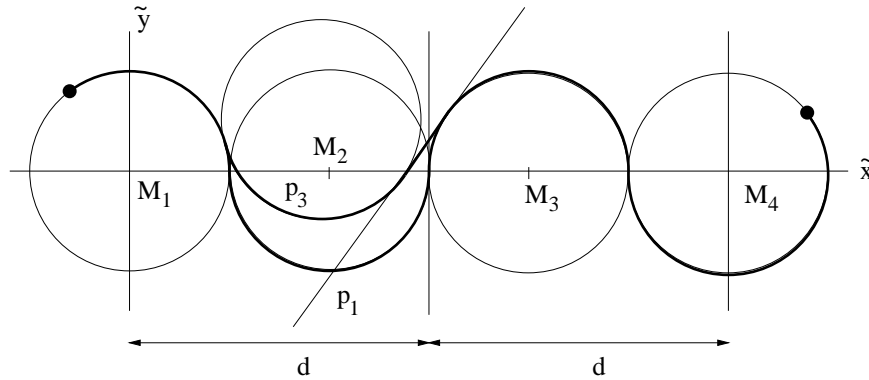
Figure 2.14: Alternative to the CCCC path if $d = 3$

first switching point and leave the other two circles unchanged. Then we take the tangent t from the new second circle to the third circle and get a new path p_3, see Figure 2.14. Between the point where the new second circle touches the first circle and the point where t touches the third circle, the part of path p_3 is convex and from Lemma 2.2.10 follows that it is shorter than the convex hull of the part of path p_1 which is again shorter than this part of path p_1 itself. Thus p_3 is shorter than p_1.

In each case we have shown that p_1 is not optimal. Therefore concatenations of four circular arcs cannot be optimal and we proved our claim. ∎

Chapter 3

Workspaces of 2D continuous robotic manipulators

As far as we know a robotic manipulator controlled by distributed bending moments has not yet been designed or built since it is very hard if not impossible to control a continuous structure at each point independently. Therefore, this chapter has to be seen as a purely theoretical investigation. Nevertheless, since the model is a very good approximation of a discrete hyper-redundant manipulator (see e.g., [14] and [15], where such robots are built and their workspaces look very similar to those obtained in this chapter), it is of interest even today.

Here we will determine the workspaces of planar continuous manipulators for arbitrary but fixed curvature constraint. At first, we will introduce the mathematical model describing this particular type of manipulator and define its workspace. Then we will investigate the workspaces of manipulators with free and prescribed terminal direction. After showing a few elementary properties of the wor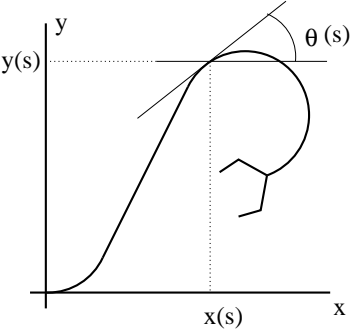kspaces, we solve optimal control problems in order to describe the boundaries of the workspaces. For various values of the curvature constraint of the manipulators we get workspaces with different topological properties.

3.1 Model of 2D continuous manipulators

A planar continuous robotic manipulator of length L (we assume that the manipulator is inextensible and normalize such that L=1) can be described by a C^1-curve in the plane which describes the shape of the robot's centerline. This centerline (in the literature often called backbone curve having in mind the backbone of an animal, in particular a snake) captures the macroscopic geometric features of the robot. Whenever the shape of the manipulator is mentioned in the sequel it is to be interpreted as the shape of the centerline. We parametrize the curve by arc-length and denote with $\theta(s)$ the angle between the x-axis and the tangent to the curve at $(x(s), y(s)) \in \mathbb{R}^2$ at the parameter value s. Further-

more, we assume that the manipulator is fixed in the origin. The curve can be described by the following equations:

$$
\begin{aligned}
x'(s) &= \cos \theta(s) \\
y'(s) &= \sin \theta(s) \\
\theta'(s) &= \kappa(s) \\
x(0) &= 0 \\
y(0) &= 0 \\
\theta(0) &= 0
\end{aligned}
\qquad (3.1)
$$

with $s \in [0,1]$ and curvature $\kappa \in \mathcal{U}_M$.

Remark 3.1.1 At this stage considering a measurable curvature seems to be far too general for realizations of manipulators and one might prefer piecewise constant functions (maybe even continuous functions). Actually, this generality is needed to prove the existence of optimal solutions of the optimal control problem introduced later. But after the solution of this problem we will see in Lemma 3.3.3 and its proof that every point in the workspace can be reached with a realization through a piecewise continuous control function with at most two discontinuities taking its values in $\{-1, 0, 1\}$. □

Due to possible physical limitations we prescribe the curvature to be uniformly bounded, $|\kappa(s)| \leq M$ for almost every $s \in [0,1]$ and some constant $M > 0$.

3.2 Description of the 2D workspaces

First, we describe mathematically what we call workspace.

Definition 3.2.1 *Let*

$$\mathcal{F} := \{(x(\cdot), y(\cdot), \theta(\cdot)) \text{ satisfying (3.1) with } \kappa \in \mathcal{U}_M\}.$$

For any $\Omega \subset \mathcal{F}$ we define

$$P_\Omega := \{(x_1, y_1) \in \mathbb{R}^2 \,:\, (x(1), y(1)) = (x_1, y_1) \text{ for some } (x(\cdot), y(\cdot), \theta(\cdot)) \in \Omega\}.$$

The workspace *of a robotic manipulator of length 1 described by system (3.1) is the set of reachable points of its* end-effector $(x(1), y(1))$:

$$W := P_\mathcal{F} \quad \text{or} \quad W_{\theta_1} := \{(x_1, y_1) \in W \,|\, \theta(1) = \theta_1 \bmod 2\pi\}$$

for some fixed $\theta_1 \in [0, 2\pi)$.

Remark 3.2.2 Since we disregard $\theta(1)$ in the first case, we do not determine the reachable set of the control system at $s = 1$ but only the 'output' $(x(1), y(1))$. □

3.2.1 The workspaces with free terminal direction

In this section we will describe and illustrate the workspaces W for different values of M. At first, we state a few basic properties of W.

Lemma 3.2.3 W *is non-empty for every $M > 0$. Furthermore, W is*

(i) *symmetric to the x-axis and*

(ii) *a path-connected subset of $\mathbb{R}^2$.*

Proof First of all, the point $(1, 0)$ can always be reached with $\kappa \equiv 0$. Let $\kappa \in \mathcal{U}_M$ be the curvature of a manipulator reaching $(x_1, y_1) \in W$.

(i) Then $-\kappa \in \mathcal{U}_M$ and the manipulator with curvature $-\kappa$ reaches the point $(x_1, -y_1) \in W$ (look at (3.1)) and we have the symmetry.

(ii) Let $a \in [0, 1]$ and $\kappa^a := (1 - a)\kappa$. Then $\kappa^a \in \mathcal{U}_M$ and the corresponding end-effector is $(x_1^a, y_1^a) \in W$. Finally, the points (x_1^a, y_1^a) describe a path between (x_1, y_1) and the point $(1, 0)$ since the solutions of this differential equation depend continuously on the parameter a. Therefore, all points in W are path-connected.

■

Proposition 3.2.4 W *is compact.*

Proof The manipulator can obviously only reach points inside the unit circle and the point $(1,0)$. Thus W is bounded and it remains to show that W is closed. Consider a sequence $\kappa_n(\cdot)_{n \in \mathbb{N}} \subset \mathcal{U}_M$ of controls with corresponding state

$$(x_n(\cdot), y_n(\cdot), \theta_n(\cdot)) : [0, 1] \to \mathbb{R}^3$$

subject to (3.1) for each $n \in \mathbb{N}$ such that $(x_n(1), y_n(1))_{n \in \mathbb{N}}$ converges to $(x_1, y_1) \in \mathbb{R}^2$. We show that there exists a function $\tilde{\kappa}(\cdot) \in \mathcal{U}_M$ with state $(\tilde{x}(\cdot), \tilde{y}(\cdot), \tilde{\theta}(\cdot))$ subject to (3.1) such that $(\tilde{x}(1), \tilde{y}(1)) = (x_1, y_1)$. Due to the parametrization by arc length we have $||(x_n'(s), y_n'(s))|| = 1$ and anyhow

$$|\theta_n(s)| = \left| \int_0^s \kappa_n(\tau)d\tau \right| \leq Ms \leq M$$

for all $s \in [0, 1]$ and all $n \in \mathbb{N}$. Thus the family $(x_n'(\cdot), y_n'(\cdot), \theta_n(\cdot))_{n \in \mathbb{N}}$ is uniformly bounded. Moreover, we have for all $s, t \in [0, 1]$ and $n \in \mathbb{N}$

$$
\begin{aligned}
||(x_n'(s), y_n'(s)) \ - \ (x_n'(t), y_n'(t))||^2 &= (\cos \theta(s) - \cos \theta(t))^2 + \\
&\quad + (\sin \theta(s) - \sin \theta(t))^2 = \\
&= 2 - 2\cos \theta(s) \cos \theta(t) - 2\sin \theta(s) \sin \theta(t) = \\
&= 2 - 2\cos (\theta(s) - \theta(t)) = 4\sin^2 \frac{\theta(s) - \theta(t)}{2} \leq |\theta_n(s) - \theta_n(t)|^2
\end{aligned}
$$

and we get

$$||(x_n'(s), y_n'(s)) - (x_n'(t), y_n'(t))|| \leq |\theta_n(s) - \theta_n(t)| \leq M|s - t|. \qquad (3.2)$$

Thus

$$||(x_n'(s), y_n'(s), \theta_n(s)) - (x_n'(t), y_n'(t), \theta_n(t))|| \leq \sqrt{2}M|s - t|$$

and the $(x_n'(\cdot), y_n'(\cdot), \theta_n(s))_{n \in \mathbb{N}}$ form an equicontinuous family on $[0, 1]$. Therefore by the Arzelà-Ascoli theorem, there exists a subsequence of $(x_n'(\cdot), y_n'(\cdot), \theta_n(\cdot))_{n \in \mathbb{N}}$ converging uniformly on $[0, 1]$ to a continuous function $(\xi(\cdot), \eta(\cdot), \tilde{\theta}(\cdot))$ with

$$\xi(s) = \cos \tilde{\theta}(s), \quad \eta(s) = \sin \tilde{\theta}(s)$$

for all $s \in [0, 1]$. For simplicity we may assume that $(x_n'(\cdot), y_n'(\cdot), \theta_n(\cdot))_{n \in \mathbb{N}}$ is itself such a sequence. Obviously, for all $s, t \in [0, 1]$

$$|\tilde{\theta}(s) - \tilde{\theta}(t)| \leq M|s - t| \qquad (3.3)$$

and $(\xi(0), \eta(0), \tilde{\theta}(0)) = (1, 0, 0)$ which shows that the initial condition of (3.1) holds for $\tilde{\theta}(\cdot)$. In particular $\tilde{\theta}(\cdot) \in \mathrm{Lip}_M[0, 1] \subset A[0, 1]$. Thus $\tilde{\theta}(\cdot)$ is differentiable almost everywhere (see e.g., [28]). We set $\tilde{\kappa}(s) := \dot{\tilde{\theta}}(s)$ for all $s \in [0, 1]$ where $\tilde{\theta}(\cdot)$ is differentiable and $\tilde{\kappa}(s) := 0$ else. Because of (3.3) we have $|\tilde{\kappa}(s)| = |\dot{\tilde{\theta}}(s)| \leq M$ for every $s \in [0, 1]$ thus $\tilde{\kappa}(\cdot) \in \mathcal{U}_M$. We set

$$\tilde{x}(s) := \int_0^s \xi(t) \, dt \quad \text{and} \quad \tilde{y}(s) := \int_0^s \eta(t) \, dt.$$

Since

$$|\tilde{x}(1) - x_n(1)| \;\leq\; \int_0^1 |\cos \tilde{\theta}(t) - \cos \theta_n(t)| \, dt \;\to\; 0 \text{ as } n \to \infty \quad \text{and}$$

$$|\tilde{y}(1) - y_n(1)| \;\leq\; \int_0^1 |\sin \tilde{\theta}(t) - \sin \theta_n(t)| \, dt \;\to\; 0 \text{ as } n \to \infty,$$

we have $(x_1, y_1) = (x(1), y(1)) \in W$ and W is closed as claimed. $\blacksquare$

In order to describe the workspaces W we follow the following program. We investigate a 2-parameter family of optimal control problems (of the Mayer type) subject to the conditions of (3.1) such that for the set of optimal solutions $\mathcal{G}$ we have $\mathrm{cl}P_{\mathcal{G}} = \partial W$. We are not able to describe $P_{\mathcal{G}}$ itself, but we will determine a 'small' set of functions $\mathcal{B}$ satisfying the necessary conditions of Pontryagin's

Maximum Principle and further geometric properties such that the following diagram holds:

$$\mathcal{F} \quad \supset \quad \mathcal{B} \quad \supset \quad \mathcal{G}$$

$$P \downarrow \qquad P \downarrow \qquad P \downarrow$$

$$W = P_{\mathcal{F}} \quad \supset \quad P_{\mathcal{B}} \quad \supset \quad P_{\mathcal{G}}$$

Using homotopies we will be able to describe W using $P_{\mathcal{B}}$.

Let us consider the following 2-parameter $((x_0, y_0) \in \mathbb{R}^2)$ family of minimization problems subject to (3.1):

$$J_{x_0,y_0} = (x(1) - x_0)^2 + (y(1) - y_0)^2 \to \min \tag{3.4}$$

while minimizing over all $(x(\cdot), y(\cdot), \theta(\cdot)) \in \mathcal{F}$ (thus $(x(1), y(1)) \in W$). This problem is in fact an optimal control (Mayer) problem since we minimize over all $\kappa \in \mathcal{U}_M$, see Definition 3.2.1. First of all, the following lemma guarantees the existence of optimal solutions.

Lemma 3.2.5 *To any $(x_0, y_0) \in \mathbb{R}^2$ a solution to problem (3.4) exists.*

Proof If $(x_0, y_0) \in W$ then obviously $J_{x_0,y_0} = 0$ and $(x(1), y(1)) = (x_0, y_0)$ itself is a solution. If $(x_0, y_0) \notin W$ then $\sqrt{J_{x_0,y_0}}$ is the euclidean distance between (x_0, y_0) and W. Since W is compact the optimal solution to (3.4) exists. ∎

Now let $\mathcal{G} \subset \mathcal{F}$ denote the set of all admissible solutions that minimize (3.4) for some parameter $(x_0, y_0) \notin W$. Then the following holds:

Proposition 3.2.6 $cl\, P_{\mathcal{G}} = \partial W$.

Proof If $(x_0, y_0) \notin W$ and $(\overline{x}(1), \overline{y}(1))_{x_0,y_0}$ is the terminal point of a corresponding optimal solution, then any point on the straight line between (x_0, y_0) and $(\overline{x}(1), \overline{y}(1))_{x_0,y_0}$ is not in W because of the minimal distance property of the point $(\overline{x}(1), \overline{y}(1))_{x_0,y_0}$. Thus $(\overline{x}(1), \overline{y}(1))_{x_0,y_0} \in \partial W$ and $P_{\mathcal{G}} \subset \partial W$.

Let $(x, y) \in \partial W$ be arbitrary. Then there exists a sequence $(x_n, y_n)_{n \in N}$ such that $(x_n, y_n) \notin W$ for each $n \in N$ and $(x_n, y_n) \to (x, y)$ as $n \to \infty$. Obviously $J_{x_n,y_n} \to 0$, $(\overline{x}(1), \overline{y}(1))_{x_n,y_n} \in P_{\mathcal{G}}$ for each $n \in \mathbb{N}$ and $(\overline{x}(1), \overline{y}(1))_{x_n,y_n} \to (x, y)$ as $n \to \infty$. Thus $(x, y) \in cl\, P_{\mathcal{G}}$ and we have

$$P_{\mathcal{G}} \subset \partial W \subset cl\, P_{\mathcal{G}}$$

and the claim follows since W is compact by Proposition 3.2.4 and so is ∂W. ∎

Now we want to construct $P_{\mathcal{B}}$. Since we desire to apply optimal control techniques, we state a version of Pontryagin's Maximum Principle (see e.g., [6]) tailored for the needs of the following analysis.

Theorem 3.2.7 (Pontryagin's Minimum Principle) *If $\kappa(\cdot) \in \mathcal{U}_M$ is an optimal control to problem (3.4) with $(x_0, y_0) \notin W$ and corresponding state function $(x(\cdot), y(\cdot), \theta(\cdot))$, then*

(i) *there exists an absolutely continuous vector function $\lambda : [0, 1] \to \mathbb{R}^3$ satisfying the adjoint equations*

$$
\begin{array}{rcl}
\lambda_1'(s) & = & -\frac{\partial}{\partial x} H(x(s), y(s), \theta(s), \lambda_1(s), \lambda_2(s), \lambda_3(s), \kappa(s)), \\
\lambda_2'(s) & = & -\frac{\partial}{\partial y} H(x(s), y(s), \theta(s), \lambda_1(s), \lambda_2(s), \lambda_3(s), \kappa(s)), \\
\lambda_3'(s) & = & -\frac{\partial}{\partial \theta} H(x(s), y(s), \theta(s), \lambda_1(s), \lambda_2(s), \lambda_3(s), \kappa(s)),
\end{array}
\tag{3.5}
$$

for almost every $s \in [0, 1]$ where the Hamiltonian *of (3.4) is given by*

$$
H : \mathbb{R}^3 \times \mathbb{R}^3 \times [-M, M] \to \mathbb{R}, \quad ((x, y, \theta), \lambda, \kappa) \mapsto \lambda_1 \cos\theta + \lambda_2 \sin\theta + \lambda_3 \kappa.
$$

(ii) *if dJ_{x_0, y_0} is not identically zero for all $(x(1), y(1))$ then $\lambda(s)$ is never zero in $[0, 1]$,*

(iii) *there exists a constant $c \in \mathbb{R}$ such that for almost every $s \in [0, 1]$*

$$
H((x(s), y(s), \theta(s)), \lambda(s), \kappa(s)) = \min_{v \in \mathcal{U}_M} H((x(s), y(s), \theta(s)), \lambda(s), v(s)) = c,
$$

(iv) *there exists a constant $\lambda_0 \geq 0$ such that the covector $(\lambda_0, \lambda_1(s), \lambda_2(s), \lambda_3(s))$ never vanishes in $[0, 1]$ and the following transversality conditions hold:*

$$
\begin{array}{rcl}
0 & = & 2\lambda_0(x(1) - x_0) - \lambda_1(1), \tag{3.6} \\
0 & = & 2\lambda_0(y(1) - y_0) - \lambda_2(1), \tag{3.7} \\
0 & = & \lambda_3(1). \tag{3.8}
\end{array}
$$

Applying Pontryagin's Maximum Principle we can collect a few essential properties of the optimal control problem (3.4) in the following lemma.

Lemma 3.2.8 *Suppose $(x(\cdot), y(\cdot), \theta(\cdot)) : [0, 1] \to \mathbb{R}^3$ is an optimal solution to (3.4) with $(x_0, y_0) \notin W$ and the corresponding optimal control $u(\cdot) \in \mathcal{U}_M$, $\lambda : [0, 1] \to \mathbb{R}^3$ as in Theorem 3.2.7 and $I \subset [0, 1]$ an open interval. Then there exists a constant $c \in \mathbb{R}$ such that*

(i) *$c = \lambda_1(s) \cos\theta(s) + \lambda_2(s) \sin\theta(s) + \lambda_3(s) \kappa(s)$ for almost every $s \in [0, 1]$.*

(ii) *$\kappa(s) = -M \; \mathrm{sign}\, \lambda_3(s)$, if $\lambda_3(s) \neq 0$.*

(iii) *$\lambda_3(\cdot) \in \mathcal{C}^1[0, 1]$ and, if there are no switching times in I, then $\lambda_3(\cdot)|_I \in \mathcal{C}^2$.*

(iv) *$(x(\cdot), y(\cdot))|_I$ is of type C, if $\lambda_3(s) \neq 0$ for all $s \in I$.*

(v) *$\lambda_1'(\cdot)_{[0,1]} \equiv \lambda_2'(\cdot)_{[0,1]} \equiv 0$ and $\lambda_3''(s) = -M^2 \lambda_3(s) + c\, M\, \kappa(s)$, if $\lambda_3(\cdot)_I \neq 0$.*

(vi) $\lambda_3(1) = 0$.

(vii) $2\lambda_0(x(1) - x_0) - \lambda_1 = 0$.

(viii) $2\lambda_0(y(1) - y_0) - \lambda_2 = 0$.

(ix) If $(x_0, y_0) \notin W$ *and* $\lambda_3(\cdot)_I \equiv 0$ *then* $(x(\cdot), y(\cdot))|_I$ *is of type L.*

Proof By Theorem 3.2.7, we have for almost every $s \in [0, 1]$

$$
\begin{aligned}
\lambda_1'(s) &= 0, \\
\lambda_2'(s) &= 0, \\
\lambda_3'(s) &= \lambda_1(s) \sin \theta(s) - \lambda_2(s) \cos \theta(s).
\end{aligned}
\tag{3.9}
$$

(i) and (ii) follow directly from Theorem 3.2.7 (iii), (iii) follows from (3.9). From (ii) it follows that $u(\cdot)|_I \equiv M$ or $u(\cdot)|_I \equiv -M$ and hence (iv). Furthermore, (3.1), (i) and (iii) yield

$$\lambda_3''(s) = (\lambda_1(s) \cos \theta(s) + \lambda_2(s) \sin \theta(s)) \kappa(s) = -M^2 \lambda_3(s) + c\,M\,\kappa(s)$$

for all $s \in I$ (the phase portrait is shown in Figure 3.1) and this proves the second
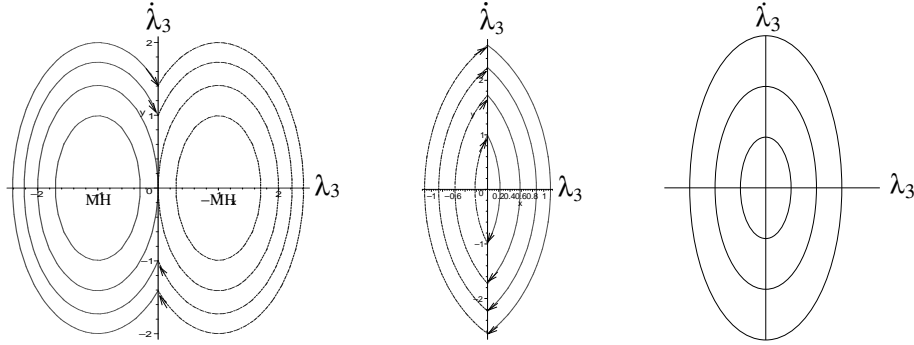
Figure 3.1: λ_3-λ_3'-phase portrait for $c < 0$, $c > 0$ and $c = 0$

part of (v). The first claim of (v) follows directly from (3.9). Moreover, (vi), (vii) and (viii) follow from (3.7). If $(x_0, y_0) \notin W$ then $\lambda_1 = \lambda_2 = 0$ is impossible since otherwise $\lambda_0 = 0$ because of (vii) and (viii) and $\lambda_3 \equiv 0$ because of (3.9) and (vi). Using this fact and substituting $\lambda_3'(\cdot)|_I \equiv 0$ into (2.5) yields that $\theta(\cdot)|_I$ has to be constant and thus $\kappa(\cdot)|_I \equiv 0$ and (ix) is shown. ∎

Definition 3.2.9 *The function* $\lambda_3 : [0, 1] \to \mathbb{R}$ *is called* switching function *(since changes of sign imply changes of control strategy). If* $\lambda_3(s_0) = 0$ *for some* $s_0 \in [0, 1]$ *and* $\lambda_3 \not\equiv 0$ *on every neighbourhood of* s_0, *then* s_0 *is called* switching parameter *or* switching time; *the corresponding* $(x(s_0), y(s_0), \theta(s_0))$ *is called* switching point. *An optimal solution is called* abnormal *if* $\lambda_0 = 0$ *and* normal *otherwise.*

Proposition 3.2.10 *The following properties hold.*

(i) *The optimal control to (3.4) for $(x_0, y_0) \notin W$ is piecewise constant and takes values in $\{-M, 0, M\}$.*

(ii) *If the optimal control takes only values in $\{-M, M\}$, then the distances between each two consecutive switching parameters and the distance between the last switching parameter and 1 are the same and not smaller than the first switching parameter.*

In other words: The shape of an optimal manipulator is a finite concatenation of C and L parts. If the shape is a concatenation of circular arcs only then the second until the last arc are of same length and not shorter than the first arc.

Proof In order to prove (i) we need to show that there are only finitely many switching points. By Lemma 3.2.8 (iii) $\lambda_3(\cdot)_{[0,1]}$ is continuous and thus the set $F := \{s \in [0,1] : \lambda_3(s) \neq 0\}$ is the union of open intervals. We will show that their number is finite. Let $I = (s_1, s_2) \in F$. Then either $s_1 = 0$ and/or $s_2 = 1$ (boundary interval, here $\lambda_3(s_2) = 0$ because of Lemma 3.2.8 (vi)) or $\lambda_3(s_1) = \lambda_3(s_2) = 0$ (interior interval). In F there are at most two boundary intervals and we assume that there are infinitely many interior intervals. On each interior interval I the function $\lambda_3(\cdot)$ has to satisfy the differential equation in Lemma 3.2.8 (v). If $c \leq 0$ then $s_2 - s_1 \geq \frac{\pi}{M}$ (see Figure 3.1) and this cannot be true for infinitely many intervals in $[0, 1]$. If $c > 0$ then $\lambda_3'(s_1) = -\lambda_3'(s_2) \neq 0$ and, by continuity arguments, all interior intervals are of same length (see also Figure 3.1). Again, this cannot be true for infinitely many intervals in $[0, 1]$ and we arrive at the desired contradiction. From Lemma 3.2.8 (iv) and (ix) the first part follows. Claim (ii) follows from Lemma 3.2.8 (v) since the phase curves in Figure 3.1 between two intersections with the axis $\lambda_3 = 0$ are always of same length. Furthermore, $\lambda_3(1) = 0$. ∎

Using geometric arguments we now determine the family of solutions $\mathcal{B}$ which is generated by the controls described in Theorem 3.2.11.

Theorem 3.2.11 *The optimal control $\kappa(\cdot)$ to (3.4) for $(x_0, y_0) \notin W$ is either $\kappa \equiv 0$ or*

$$\kappa(s) = \begin{cases} \pm M & : \quad 0 \leq s < s_0 \\ 0 & : \quad s_0 \leq s \leq 1 \end{cases}$$

if $\kappa \equiv 0$ on some interval $I \subset [0, 1]$ or

$$\kappa(s) = \begin{cases} \pm M & : \quad 0 \leq s < s_0 \\ \mp M & : \quad s_0 \leq s \leq 1 \end{cases}$$

with $s_0 \leq \frac{1}{2}$. In other words: The shape of a manipulator solving (3.4) for $(x_0, y_0) \notin W$ is of the type

(i) *CL or L, if the shape is partly of type L,*

(ii) *CC or C, if the shape is a concatenation of C parts only. In the CC case the first arc is not longer than the second.*

Remark 3.2.12 The set $P_\mathcal{B}$ is the union of the C^+L, C^-L, C^+C^- and the C^-C^+ loci (the latter two reduced to those with switching parameter $s_0 \leq \frac{1}{2}$), see Figure 3.2 for an illustration of the CL locus. Each locus is a parametrized curve in $\mathbb{R}^2$ with the switching time $s_0 \in [0,1]$ (or $s_0 \in [0, \frac{1}{2}]$) being the parameter, see (3.12). Since the parameter set is compact and the solution of the differential equation (3.1) depends continuously on the switching parameter (and so does the corresponding terminal point $(x(1), y(1))$) it follows that each of the four loci mentioned is compact and thus also $P_\mathcal{B}$. We finally have

$$\partial W = \operatorname{cl} P_\mathcal{G} \subset P_\mathcal{B}.$$

$\square$
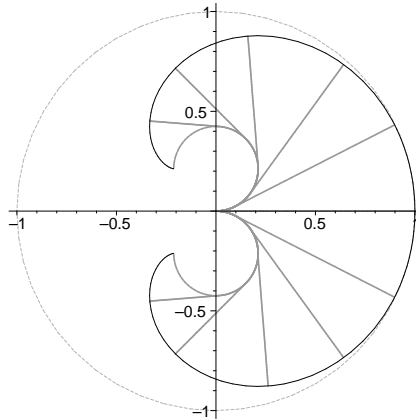
Figure 3.2: The CL locus with manipulators of type CL, $M = \frac{3\pi}{2}$

Remark 3.2.13 The workspaces W (in particular their boundaries ∂W) for different values of M can be visualized as depicted in Figure 3.3. $\square$

In order to prove Theorem 3.2.11 we first state a lemma which we prove in Section 3.3.

Lemma 3.2.14 *Concatenations of three or more circular arcs cannot be optimal for (3.4) with $(x_0, y_0) \notin W$.*

With the help of this result we can prove Theorem 3.2.11.
Proof [Theorem 3.2.11]
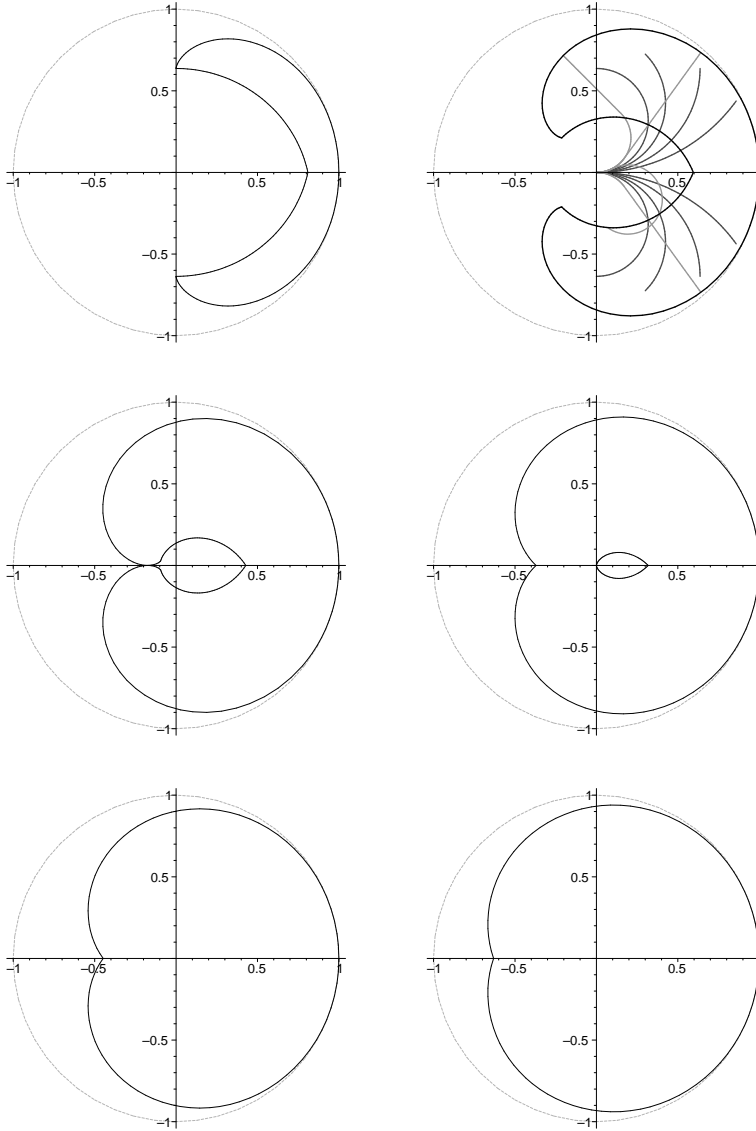
Figure 3.3: The workspaces with curvature bounds π, $3\pi/2$, $3\pi/2 + 1$, 2π, $2\pi + \arccos(23/27)$ and 3π. The top right picture also shows four optimal shapes of manipulators reaching ∂W and eight C^∞-manipulators reaching the interior.

(i) Let $0 \leq s_0 \leq s_1 < s_2 \leq s_3 \leq 1$ and suppose

$$\lambda_3(s) \begin{cases} \neq 0 & , \quad \text{for all } s \in (s_0, s_1) \\ = 0 & , \quad \text{for all } s \in [s_1, s_2] \\ \neq 0 & , \quad \text{for all } s \in (s_2, s_3). \end{cases}$$

Then by Lemma 3.2.8 (vi), $(x(\cdot), y(\cdot))|_{[s_1, s_2]}$ is of type L. We show that if $c \geq 0$ then $s_0 = s_1 = 0$, $s_2 = s_3 = 1$ and $(x(\cdot), y(\cdot))|_{[0,1]}$ is of type L. If $c < 0$ then $s_1 < \frac{2\pi}{M}$, $s_2 = s_3 = 1$ and $(x(\cdot), y(\cdot))|_{[0,1]}$ is of type CL.

If $c \geq 0$ then by assumption $\lambda_3(s_1) = \lambda_3'(s_1) = \lambda_3(s_2) = \lambda_3'(s_2) = 0$. Thus, by Lemma 3.2.8 (ii) and (v), we get $\lambda_3(\cdot)|_{(s_0,s_1)} \equiv \lambda_3(\cdot)|_{(s_2,s_3)} \equiv 0$, see also Figure 3.1. Therefore, both intervals (s_0, s_1) and (s_2, s_3) have to be empty and we have proved the claim for $c \geq 0$.

Now consider $c < 0$. First assume that $s_2 < 1$. Since by Lemma 3.2.8 (vii) $\lambda_3(1) = 0$, we may increase the value of s_3 such that $\lambda_3(s_3) = 0$. On the interval (s_2, s_3), the solution of the differential equation in Lemma 3.2.8 (v) is given by $\lambda_3(s) = A \sin(M s + \varphi) + c$ or $\lambda_3(s) = A \sin(M s + \varphi) - c$ for some suitable constants A and φ. From $\lambda_3(s_2) = \lambda_3'(s_2) = 0 = \lambda_3(s_3)$ and the special form of the solution it follows immediately that both s_2 and s_3 are local extrema of λ_3 of the same type, $\lambda_3'(s_3) = 0$ and $s_3 - s_2 = 2\pi$, see also Figure 3.1. Therefore, $(x(\cdot), y(\cdot))|_{[s_2,s_3]}$ is a full circle which can be shifted to the origin without changing $(x(1), y(1))$. This can be repeated until $s_2 = s_3 = 1$. On the other hand, by analogous arguments, it can be shown that the value of s_0 can be decreased to $s_0 = 0$ such that $\lambda_3(\cdot)|_{[s_0,s_1)} \neq 0$, $s_1 < \frac{2\pi}{M}$ and the claim follows.

(ii) If the shape of the manipulator is a finite concatenation of C parts, then it is of type CC or C due to Lemma 3.2.14. By Proposition 3.2.10 the first arc cannot be longer than the second and we are done.

$\blacksquare$

Remark 3.2.15 The problem of finding the workspace if the initial direction is free and the terminal direction is prescribed to be that of the positive x-axis is dual to the problem above and gives exactly the same workspaces. For different terminal directions θ_1 the workspaces are just rotations around the origin by the angle θ_1 of the workspaces in Figure 3.3. $\square$

3.2.2 The workspaces with prescribed terminal direction

Similarily to the previous section we have the following result.

Proposition 3.2.16 W_{θ_1} *is compact for every* $\theta_1 \in (-\pi, \pi]$.

Proof The proof works exactly the same way as the proof of Proposition 3.2.4.

$\blacksquare$

In order to determine the boundary of W_{θ_1} we consider (3.4) again and minimize over all $(x(\cdot), y(\cdot), \theta(\cdot)) \in \mathcal{F}$ such that $(x(1), y(1)) \in W_{\theta_1}$. Analogously to the previous section we determine a family of functions containing the optimal solutions which is sufficiently small to determine the workspace W_{θ_1}.

The result of Proposition 3.2.10 is also valid here and optimal solutions are finite concatenations of C and L parts. The main result is quite similar to Theorem 3.2.11.

Theorem 3.2.17 *Every point on the boundary of the workspace W_{θ_1} of the manipulator described by system (3.1) and prescribed terminal direction $\theta(1) = \theta_1$ mod 2π can be reached by a manipulator of the types CLC, CCC and their subtypes (CL, LC, CC, L or C).*

Remark 3.2.18 The workspaces for different values of M and the terminal direction θ_1 can be visualized as depicted in Figures 3.4 and 3.5. $\quad\square$
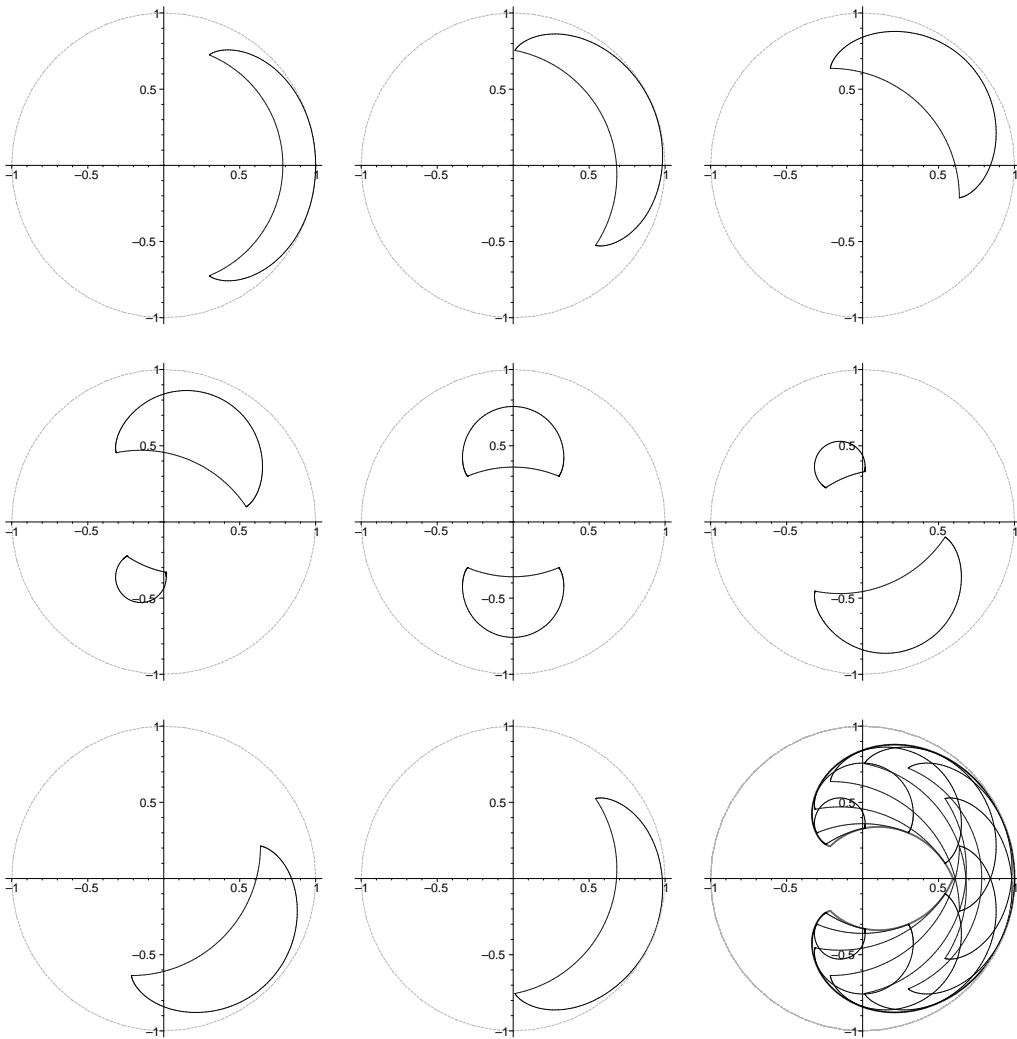
Figure 3.4: The workspaces with curvature bound $M = 3\pi/2$, terminal directions $k\pi/4$, $k = 0, \ldots, 7$, and their union

In order to prove Theorem 3.2.17 we need the following lemma which will be proved in Section 3.3.
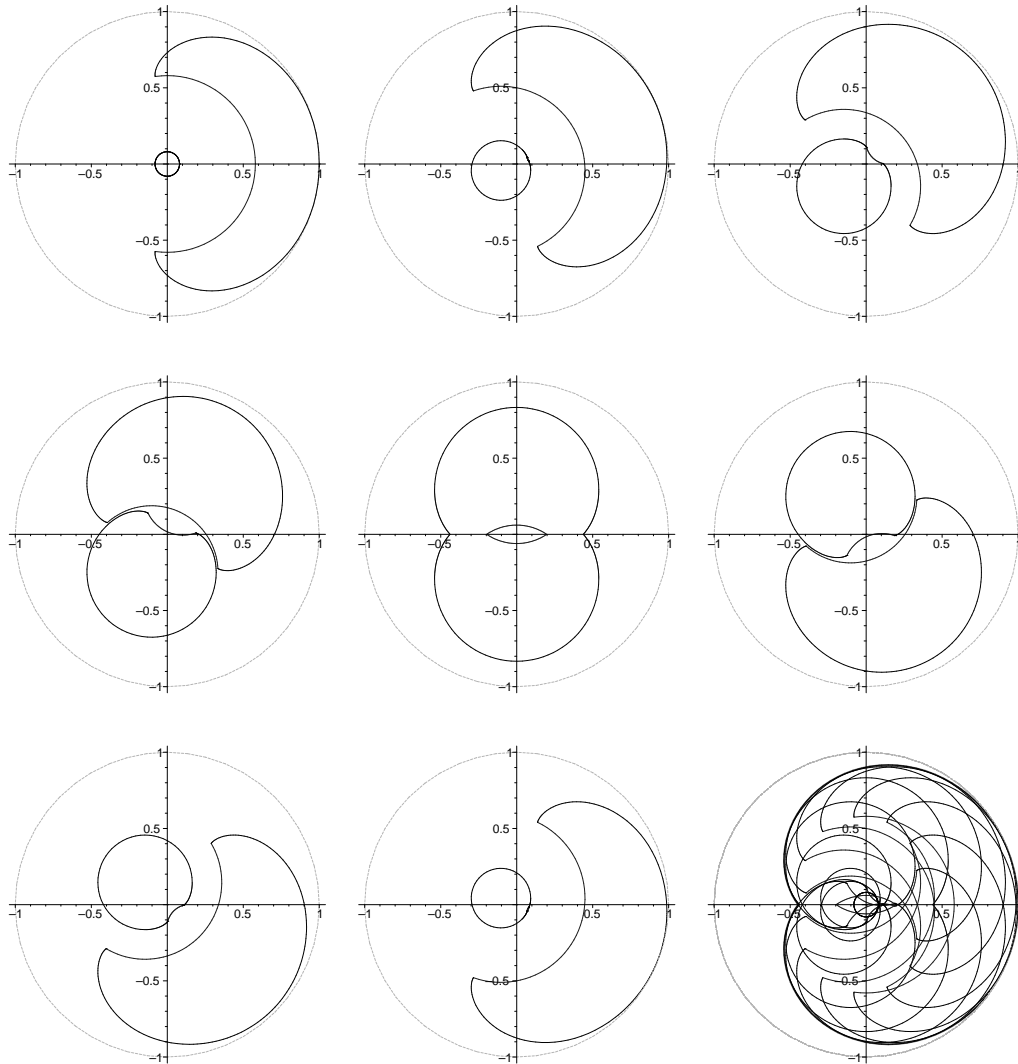
Figure 3.5: The workspaces with curvature bound $M = 2\pi + \arccos(23/27)$ and terminal directions $\nu\pi/4$, $\nu = 0, \ldots, 7$, and comparison with the workspace of the manipulator with free terminal direction (cf. Figure 3.3)

Lemma 3.2.19 *Concatenations of four or more circular arcs cannot be optimal for (3.4) with prescribed terminal direction θ_1 and $(x_0, y_0) \notin W$.*

With this result at hand we can easily prove Theorem 3.2.17.

Proof [of Theorem 3.2.17] The proof works similar to the proof of Theorem 3.2.11, just the transversality condition $\lambda_3(1) = 0$ (Lemma 3.2.8 (vi)) drops here. Therefore, if a straight line segment occurs, we are limited to CLC shapes. From Lemma 3.2.19 we know that concatenations of four or more circular arcs cannot

be optimal and we are done.   ■

Remark 3.2.20 The interior of the workspaces can even be reached by C^2- or C^∞-manipulators.   ☐

3.3   Technical proofs

In this section we present all the missing technical proofs.

3.3.1   Proofs of Section 3.2.1

First we need a few more results to prove the main lemma. We introduce some

$$C_b \quad \text{circle of radius } b = \frac{2\sqrt{2}}{M}\sqrt{1 - \cos\frac{M}{2}} \text{ around the origin}$$

further notation: C_1 circle of radius $\frac{1}{M}$ around $(0, \frac{1}{M})$

$$C_2 \quad \text{circle of radius } \frac{1}{M} \text{ around } (0, -\frac{1}{M})$$

Lemma 3.3.1 *Let $M \in (0, 3\pi)$. Then the end-effectors of manipulators of the CC type lie inside C_b and the end-effectors of manipulators of the $C\cdots C$ type (more than two circular arcs) lie outside C_b.*

Proof   Because of symmetry we just consider manipulators of the $C^+C^-\cdots$ type with n switchings here. Since by Proposition 3.2.10 the second until the last arc are of same length, it is easy to compute that the distance between two switching parameters is $\Delta s = \frac{1-s_0}{n}$ with s_0 being the first switching parameter. Therefore, the coordinates of the terminal point $(x_n^{s_0}(1), y_n^{s_0}(1))$ of a concatenation of $n \in \mathbb{N}$ circular arcs depend on the first switching parameter s_0, the curvature bound M and the number of switchings n only. On the interval $[0, s_0]$ we have $\theta(\sigma) = M\sigma$ and

$$x(s_0) - x(0) = \int_0^{s_0} \cos M\sigma d\sigma = \frac{1}{M}\sin Ms_0,$$

on the interval $[s_0, s_0 + \Delta s]$ we have $\theta(\sigma) = M(2s_0 - \sigma)$ (on all further intervals we similarly get the same values since the intervals are all of same length) and

$$x(s_0 + \Delta s) - x(s_0) = \int_0^{\Delta s} \cos M(s_0 - \sigma)d\sigma = \frac{1}{M}\sin Ms_0 - \frac{1}{M}\sin M(s_0 - \Delta s).$$

Equivalent results hold for the y values and by simple addition we get

$$x_n^{s_0}(1) = \frac{1}{M}\left[(n+1)\sin Ms_0 - n\sin\frac{(n+1)Ms_0 - M}{n}\right], \qquad (3.10)$$

$$y_n^{s_0}(1) = \frac{1}{M}\left[1 - (n+1)\cos Ms_0 + n\cos\frac{(n+1)Ms_0 - M}{n}\right]. \qquad (3.11)$$

The distance of the end-effector from the origin is

$$
\begin{aligned}
D_n^{s_0}(1) \;=\;& \frac{1}{M}\Big[(n+1)^2 + 1 + n^2 - 2(n+1)\cos Ms_0 - \\
& - 2n(n+1)\cos\left(\frac{Ms_0 - M}{n}\right) + 2n\cos\left(\frac{(n+1)Ms_0 - M}{n}\right)\Big]^{\frac{1}{2}}.
\end{aligned}
$$

The first arc is at most as long as the others, that gives $s_0 \leq \frac{1}{n+1}$. Now consider the CC shapes first, i.e., $n = 1$. If $M \in (\pi, 3\pi)$, we have

$$
\begin{aligned}
(D_1^{s_0}(1))^2 \;=\;& \frac{1}{M^2}\left[6 - 4\cos Ms_0 - 4\cos(Ms_0 - M) + 2\cos(2Ms_0 - M)\right] \leq \\
\leq\;& \frac{1}{M^2}\left[8 - 4\cos Ms_0 - 4\cos(Ms_0 - M)\right] \leq \frac{8}{M^2}\left(1 - \cos\frac{M}{2}\right)
\end{aligned}
$$

since it is easy to check that $[-\cos Ms_0 - \cos(Ms_0 - M)]$ takes its maximum on the interval $[0, \frac{1}{2}]$ at $s_0 = \frac{1}{2}$. Actually, $(D_1^{\frac{1}{2}}(1))^2 = \frac{8}{M^2}\left(1 - \cos\frac{M}{2}\right)$. If $M \in (0, \pi]$, we have the following:

$$
\begin{aligned}
M^2\frac{\partial}{\partial s_0}(D_1^{s_0}(1))^2 \;=\;& 4M\sin Ms_0 + 4M\sin(Ms_0 - M) - 4M\sin(2Ms_0 - M) = \\
=\;& -16M\sin\left(\frac{2Ms_0 - M}{2}\right)\sin(Ms_0)\sin(M - Ms_0) \geq 0
\end{aligned}
$$

for $s_0 \in [0, \frac{1}{2}]$. Consequently, the maximum on this interval is at $s_0 = \frac{1}{2}$. Finally, we have for all $M \in (0, 3\pi)$:

$$
(D_1^{s_0}(1))^2 \leq \left(D_1^{\frac{1}{2}}(1)\right)^2 = \frac{8}{M^2}\left(1 - \cos\frac{M}{2}\right) \quad \text{for } s_0 \in \left[0, \frac{1}{2}\right].
$$

Therefore, we have an upper bound of the distances of end-effectors of the CC locus to the origin depending on M only. Now we show that this is also a lower bound for the distances of end-effectors of strategies with more than two circular arcs by showing that $(D_n^0(1))^2 \geq \frac{8}{M^2}\left(1 - \cos\frac{M}{2}\right)$ for all $n \geq 2$ and that $(D_n^{s_0}(1))^2$ is monotonously increasing with $s_0 \in [0, \frac{1}{n+1}]$ for all $n \geq 2$. We have

$$
(D_n^0(1))^2 \;=\; \frac{2n^2}{M^2}\left(1 - \cos\frac{M}{n}\right)
$$

and this is monotonically increasing with growing $n \geq 2$. To prove that we consider $(D_n^0(1))^2$ as a function of $n \in \mathbb{R}$, differentiate with respect to n and get

$$
\frac{\partial(D_n^0(1))^2}{\partial n} \;=\; \frac{2n}{M^2}\left[2\left(1 - \cos\frac{M}{n}\right) - \frac{M}{n}\sin\frac{M}{n}\right] \geq 0
$$

as long as $\frac{M}{n} \leq 2\pi$ and this is the case for the considered values of M and n. Futhermore,

$$
\begin{aligned}
\frac{\partial}{\partial s_0}(D_n^{s_0}(1))^2 &= \frac{1}{M^2}\left[2M(n+1)\sin Ms_0 + 2M(n+1)\sin\left(\frac{Ms_0 - M}{n}\right) - \right. \\
&\quad\left. -2M(n+1)\sin\left(\frac{(n+1)Ms_0 - M}{n}\right)\right] = \\
&= -\frac{8(n+1)}{M}\sin\left(\frac{(n+1)Ms_0 - M}{2n}\right)\sin\left(\frac{Ms_0}{2}\right)\cdot \\
&\quad\cdot\sin\left(\frac{M(1-s_0)}{2n}\right)
\end{aligned}
$$

and this is not negative for all $n \geq 2$ and $s_0 \in [0, \frac{1}{n+1}]$ since we have

$$
\frac{(n+1)Ms_0 - M}{2n} \in \left[-\frac{3\pi}{4}, 0\right], \quad \frac{Ms_0}{2} \in \left(0, \frac{\pi}{2}\right) \quad \text{and} \quad \frac{M(1-s_0)}{2n} \in \left[0, \frac{3\pi}{4}\right]
$$

and therefore

$$
\sin\left(\frac{(n+1)Ms_0 - M}{2n}\right) \leq 0, \quad \sin\left(\frac{Ms_0}{2}\right) \geq 0 \quad \text{and} \quad \sin\left(\frac{M(1-s_0)}{2n}\right) \geq 0.
$$

This finally gives us

$$
(D_1^{s_0}(1))^2 \leq \left(D_1^{\frac{1}{2}}(1)\right)^2 = \frac{8}{M^2}\left(1 - \cos\frac{M}{2}\right) \leq (D_n^0(1))^2 \leq (D_n^{s_0}(1))^2
$$

for all $n \geq 2$, $s_0 \in \left[0, \frac{1}{n+1}\right]$ and $M \in [0, 3\pi)$ and the upper bound for the CC locus is actually a lower bound for the end-effectors of the strategies with concatenations of more than two circular arcs. ∎

Lemma 3.3.2 *Let $M \in (0, 3\pi)$. Then the end-effectors of manipulators consisting of concatenations of more than two circular arcs lie between C_b and the CL locus (we denote this set by G).*

Proof If $M \leq \pi$, C_b may not contain C_1 and C_2, but the manipulator cannot reach inside C_1 and C_2 by Remark 2.2.9. If $3\pi > M > \pi$, C_b contains C_1 and C_2 since $\frac{8}{M^2}\left(1 - \cos\frac{M}{2}\right) \geq \frac{4}{M^2}$ and end-effectors of concatenations of more than two circular arcs always lie outside C_1 and C_2. Now we assume that one of these end-effectors lies outside C_b and outside G. Since it necessarily lies outside C_1 and C_2, the shortest manipulator reaching this point would have to be of the CL type by Theorem 2.2.8 and longer than 1 (either the C part of the shortest manipulator reaching that point (P_1 in Figure 3.6) is already longer than 1 or the L part crosses the CL locus (P_2 in Figure 3.6)) which gives a contradiction to $L = 1$. Therefore, the end-effectors of the manipulators considered lie in set G. ∎
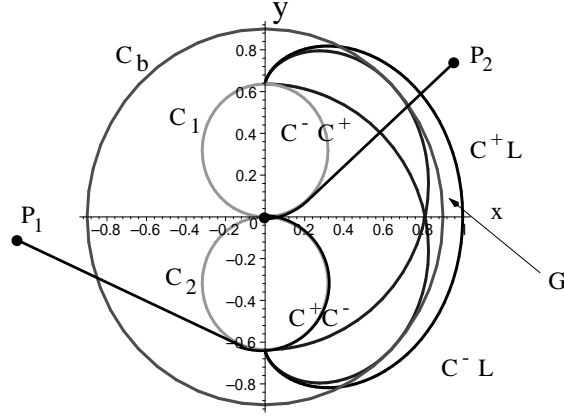
Figure 3.6: The manipulator cannot reach outside set G, here $M = \pi$

Lemma 3.3.3 *The set between the CL locus and the CC loci can be reached by the manipulator.*

Proof The C^-C^+ locus can be continuously deformed to the CL locus via the following C^-C^+L loci depending on the parameter $\alpha \in [0, 1]$:

$$\tilde{x}_1(s_0, \alpha) = \frac{2}{M} \sin(Ms_0(1-\alpha)) + \frac{1}{M} \sin(M(1-2s_0) + 2\alpha s_0 \cos(M(1-2s_0))),$$

$$\tilde{y}_1(s_0, \alpha) = \frac{1}{M}(-1 + 2\cos(Ms_0(1-\alpha))) - \frac{1}{M} \cos(M(1-2s_0)) +$$
$$+ 2\alpha s_0 \sin(M(1-2s_0))$$

for all $s_0 \in [0, \frac{1}{2}]$ and

$$\tilde{x}_2(s_0, \alpha) = \frac{2}{M} \sin(M(s_0 + \alpha(s_0 - 1))) + \frac{1}{M} \sin(M(1-2s_0) +$$
$$2\alpha(1-s_0) \cos(M(1-2s_0)),$$

$$\tilde{y}_2(s_0, \alpha) = \frac{1}{M}(-1 + 2\cos(M(s_0 + \alpha(s_0 - 1)))) - \frac{1}{M} \cos(M(1-2s_0)) +$$
$$+ 2\alpha(1-s_0) \sin(M(1-2s_0))$$

for all $s_0 \in [\frac{1}{2}, 1]$. Analogously, the C^+C^- locus can be continuously deformed to the CL locus via C^+C^-L loci. Therefore, all interior points between the strategies mentioned above (and obviously also the set G) can be reached, see Figure 3.7. ∎

Now we can prove the lemma needed in Section 3.2.1

Figure 3.7: Every point between the CC and the CL locus can be reached, here $M = \frac{3\pi}{2}$

Lemma 3.2.14 *Concatenations of three or more circular arcs cannot be optimal for (3.4) with $(x_0, y_0) \notin W$.*
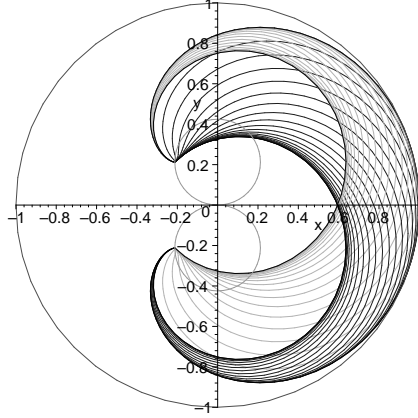
Proof   We first assume $M \in (0, 3\pi)$. Later we will show that only manipulators of the CL type can be optimal for larger M.

In Lemma 3.3.1 we saw that the end-effectors of manipulators of the CC type lie inside C_b and the end-effectors of manipulators of the C$\cdots$C type (more than two circular arcs) lie outside this circle. From Lemma 3.3.2 we know that the end-effectors of concatenations of more than two circular arcs lie between C_b and the CL locus (set G). The C^+C^-, C^-C^+, C^+L and the C^-L loci are parametrized curves with the switching point $s_0 \in [0, 1]$ being the parameter:

$$
\begin{aligned}
x_2^{s_0} &= \frac{2 \sin M s_0}{M} - \frac{\sin(2M s_0 - M)}{M}, \\
y_2^{s_0} &= \pm \frac{(1 - 2\cos M s_0)}{M} \pm \frac{\cos(2M s_0 - M)}{M}, \\
x_{C^\pm L}^{s_0} &= \frac{\sin M s_0}{M} + (1 - s_0)\cos M s_0, \\
y_{C^\pm L}^{s_0} &= \pm\frac{1 - \cos M s_0}{M} \pm (1 - s_0)\sin M s_0.
\end{aligned}
\tag{3.12}
$$

In Lemma 3.3.3 it was shown that the set bounded by the CL locus and the CC loci can be reached and the C$\cdots$C loci lie inside this set. Therefore, the C$\cdots$C strategy cannot be better than the CC or CL strategy for the problem (3.4) by Lemma 3.2.6

Now we will describe the workspaces. The loci given by (3.12) depend continuously on the bound M of the curvature. As M tends to zero, the workspace contracts to the point $(1, 0)$. For different M and free terminal direction, the

workspaces are connected, the boundaries in the upper (lower) half plane are given by C^+L and C^-C^+ (C^-L and C^+C^-) loci and look as in Figure 3.3. The following geometric arguments can be found in [16] and we will just state them here. If $M < \frac{3\pi}{2} + 1$, the reachability set is simply connected. The set grows continuously and for $M = \frac{3\pi}{2} + 1$ the C$^+$L and the C$^-$L locus touch each other. If $\frac{3\pi}{2} + 1 \le M < 2\pi + \arccos(23/27)$ (this value occurs when the two cardioids described by the first two equations of (3.12) touch the x-axis) the workspace has a 'hole' which is bounded by the CC loci and the CL locus as $\frac{3\pi}{2} + 1 \le M < 2\pi$ and by CC loci only as $2\pi \le M < 2\pi + \arccos(23/27)$. If $M > 2\pi + \arccos(23/27)$ (and this also covers the case $M \ge 3\pi$), the workspace is simply connected again and the CC strategies can reach interior points only which is also true for concatenations of more than two circular arcs using the same arguments as above and Theorem 2.2.8. As M tends to infinity, the boundary of the workspace obviously tends to a circle of radius 1 around the origin. $\blacksquare$

3.3.2 Proofs of Section 3.2.2

In order to prove the main result we need a two more lemmas.

Lemma 3.3.4 *The end-effector of a manipulator of the $C^+C^-C^+$ type or of the $C^-C^+C^-$ type lies on the circle of radius*

$$\frac{4}{M}\left|\sin\left(\frac{M + 2k\pi - \theta_1}{4}\right)\right| \quad around \quad \left(\frac{1}{M}\sin\theta_1, \frac{1}{M}(1 - \cos\theta_1)\right)$$

or on the circle of radius

$$\frac{4}{M}\left|\sin\left(\frac{M + 2k\pi + \theta_1}{4}\right)\right| \quad around \quad \left(-\frac{1}{M}\sin\theta_1, -\frac{1}{M}(1 - \cos\theta_1)\right),$$

respectively.

Proof First we determine the possible coordinates of the end-effectors of the $C^+C^-C^+$ strategy. We denote with s_1 the parameter of the first switching point, with s_2 the distance between the first and the second switching parameter and with s_3 the distance between the second switching parameter and 1. The terminal angle is $\theta(1) = \theta_1 - 2k\pi$ for some $k \in \mathbb{Z}$ ($|k|$ is the number of additional 2π turns and the sign $+/-$ tells if turning clockwise/anticlockwise). The possible values of k depend on M. Later we will consider $M \in [0, 3\pi]$ and for these values of M the only values k can take are $0, \pm 1$. The following equations hold:

$$s_1 + s_2 + s_3 = 1,$$
$$M(s_1 - s_2 + s_3) = \theta_1 - 2k\pi.$$

With these equations we can eliminate s_2 and s_3 and get

$$\sigma \in [0, s_1] \quad \Rightarrow \quad \theta(\sigma) = M\sigma,$$
$$\sigma \in [s_1, s_1 + s_2] \quad \Rightarrow \quad \theta(\sigma) = M(2s_1 - \sigma) \text{ and}$$
$$\sigma \in [s_1 + s_2, 1] \quad \Rightarrow \quad \theta(\sigma) = M(-2s_2 + \sigma).$$

Now we can simply integrate and get for $s_1 \in [0, 1]$

$$x(s_1) - x(0) \quad = \quad \int_0^{s_1} \cos M\sigma d\sigma = \frac{1}{M} \sin Ms_1,$$

and for every $s_2 \in [0, 1 - s_1]$

$$x(s_1 + s_2) - x(s_1) \quad = \quad \int_0^{s_2} \cos M(s_1 - \sigma) d\sigma =$$
$$= \quad \frac{1}{M} \sin Ms_1 - \frac{1}{M} \sin\left(Ms_1 - \frac{M - \theta_1 + 2k\pi}{2}\right),$$
$$x(1) - x(s_1 + s_2) \quad = \quad \int_0^{s_3} \cos M(s_1 - s_2 + \sigma) d\sigma =$$
$$= \quad \frac{1}{M} \sin \theta_1 - \frac{1}{M} \sin\left(Ms_1 - \frac{M - \theta_1 + 2k\pi}{2}\right).$$

The y-values can be computed similarily. The coordinates of the end-effectors depend on the parameter of the first switching point only and look as

$$x_{3+}^{s_1} \quad = \quad \frac{1}{M}\left[2\sin Ms_1 + 2\sin\left(\frac{M + 2k\pi - \theta_1}{2} - Ms_1\right) + \sin \theta_1\right],$$
$$y_{3+}^{s_1} \quad = \quad \frac{1}{M}\left[1 - 2\cos Ms_1 + 2\cos\left(\frac{M + 2k\pi - \theta_1}{2} - Ms_1\right) - \cos \theta_1\right]$$

for some $k \in \mathbb{Z}$. They lie on a circle, since

$$x_{3+}^{s_1} - \frac{1}{M}\sin \theta_1 \quad = \quad \frac{4}{M} \sin\left(\frac{M + 2k\pi - \theta_1}{4}\right) \cos\left(Ms_1 - \frac{M + 2k\pi - \theta_1}{4}\right),$$
$$y_{3+}^{s_1} - \frac{1}{M}(1 - \cos \theta_1) \quad = \quad -\frac{4}{M} \sin\left(\frac{M + 2k\pi - \theta_1}{4}\right) \sin\left(Ms_1 - \frac{M + 2k\pi - \theta_1}{4}\right)$$

and

$$\left(x_{3+}^{s_1} - \frac{\sin \theta_1}{M}\right)^2 + \left(y_{3+}^{s_1} - \frac{1 - \cos \theta_1}{M}\right)^2 = \frac{16}{M^2} \sin^2\left(\frac{M + 2k\pi - \theta_1}{4}\right).$$

Analogously, the possible coordinates of the end-effectors of the $C^-C^+C^-$ strategy look as

$$x_{3-}^{s_1} = \frac{1}{M}\left[2\sin Ms_1 + 2\sin\left(\frac{M+2k\pi+\theta_1}{2} - Ms_1\right) - \sin\theta_1\right],$$

$$y_{3-}^{s_1} = \frac{1}{M}\left[-1 + 2\cos Ms_1 - 2\cos\left(\frac{M+2k\pi+\theta_1}{2} - Ms_1\right) + \cos\theta_1\right]$$

for some $k \in \mathbb{Z}$. They also lie on a circle, since

$$\left(x_{3-}^{s_1} + \frac{\sin\theta_1}{M}\right)^2 + \left(y_{3-}^{s_1} + \frac{1-\cos\theta_1}{M}\right)^2 = \frac{16}{M^2}\sin^2\left(\frac{M+2k\pi+\theta_1}{4}\right).$$

∎

Lemma 3.3.5 *Manipulators of the $C\cdots C$ type (with more than three circular arcs) can only reach outside the circles that can be reached by the manipulators of the CCC type.*

Proof In order to determine the possible coordinates of the end-effectors of the strategies with $2m$ arcs, $m \in \mathbb{N}$, we need the fact that the second until the $2m-1$st arc are of same length. We denote the difference between two switching parameters with Δs, the first switching parameter with s_1 and the difference between the last parameter and 1 with s_e. We have

$$s_1 + 2(m-1)\Delta s + s_e = 1$$
$$\pm M(s_1 - s_e) = \theta_1 - 2k\pi$$

for some $k \in \mathbb{Z}$. With these equations we can, again, eliminate Δs and s_e. Therefore, the end-effectors depend on the first switching point s_1 only and after integration like in the CCC case they look as

$$x_{2m,\pm}^{s_1} = \frac{1}{M}\left[2m\sin Ms_1 + 2(m-1)\sin\left(\frac{M+2k\pi\pm\theta_1-2mMs_1}{2(m-1)}\right) \mp \sin\theta_1\right],$$

$$y_{2m,\pm}^{s_1} = \pm\frac{1}{M}\left[1 - 2m\cos Ms_1 + 2(m-1)\cos\left(\frac{M+2k\pi\pm\theta_1-2mMs_1}{2(m-1)}\right)\right.$$
$$\left. + \cos\theta_1\right].$$

With the same notation as above for the strategy with $2m+1$ arcs we have

$$s_1 + (2m-1)\Delta s + s_e = 1$$
$$\pm M(s_1 - \Delta s + s_e) = \theta_1 - 2k\pi$$

for some $k \in \mathbb{Z}$ and the coordinates of the end-effectors of the $C^+ C^- \cdots C^+$ and the $C^- C^+ \cdots C^-$ strategy with $2m + 1$ arcs look as

$$x_{2m+1,\pm}^{s_1} = \frac{1}{M} \left[2m \sin M s_1 + 2m \sin \left(\frac{M + 2k\pi \mp \theta_1}{2m} - M s_1 \right) \pm \sin \theta_1 \right],$$

$$y_{2m+1,\pm}^{s_1} = \pm \frac{1}{M} \left[1 - 2m \cos M s_1 + 2m \cos \left(\frac{M + 2k\pi \mp \theta_1}{2m} - M s_1 \right) - \cos \theta_1 \right],$$

for some $k \in \mathbb{Z}$. From the equations above we get

$$x_{2m,\pm}^{s_1}(\theta_1) = x_{2m,\mp}^{s_1}(-\theta_1),$$
$$y_{2m,\pm}^{s_1}(\theta_1) = -y_{2m,\mp}^{s_1}(-\theta_1)$$

and the same is true in the odd case. Because of this symmetry with respect to the x-axis we only need to consider terminal directions $\theta_1 \in [0, \pi]$ instead of $(-\pi, \pi]$. Now we show that the manipulators with concatenations of more than three circular arcs can only reach outside the circles reached by manipulators of the CCC shape. We furthermore introduce the following notation (distances of the end-effectors of the manipulators with concatenations of more than three circular arcs from the centers of the corresponding circles of the CCC loci with $k = 0$ up to the factor M) for an even number of circular arcs:

$$A_{2m}^+(s_1) := (M x_{2m,+}^{s_1} + \sin \theta_1)^2 + (M y_{2m,+}^{s_1} + 1 - \cos \theta_1)^2 =$$

$$= 8 \left[(m^2 - m + 1) - m(m - 1) \cos \left(\frac{2M s_1 - (M + \theta_1)}{2(m - 1)} \right) - \right.$$

$$\left. - m \cos M s_1 + (m - 1) \cos \left(\frac{2m M s_1 - (M + \theta_1)}{2(m - 1)} \right) \right]$$

and

$$A_{2m}^-(s_1) := \left[(M x_{2m,-}^{s_1} + \sin \theta_1)^2 + (M y_{2m,-}^{s_1} + 1 - \cos \theta_1)^2 \right] =$$

$$= 8 \left[(m^2 - m + 1) - m(m - 1) \cos \left(\frac{2M s_1 - M + \theta_1}{2(m - 1)} \right) - \right.$$

$$\left. - m \cos(M s_1 + \theta_1) + (m - 1) \cos \left(\frac{2m M s_1 - M + (2m - 1)\theta_1}{2(m - 1)} \right) \right],$$

and for an odd number of circular arcs:

$$A_{2m+1}^+(s_1) := \left[(M x_{2m+1,+}^{s_1} - \sin \theta_1)^2 + (M y_{2m+1,+}^{s_1} - 1 + \cos \theta_1)^2 \right] =$$

$$= 16 m^2 \sin^2 \left(\frac{M - \theta_1}{4m} \right) > 16 \sin^2 \left(\frac{M - \theta_1}{4} \right),$$

$$A_{2m+1}^-(s_1) := \left[(M x_{2m+1,-}^{s_1} + \sin \theta_1)^2 + (M y_{2m+1,-}^{s_1} + 1 - \cos \theta_1)^2 \right] =$$

$$= 16 m^2 \sin^2 \left(\frac{M + \theta_1}{4m} \right) > 16 \sin^2 \left(\frac{M + \theta_1}{4} \right)$$

for $M \in (0, 3\pi]$, $\theta_1 \in [0, \pi]$ and $m \geq 2$. Therefore, the odd cases are done. Since

$$
\begin{aligned}
\left(A_{2m}^+(s_1)\right)' &= 8Mm \left[\sin\left(\frac{2Ms_1 - (M + \theta_1)}{2(m-1)} \right) + \sin Ms_1 - \right. \\
&\quad \left. - \sin\left(\frac{2mMs_1 - (M + \theta_1)}{2(m-1)} \right) \right] = \\
&= 32Mm \sin\left(\frac{2Mms_1 - (M + \theta_1)}{4(m-1)} \right) \sin\left(\frac{2Ms_1 - (M + \theta_1)}{4(m-1)} \right) \cdot \\
&\quad \cdot \sin \frac{Ms_1}{2}
\end{aligned}
$$

on the one hand and

$$
\begin{aligned}
\left(A_{2m}^-(s_1)\right)' &= 8Mm \left[\sin\left(\frac{2Ms_1 - M + \theta_1}{2(m-1)} \right) + \sin(Ms_1 + \theta_1) - \right. \\
&\quad \left. - \sin\left(\frac{2mMs_1 - M + (2m-1)\theta_1}{2(m-1)} \right) \right] = \\
&= 32Mm \sin\left(\frac{2Ms_1 - M + \theta_1}{4(m-1)} \right) \sin\left(\frac{2Mms_1 - M + (2m-1)\theta_1}{4(m-1)} \right) \cdot \\
&\quad \cdot \sin \frac{Ms_1 + \theta_1}{2}
\end{aligned}
$$

on the other hand, the extrema of $A_{2m}^+(s_1)$ are at

$$
s_{1,1}^+ = 0 + \frac{2l\pi}{M}, \quad s_{1,2}^+ = \frac{M + \theta_1}{2M} + \frac{2(m-1)l\pi}{M} \quad \text{and} \quad s_{1,3}^+ = \frac{M + \theta_1}{2mM} + \frac{2(m-1)l\pi}{mM},
$$

the extrema of $A_{2m}^-(s_1)$ are at

$$
\begin{aligned}
s_{1,1}^- &= -\frac{\theta_1}{M} + \frac{2l\pi}{M}, \quad s_{1,2}^- = \frac{M - \theta_1}{2M} + \frac{2(m-1)l\pi}{M} \quad \text{and} \\
s_{1,3}^- &= \frac{M - (2m-1)\theta_1}{2mM} + \frac{2(m-1)l\pi}{mM}
\end{aligned}
$$

for $l \in \mathbb{Z}$. Evaluating the functions at the extremal points (with $l = 0, 1$), we

get:

$$A_{2m}^+(0) = 16(m-1)^2 \sin^2\left(\frac{M+\theta_1}{4(m-1)}\right),$$

$$A_{2m}^+\left(\frac{2\pi}{M}\right) = 16(m-1)^2 \sin^2\left(\frac{M+\theta_1}{4(m-1)} - \frac{\pi}{m-1}\right),$$

$$A_{2m}^+\left(\frac{M+\theta_1}{2M}\right) = 16 \sin^2\left(\frac{M+\theta_1}{4}\right),$$

$$A_{2m}^+\left(\frac{M+\theta_1}{2M} + \frac{2(m-1)\pi}{M}\right) = 16 \sin^2\left(\frac{M+\theta_1}{4}\right),$$

$$A_{2m}^+\left(\frac{M+\theta_1}{2mM}\right) = A_{2m}^-\left(\frac{M-(2m-1)\theta_1}{2mM}\right) = 16m^2 \sin^2\left(\frac{M+\theta_1}{4m}\right),$$

$$A_{2m}^+\left(\frac{M+\theta_1}{2mM} + \frac{2(m-1)\pi}{mM}\right) = 16m^2 \sin^2\left(\frac{M+\theta_1}{4m} - \frac{\pi}{m}\right),$$

and for

$$A_{2m}^-\left(-\frac{\theta_1}{M}\right), \; A_{2m}^-\left(-\frac{\theta_1}{M} + \frac{2\pi}{M}\right), \; A_{2m}^-\left(\frac{M-\theta_1}{2M}\right), \; A_{2m}^-\left(\frac{M-\theta_1}{2M} + \frac{2(m-1)\pi}{M}\right),$$

$$A_{2m}^-\left(\frac{M-(2m-1)\theta_1}{2mM}\right) \;\; \text{and} \;\; A_{2m}^-\left(\frac{M-(2m-1)\theta_1}{2mM} + \frac{2(m-1)\pi}{mM}\right)$$

we get the same values in the same order. All these values are greater or equal to $16 \sin^2\left(\frac{M+\theta_1}{4}\right)$ for $M \in [0, 3\pi]$, $\theta_1 \in [0, \pi]$ and $m \geq 2$. This can be easily verified by observing that $\frac{M+\theta_1}{4} \in [0, \pi]$ and that $m^2 \sin(\frac{x}{m})^2$ and $m^2 \sin(\frac{x-\pi}{m})^2$ are montonically increasing with $m \geq 1$ and any fixed $x \in [0, \pi]$. ∎

With these results at hand we can now prove the main result.

Lemma 3.2.19 *Concatenations of four or more circular arcs cannot be optimal and the workspaces look as in Figures 3.4 and 3.5.*

Proof Lemma 3.3.4 showed that the coordinates of the end-effector of a manipulator of the $C^+C^-C^+$ type $(x_{3+}^{s_1}, y_{3+}^{s_1})$ fulfill

$$\left(x_{3+}^{s_1} - \frac{\sin\theta_1}{M}\right)^2 + \left(y_{3+}^{s_1} - \frac{1-\cos\theta_1}{M}\right)^2 = \frac{16}{M^2} \sin^2\left(\frac{M+2k\pi-\theta_1}{4}\right)$$

and the coordinates of the end-effector of a manipulator of the $C^-C^+C^-$ type $(x_{3-}^{s_1}, y_{3-}^{s_1})$ fulfill

$$\left(x_{3-}^{s_1} + \frac{\sin\theta_1}{M}\right)^2 + \left(y_{3-}^{s_1} + \frac{1-\cos\theta_1}{M}\right)^2 = \frac{16}{M^2} \sin^2\left(\frac{M+2k\pi+\theta_1}{4}\right).$$

At this point we confine our investigation to $M \in (0, 3\pi]$ and $k = 0$ ($k \in \{-1, 0, 1\}$ anyhow for these values of M and the computations with $k = \pm 1$ are exactly the same). In the end we will be able to show that for larger values of M the workspace is simply connected and bounded by the CLC loci only (concatenations of circular arcs are irrelevant then).

Lemma 3.3.5 tells us that manipulators of the C$\cdots$C type (with more than three circular arcs) can only reach outside these circles. Using the same homotopy arguments as in the proof of Lemma 3.2.14 the set between the locus of points reached with CCC shapes and the locus of points reached with CLC shapes (we now call this reagion G) can be reached. Considering all manipulators reaching outside the circles mentioned, the shortest manipulators are of the CLC shape, see [37]. Using similar arguments as in the proof of Lemma 3.2.14 again the shortest manipulator reaching points outside set G would have to be longer than 1 and this is a contradiction to the normalization $L = 1$. Therefore, all manipulators of the C$\cdots$C type (with more than three circular arcs) reach inside the set G (with $k = 0$) and thus cannot deliver optimal solutions.

Now we give a description of the possible workspaces for different values of M and θ_1. If $M < \theta_1$, the workspace is obviously empty, if $\theta_1 \le M < 2\pi - \theta_1$, the manipulator cannot bend a total angle of $|\theta_1 + 2\nu\pi|$ for any $\nu \ne 0$. This is exactly the case discussed above ($k = 0$). Actually, the workspace is bounded by the CLC and the $C^- C^+ C^-$ locus and simply connected since both CCC loci can be continuously deformed to the CLC locus. It is also symmetric to the straight line through the origin and the centers of the CCC loci (which are circles).

For values of M slightly larger than $2\pi - \theta_1$ another simply connected set can be reached additionally ($k = 1$). This set is bounded by the CLC and the $C^+ C^- C^+$ locus. Now we distinguish two cases, namely $0 \le \theta_1 \le \pi/2$ and $\pi/2 < \theta_1 \le \pi$.

If $\pi/2 < \theta_1 \le \pi$ and as M grows, both sets grow and at a certain point these two sets begin to overlap, the workspace is connected then. The two overlapping sets join to one simply connected set whenever the $C^+ C^- C^+$ locus of the second set and the $C^- C^+ C^-$ locus of the first set intersect in exactly one point. We have $2\pi - \theta_1 \le M \le 2\pi + \theta_1$ in this case.

If $0 \le \theta_1 \le \pi/2$, the boundary of the second set is given by the CLC locus only whenever $M \ge 2\pi + \theta_1$ (the latter is exactly the value of M when the two sets join to one simply connected set whith $\theta_1 = \pi/2$). If $0 \le \theta_1 < \pi/2$, the two sets begin to overlap at a certain value of M and the overlapping sets join to one simply connected set whenever the $C^+ L C^-$ and the $C^- L C^+$ locus of the second set intersect on the $C^- C^+ C^-$ locus of the first set ($3\pi > M > 2\pi + \theta_1$ here).

Whenever M is larger, the workspace is simply connected (with [37] again) and the boundary is reached with manipulators of the shape CLC only. With this argument we cover also the case $M > 3\pi$ which we excluded in the beginning.

The workspaces look as can be seen in Figures 3.4 and 3.5. Obviously, the union of the workspaces with all possible terminal directions gives the workspace with free terminal direction. This can be seen in the last pictures of Figures 3.4 and

3.5.   ∎

Chapter 4

An approach to workspaces of 3D continuous robotic manipulators

In this chapter we extend the results of Chapter 3 to the 3D case. Up to a certain point this is pursued with the same methods. But since motions in space are only achieved by using at least two controls, we are no longer in the simple single input case. This complicates the situation drastically and we are not able to completely determine the workspaces.

4.1   Model and basic properties

Since a continuous robotic manipulator of length L can also be seen as an inextensible elastic rod, we adopt some basic notation from [22]. We parametrize the backbone curve $x : [0, L] \to \mathbb{R}^3$ by arc-length and let $e_1 = (1, 0, 0)^T$, $e_2 = (0, 1, 0)^T$ and $e_3 = (0, 0, 1)^T$. We assume that there exist body-fixed orthonormal axes $a_1(\cdot), a_2(\cdot), a_3(\cdot) : [0, L] \to \mathbb{R}$ that are continuous and that the manipulator can rotate around these axes at each parameter value $s \in [0, L]$ with velocities $u_1(s)$, $u_2(s)$ and $u_3(s)$. Furthermore, we fix it at the origin. The curve can then be described by the following equations, see also Figure 4.1:

$$
\begin{aligned}
x' &= a_1 \\
a_1' &= u_3 a_2 \; - \; u_2 a_3 \\
a_2' &= -u_3 a_1 \qquad + \qquad u_1 a_3 \\
a_3' &= u_2 a_1 \; - \; u_1 a_2 \\
x(0) &= 0 \\
a_i(0) &= e_i, \quad i = 1, 2, 3
\end{aligned}
\tag{4.1}
$$

with $s \in [0, L]$ and $u_i \in \mathcal{U}_1$, $i = 1, 2, 3$, due to possible physical limitations. Note that the differential equations in (4.1) are the well-known equations for the
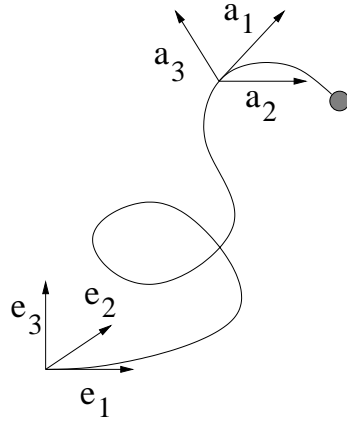
Figure 4.1: 3D robotic manipulator with body-fixed principal axes

motions of a rigid body. We set $R := (a_1, a_2, a_3) \in \mathbb{R}^{3 \times 3}$ and

$$S(u) := \begin{pmatrix} 0 & -u_3 & u_2 \\ u_3 & 0 & -u_1 \\ -u_2 & u_1 & 0 \end{pmatrix}.$$

Then the control system (4.1) can be written as

$$x' = Re_1, \quad R' = RS(u), \quad x(0) = 0, \quad R(0) = I_3. \tag{4.2}$$

4.1.1 Illustration of the model

We want to illustrate why we don't describe the backbone curve with $x' = t$ and the well-know 3D Frenet equations

$$\begin{aligned} t' &= & \kappa n & \\ n' &= -\kappa t &+& \tau b \\ b' &= & -\tau n & \end{aligned}$$

with tangent t, normal n and binormal b.

These equations are only valid for C^3 space curves that do not contain straight line segments. But here we have, in general, only continuously differentiable curves as in the 2D case, in particular when switchings between space and plane curves occur. Furthermore, we will definetly not exclude straight line segments since the point $(L, 0, 0)$ can only be reached with a straight line. Nevertheless, the following is true.

Lemma 4.1.1 *If the controls u_1, u_2 and u_3 are constant and not $u_2 = u_3 = 0$, then the solution x of (4.2) is a helix with curvature $\kappa = \sqrt{u_2^2 + u_3^2}$ and torsion $\tau = u_1$ if $u_1 \neq 0$ or a circle with radius $1/\sqrt{u_2^2 + u_3^2}$ if $u_1 = 0$.*

Proof Let $\kappa = \sqrt{u_2^2 + u_3^2}$, $\tau = u_1$, $t = a_1$, $n = \frac{1}{\kappa}(-u_3 a_2 + u_2 a_3)$ and $b = \frac{1}{\kappa}(u_3 a_3 + u_2 a_2)$. Then

$$
\begin{aligned}
t' &= a_1' = -u_3 a_2 + u_2 a_3 = \kappa n, \\
n' &= \frac{1}{\kappa}(-u_3 a_2' + u_2 a_3') = \frac{1}{\kappa}(-u_3^2 a_1 + u_1 u_3 a_3 - u_2^2 a_1 + u_1 u_2 a_2) = \\
&= -\kappa a_1 + \frac{u_1}{\kappa}(u_3 a_3 + u_2 a_2) = -\kappa t + \tau b, \\
b' &= \frac{1}{\kappa}(u_3 a_3' + u_2 a_2') = \frac{1}{\kappa}(-u_2 u_3 a_1 + u_1 u_3 a_2 + u_2 u_3 a_1 - u_1 u_2 a_3) = \\
&= -\frac{u_1}{\kappa}(u_3 a_2 - u_2 a_3) = -\tau n.
\end{aligned}
$$

These are the Frenet differential equations and t, n and b are tangent, normal and binormal. The curvature κ and torsion τ are both constant and the curve is a helix. If $u_1 = 0$ the equations reduce to the 2D Frenet equations and we are done. ∎

Remark 4.1.2 If $u_2 = u_3 = 0$ then the solution x of (4.2) is obviously a straight line segment. □

The following example illustrates that we cannot describe the manipulator with a continuous Frenet coordinate frame.

Example 4.1.3 Consider a manipulator of length L and assume that $u_2 = 0$. On the interval $I_1 = [0, \frac{L}{2}]$ let $u_1 = u_3 = 1$ and on the interval $I_2 = (\frac{L}{2}, L]$ let $u_1 = u_3 = -1$. Then from Lemma 4.1.1 and its proof follows that on I_1 the curve is a helix with $\kappa = \tau = 1$ and $t = a_1$, $n = -a_2$ and $b = a_3$. On I_2 the curve is a helix with $\kappa = -\tau = 1$ and $t = a_1$, $n = a_2$ and $b = -a_3$. Since a_2 and a_3 are continuous (in particular in $\frac{L}{2}$), the Frenet coordinate frame is rotated by π around the tangent in the point at parameter $\frac{L}{2}$ and obviously not continuous. □

4.1.2 Basic properties

We first want to define the term workspace properly and determine a few of its elementary properties.

Definition 4.1.4 (Workspace) *Let $\mathcal{U} := \{u = (u_1, u_2, u_3) : u_i \in \mathcal{U}_1\}$ and*

$$\mathcal{F} := \{(x(\cdot), R(\cdot)) \text{ satisfying (4.2) with } u \in \mathcal{U}\}.$$

For any $\Omega \subset \mathcal{F}$ we define

$$P_\Omega := \{x_1 \in \mathbb{R}^3 : x(1) = x_1 \text{ for some } (x(\cdot), R(\cdot)) \in \Omega\}.$$

The workspace W *of a robotic manipulator of length L described by system (4.2) is the set of reachable points of its* end-effector $x(L)$, *that is $W := P_\mathcal{F}$.*

Now we will state a few elementary properties of the workspace W.

Lemma 4.1.5 W *is non-empty. Furthermore, W is*

(i) *symmetric to the e_1-e_2- and the e_1-e_3-plane and*

(ii) *a path-connected subset of $\mathbb{R}^3$.*

Proof First of all, the point $(L, 0, 0)$ can always be reached with $u \equiv 0$. Now denote any $y \in \mathbb{R}^3$ in components by $y = (y^1, y^2, y^3)$. Let $u \in \mathcal{U}$ be the control of a manipulator with centerline $x(\cdot)$ reaching $x_1 \in W$.

(i) We will show that there exists a control $\tilde{u} \in \mathcal{U}$ such that the corresponding curve $\tilde{x}$ is symmetric to x with respect to the e_1-e_3-plane and thus $\tilde{x}_1 = (x_1^1, -x_1^2, x_1^3) \in W$. Let $\tilde{u}_1 := -u_1$, $\tilde{u}_2 := u_2$ and $\tilde{u}_3 := -u_3$. Then by (4.2) we get

$$\begin{pmatrix} \tilde{a}_1^1 \\ \tilde{a}_1^2 \\ \tilde{a}_1^3 \end{pmatrix} = \begin{pmatrix} a_1^1 \\ -a_1^2 \\ a_1^3 \end{pmatrix}, \quad \begin{pmatrix} \tilde{a}_2^1 \\ \tilde{a}_2^2 \\ \tilde{a}_2^3 \end{pmatrix} = \begin{pmatrix} -a_2^1 \\ a_2^2 \\ -a_2^3 \end{pmatrix}, \quad \begin{pmatrix} \tilde{a}_3^1 \\ \tilde{a}_3^2 \\ \tilde{a}_3^3 \end{pmatrix} = \begin{pmatrix} a_3^1 \\ -a_3^2 \\ a_3^3 \end{pmatrix}.$$

and, by (4.2) again, $\tilde{x} = (x^1, -x^2, x^3)$ and we proved the symmetry to the e_1-e_3-plane. The symmetry to the e_1-e_2-plane follows by analogous arguments ($\tilde{u}_1 := -u_1$, $\tilde{u}_2 := -u_2$ and $\tilde{u}_3 := u_3$).

(ii) Let $a \in [0, 1]$ and $u^a := (1-a)u$. Then $u^a \in \mathcal{U}$ and the corresponding end-effector is $x_1^a \in W$. Finally, the points x_1^a describe a path between x_1 and the point $(L, 0, 0)$ and, since the solutions are continuously dependent on the parameter a, all points in W are path-connected.

This concludes the proof.   ■

Proposition 4.1.6 W *is compact.*

Proof The manipulator can obviously only reach points inside the unit circle and the point (L,0,0). Thus W is bounded and it remains to show that W is closed.
Consider a sequence $u^n(\cdot)_{n \in \mathbb{N}} \subset \mathcal{U}$ of controls with corresponding state

$$(x^n(\cdot), R^n(\cdot)) : [0, 1] \to \mathbb{R}^3 \times \mathbb{R}^9$$

subject to (4.2) for each $n \in \mathbb{N}$ such that $(x^n(1))_{n \in \mathbb{N}}$ converges to $x_1 \in \mathbb{R}^3$. We show that there exists a function $\tilde{u}(\cdot) \in \mathcal{U}$ with state $(\tilde{x}(\cdot), \tilde{R}(\cdot))$ subject to (4.2) such that $\tilde{x}(L) = x_1$.

Due to the parametrization by arc length we have $||(x^n)'(s)|| = 1$ for all $n \in \mathbb{N}$ and $s, t \in [0, L]$ and thus

$$||x(s) - x(t)|| \le |s - t|.$$

Let $||R|| := \sup_{||x||=1} ||Rx||$ and $||(x, R)|| := ||x|| + ||R||$ (it should be obvious in the sequel which norm is taken for different terms). Then $||R^n(s)|| = 1$ for all $n \in \mathbb{N}$ and $s \in [0, L]$ and the family $((x^n)', R^n)$ is uniformly bounded.
It is easy to see that $||S(u)|| \le \sum_{i=1}^{3} |u_i| \le 3$ and thus

$$||R^n(s) - R^n(t)|| = \left\| \int_t^s (R^n)'(\sigma) \, d\sigma \right\| \le \int_t^s ||R^n(\sigma)|| \; ||S(u^n(\sigma))|| \, d\sigma \le 3|s - t|.$$

Then

$$||((x^n)'(s), R^n(s)) - ((x^n)'(t), R^n(t))|| \le 4|s - t|$$

and the $((x^n)', R^n)$ form an equicontinuous family on $[0, L]$. By the Arzelà-Ascoli theorem, there exists a subsequence of $((x^n)'(\cdot), R^n(\cdot))_{n \in \mathbb{N}}$ converging uniformly on $[0, L]$ to a continuous function $(\xi(\cdot), \tilde{R}(\cdot))$ with

$$\xi(s) = \tilde{R}(s) e_1$$

for all $s \in [0, L]$. For simplicity we may assume that $((x^n)'(\cdot), R^n(\cdot))_{n \in \mathbb{N}}$ is itself such a sequence. Obviously, $\tilde{R}(s) \in SO_3(\mathbb{R})$ for all $s \in [0, L]$ and $(\xi(0), \tilde{R}(0)) = (e_1, I_3)$ which shows that the initial condition of (4.2) holds for $\tilde{R}(\cdot)$.
In particular $\tilde{R}(\cdot) \in \mathrm{Lip}_3[0, L] \subset A[0, L]$. Thus $\tilde{R}(\cdot)$ is differentiable almost everywhere (see e.g. [28]). We define $\tilde{u}$ by $\tilde{R}'(s) = \tilde{R}(s) S(\tilde{u}(s))$ for all $s \in [0, L]$ where $\tilde{R}(\cdot)$ is differentiable and $\tilde{u}(s) := 0$ else. We set

$$\tilde{x}(s) := \int_0^s \xi(\sigma) \, d\sigma.$$

Since

$$||\tilde{x}(L) - x^n(L)|| \le \int_0^L ||\tilde{R}(\sigma) - R^n(\sigma)|| \; ||e_1|| \, dt \to 0 \text{ as } n \to \infty$$

we have $\tilde{x}(0) = 0$ and $\tilde{x}(L) = x_1$.
In order to show that $\tilde{x}(L) \in W$ and thus W is closed as claimed we need to show that $\tilde{u} \in \mathcal{U}$. To do so we introduce a new matrix norm

$$||(a_{ij})_{i,j=1,2,3}||_m := \max_{i,j=1,2,3} |a_{ij}|.$$

Let $s_0 \in (0, L)$ such that $\tilde{R}$ is differentiable at s_0 and $\epsilon > 0$ be fixed. Then there exists a $\delta > 0$ such that $\tilde{R}$ is differentiable on $[s_0, s_0 + \delta]$,

$$||R^n(s_0 + \mu) - R^n(s_0)||_m \leq \frac{\epsilon}{6}$$

for all $n \in \mathbb{N}$ and $\mu \in [0, \delta]$ and

$$\left\| \tilde{R}'(s_0) - \frac{\tilde{R}(s_0 + \delta) - \tilde{R}(s_0)}{\delta} \right\|_m \leq \frac{\epsilon}{4}.$$

Then we have

$$
\begin{aligned}
S(\tilde{u}(s_0)) &= \tilde{R}^T(s_0)\tilde{R}'(s_0) = \left[(R^n)^T(s_0) + (\tilde{R}^T(s_0) - (R^n)^T(s_0)) \right] \tilde{R}'(s_0) = \\
&= (R^n)^T(s_0)\tilde{R}'(s_0) + (\tilde{R}^T(s_0) - (R^n)^T(s_0))\tilde{R}'(s_0) = \\
&= (R^n)^T(s_0)\tilde{R}'(s_0) + \alpha^n = \\
&= (R^n)^T(s_0)\frac{\tilde{R}(s_0 + \delta) - \tilde{R}(s_0)}{\delta} + \\
&\quad + (R^n)^T(s_0)\left[\tilde{R}'(s_0) - \frac{\tilde{R}(s_0 + \delta) - \tilde{R}(s_0)}{\delta} \right] + \alpha^n = \\
&= (R^n)^T(s_0)\frac{\tilde{R}(s_0 + \delta) - \tilde{R}(s_0)}{\delta} + \beta^n + \alpha^n = \\
&= (R^n)^T(s_0)\frac{R^n(s_0 + \delta) - R^n(s_0)}{\delta} + \beta^n + \alpha^n + \\
&\quad + (R^n)^T(s_0)\left[\frac{\tilde{R}(s_0 + \delta) - R^n(s_0 + \delta) - \tilde{R}(s_0) + R^n(s_0)}{\delta} \right] = \\
&= (R^n)^T(s_0)\frac{R^n(s_0 + \delta) - R^n(s_0)}{\delta} + \gamma^n + \beta^n + \alpha^n
\end{aligned}
$$

with

$$
\begin{aligned}
\alpha^n &= (\tilde{R}^T(s_0) - (R^n)^T(s_0))\tilde{R}'(s_0), \\
\beta^n &= (R^n)^T(s_0)\left[\tilde{R}'(s_0) - \frac{\tilde{R}(s_0 + \delta) - \tilde{R}(s_0)}{\delta} \right] \quad \text{and} \\
\gamma^n &= (R^n)^T(s_0)\left[\frac{\tilde{R}(s_0 + \delta) - R^n(s_0 + \delta) - \tilde{R}(s_0) + R^n(s_0)}{\delta} \right].
\end{aligned}
$$

For sufficiently large $N \in \mathbb{N}$, we have $||\alpha^n + \beta^n + \gamma^n||_m \leq \frac{\epsilon}{2}$ for all $n \geq N$. Thus

$$
\begin{aligned}
||S(\tilde{u}(s_0))||_m \;&\leq\; \left\| (R^n)^T(s_0) \frac{R^n(s_0+\delta) - R^n(s_0)}{\delta} \right\|_m + \frac{\epsilon}{2} = \\
&=\; \left\| \frac{(R^n)^T(s_0)}{\delta} \int_{s_0}^{s_0+\delta} (R^n)'(\sigma)\, d\sigma \right\|_m + \frac{\epsilon}{2} \leq \\
&\leq\; \frac{1}{\delta} \int_{s_0}^{s_0+\delta} \left\| \left[(R^n)^T(s_0) - (R^n)^T(\sigma) + (R^n)^T(\sigma) \right] \cdot \right. \\
&\qquad \left. \cdot\, R^n(\sigma) S(u^n(\sigma)) \right\|_m \, d\sigma + \frac{\epsilon}{2} \leq \\
&\leq\; \frac{1+3\frac{\epsilon}{6}}{\delta} \int_{s_0}^{s_0+\delta} \left\| (R^n)^T(\sigma) R^n(\sigma) S(u^n(\sigma)) \right\|_m \, d\sigma + \frac{\epsilon}{2} \leq \\
&\leq\; 1 + \frac{\epsilon}{2} + \frac{\epsilon}{2} = 1 + \epsilon.
\end{aligned}
$$

Since this is true for all $\epsilon > 0$ we have $||S(\tilde{u}(s_0))||_m \leq 1$, $\tilde{u} \in \mathcal{U}$ and thus the claim. ∎

4.1.3 Auxiliary optimal control problem

In order to determine the workspace W we try to describe the boundary ∂W of W as in Chapter 3. Again, we investigate a 3-parameter family of optimal control problems (of the Mayer type) subject to (4.2), namely finding the shortest (euclidean) distance between points $x_0 \in \mathbb{R}^3$ outside W and the compact set W itself.

Let $\mathcal{G}$ denote the family of optimal solutions to all parameter values $x_0 \notin W$. With the help of Pontryagin's Maximum Principle we obtain a few necessary conditions which have to hold for every $(x(\cdot), R(\cdot)) \in \mathcal{G}$. We denote the set of functions fulfilling the necessary conditions by $\mathcal{B}$. In Proposition 4.1.8 we will show that the closure of $P_\mathcal{G}$ is equal to ∂W and in Conjecture 4.3.4 we describe a family $\mathcal{B}_1 \subset \mathcal{B}$ which may contain $\mathcal{G}$ and get the following diagram:

$$
\begin{array}{ccccccc}
\mathcal{F} & \supset & \mathcal{B} & \supset & \mathcal{B}_1 & \supset & \mathcal{G} \\
P \downarrow & & P \downarrow & & P \downarrow & & P \downarrow \\
W = P_\mathcal{F} & \supset & P_\mathcal{B} & \supset & P_{\mathcal{B}_1} & \supset & P_\mathcal{G}
\end{array}
$$

Now we consider the following 3-parameter ($x_0 \in \mathbb{R}^3$) family of minimization problems:

$$J_{x_0} = ||x(1) - x_0||^2 \to \min \tag{4.3}$$

while minimizing over all $(x(\cdot), R(\cdot)) \in \mathcal{F}$ (thus $x(1) \in W$). This problem is in fact an optimal control problem (of the Mayer type) since it is the same as minimizing over all $u \in \mathcal{U}$, see Definition 4.1.4. We will show that $\mathrm{cl} P_{\mathcal{G}} = \partial W$. First of all, the following lemma guarantees the existence of optimal solutions.

Lemma 4.1.7 *To any $x_0 \in \mathbb{R}^3$ a solution to problem (4.3) exists.*

Proof If $x_0 \in W$ then obviously $J_{x_0} = 0$ and x_0 itself is a solution. If $x_0 \notin W$ then $\sqrt{J_{x_0}}$ is the euclidean distance between x_0 and W. Since W is compact the optimal solution to (4.3) exists. ∎

Now let $\overline{u}_{x_0} \in \mathcal{U}$ be an optimal control to (4.3) for some parameter $x_0 \notin W$ and denote with $(\overline{x}(\cdot), \overline{R}(\cdot))_{x_0}$ the corresponding state. Then $\mathcal{G}$ is the set of all these solutions and the following holds:

Proposition 4.1.8 *$clP_{\mathcal{G}} = \partial W$.*

Proof If $x_0 \notin W$ then any point on the straight line between x_0 and $\overline{x}(1)_{x_0}$ is not in W because of the minimal distance property of the point $\overline{x}(1)_{x_0}$. Thus $\overline{x}(1)_{x_0} \in \partial W$ and $P_{\mathcal{G}} \subset \partial W$.
Let $x \in \partial W$ be arbitrary. Then there exists a sequence $(x_n)_{n \in N}$ such that $x_n \notin W$ for each $n \in N$ and $x_n \to x$ as $n \to \infty$. Obviously $J_{x_n} \to 0$, $\overline{x}(1)_{x_n} \in P_{\mathcal{G}}$ for each $n \in \mathbb{N}$ and $\overline{x}(1)_{x_n} \to x$ as $n \to \infty$. Thus $x \in \mathrm{cl}\, P_{\mathcal{G}}$ and we have

$$P_{\mathcal{G}} \subset \partial W \subset \mathrm{cl}\, P_{\mathcal{G}}$$

and the claim follows since ∂W is compact by Proposition 4.1.6. ∎

4.2   Differential geometric description

Since a continuous robotic manipulator can also be seen as an elastic rod which is treated in Chapter 12 in [22], we introduce similar notation here. The underlying manifold is the group of motions in $\mathbb{R}^3$ namely $\mathrm{SE}_3(\mathbb{R}) = \mathbb{R}^3 \times \mathrm{SO}_3(\mathbb{R})$ since $x \in \mathbb{R}^3$ and $R(s) \in \mathrm{SO}_3(\mathbb{R})$ for all $s \in [0, L]$. Let

$$\tilde{A}_4 := \begin{pmatrix} 0 & 0 & 0 \\ 0 & 0 & -1 \\ 0 & 1 & 0 \end{pmatrix}, \quad \tilde{A}_5 := \begin{pmatrix} 0 & 0 & 1 \\ 0 & 0 & 0 \\ -1 & 0 & 0 \end{pmatrix}, \quad \tilde{A}_6 := \begin{pmatrix} 0 & -1 & 0 \\ 1 & 0 & 0 \\ 0 & 0 & 0 \end{pmatrix},$$

$$A_j := \left(\begin{array}{c|c} 0 & 0 \\ \hline 0 & \tilde{A}_j \end{array} \right), \qquad A_i := \left(\begin{array}{c|c} 0 & 0 \\ \hline e_i & 0 \end{array} \right), \qquad g := \left(\begin{array}{c|c} 1 & 0 \\ \hline x & R \end{array} \right),$$

with $i = 1, 2, 3$ and $j = 4, 5, 6$. Then the manifold $SE_3(\mathbb{R})$ is isomorphic to

$$M := \left\{ g = \left(\begin{array}{c|c} 1 & 0 \\ \hline x & R \end{array} \right) , x \in \mathbb{R}^3, R \in \mathrm{SO}_3(\mathbb{R}) \right\}.$$

M is a subgroup of $\mathrm{GL}_4(\mathbb{R})$ with the usual matrix multiplication and it is well-known that M is even a Lie group. The equations (4.2) can be rewritten as $g(0) = I_4$ and

$$\dot{g} = \left(\begin{array}{c|c} 0 & 0 \\ \hline a_1 & RS(u) \end{array} \right) = g \left(A_1 + \sum_{i=1}^{3} u_i A_{3+i} \right).$$

Thus the considered control vector fields are left-invariant which is true for all vector fields on M, see [22].

Now there are different ways to find necessary conditions for optimality of 4.3 via Pontryagin's Maximum Principle (PMP). One way is to follow [22] and introduce the natural symplectic form on the cotangent bundle T^*M of the manifold M. Via this symplectic form the Hamiltonian $H_X : T^*M \to \mathbb{R}$ associated with a vector field X on M is given as well as the Poisson bracket on T^*M. With these tools at hand the PMP on manifolds can be applied.

We will follow two slightly different approaches. At first we consider M as a submanifold of $\mathbb{R}^{12}$ and apply classical $\mathbb{R}^{12}$ optimal control techniques as in Chapter 3 at the cost of a higher dimension of the problem.

The second approach affords more knowledge of differential geometry. It is closer to the approach in [22], only an appropiate change of coordinates in T_gM and T_g^*M is applied as in [39].

Let $g \in M$, $\mathrm{tr}\,()$ denote the trace of a matrix and

$$\mathbb{R}^{12} \approx \left\{ r = \left(\begin{array}{c|c} 1 & 0 \\ \hline y & B \end{array} \right) , y \in \mathbb{R}^3, B \in \mathbb{R}^{3 \times 3} \right\},$$

$$T_g\mathbb{R}^{12} \approx \left\{ Y = \left(\begin{array}{c|c} 0 & 0 \\ \hline v & F \end{array} \right) , v \in \mathbb{R}^3, F \in \mathbb{R}^{3 \times 3} \right\},$$

$$T_g^*\mathbb{R}^{12} \approx \left\{ \beta = \left(\begin{array}{c|c} 0 & \mu^T \\ \hline 0 & \Lambda^T \end{array} \right) , \mu \in \mathbb{R}^3, \Lambda \in \mathbb{R}^{3 \times 3} \right\},$$

$$\langle \beta, Y \rangle = \mathrm{tr}\,(\beta Y) = \mu^T v + \mathrm{tr}\,\left(\Lambda^T F \right) \quad \text{(one-form)}.$$

Since all vector fields on M are left invariant and

$$T_e M = \left\{ X = \left(\begin{array}{c|c} 0 & 0 \\ \hline v & S \end{array} \right) , v \in \mathbb{R}^3, S \in \mathrm{so}_3(\mathbb{R}) \right\},$$

we get

$$T_g M \;=\; \left\{ X = g\left(\begin{array}{c|c} 0 & 0 \\ \hline v & S \end{array} \right) = \left(\begin{array}{c|c} 0 & 0 \\ \hline Rv & RS \end{array} \right), v \in \mathbb{R}^3, S \in \mathrm{so}_3(\mathbb{R}) \right\}$$

and via the introduced one-form also

$$T_g^* M \;=\; \left\{ \omega = \left(\begin{array}{c|c} 0 & \mu^T R^T \\ \hline 0 & \tilde{S}^T R^T \end{array} \right), \mu \in \mathbb{R}^3, \tilde{S} \in \mathrm{so}_3(\mathbb{R}) \right\}$$

4.2.1   M as a submanifold of $\mathbb{R}^{12}$

Via the one-form introduced above we can define the Hamiltonians on $T^*\mathbb{R}^{12}$ and T^*M which we need to apply Pontryagin's Maximum Principle. Let

$$H_i := \langle \beta, g A_i \rangle, \quad i = 1, \dots, 6$$

and

$$H := \left\langle \beta, g\left(A_1 + \sum_{i=1}^{3} u_i A_{3+i} \right) \right\rangle = H_1 + \sum_{i=1}^{3} u_i H_{3+i} \qquad (4.4)$$

With $\lambda_1, \lambda_2, \lambda_3 \in \mathbb{R}^3$ and $\Lambda = (\lambda_1, \lambda_2, \lambda_3) \in \mathbb{R}^{3 \times 3}$ we have

$$H_1 = \mu^T a_1, \quad H_2 = \mu^T a_2, \quad H_3 = \mu^T a_3,$$
$$H_4 = \lambda_2^T a_3 - \lambda_3^T a_2, \quad H_5 = \lambda_3^T a_1 - \lambda_1^T a_3, \quad H_6 = \lambda_1^T a_2 - \lambda_2^T a_1.$$

Since we want to apply optimal control techniques, we state a version of Pontryagin's Maximum Principle (see e.g. [6]) tailored for the needs of the following analysis.

Theorem 4.2.1 (Pontryagin's Minimum Principle) *If $u(\cdot) \in \mathcal{U}$ is an optimal control to problem (4.3) with $x_0 \notin W$ and corresponding state $(x(\cdot), R(\cdot))$, then*

(i) there exists an absolutely continuous function $(\mu, \Lambda) : [0, L] \to \mathbb{R}^3 \times \mathbb{R}^{3 \times 3}$ satisfying the adjoint equations

$$\begin{aligned} \mu_i'(s) &= -\tfrac{\partial}{\partial x_i} H(x(s), R(s), \mu(s), \Lambda(s), u(s)), \quad i\text{=}1,2,3, \\ \Lambda_{ij}'(s) &= -\tfrac{\partial}{\partial R_{ij}} H(x(s), R(s), \mu(s), \Lambda(s), u(s)), \quad i,j\text{=}1,2,3 \end{aligned} \qquad (4.5)$$

for almost every $s \in [0, L]$ where the Hamiltonian *of (4.3)*

$$H : \mathbb{R}^3 \times \mathbb{R}^{3 \times 3} \times \mathbb{R}^3 \times \mathbb{R}^{3 \times 3} \times [-1, 1]^3 \;\to\; \mathbb{R},$$

$$(x, R, \mu, \Lambda, u) \;\mapsto\; H_1 + \sum_{i=1}^{3} u_i H_{3+i}.$$

is given by (4.4).

(ii) *if dJ_{x_0} is not identically zero for all $x(L)$ then $(\mu(s), \Lambda(s)) \neq 0$ on $[0, L]$,*

(iii) *there exists a constant $c \in \mathbb{R}$ such that for almost every $s \in [0, L]$*

$$H(x(s), R(s), \mu(s), \Lambda(s), u(s)) = \min_{v \in \mathcal{U}} H(x(s), R(s), \mu(s), \Lambda(s), v(s)) = c,$$

(iv) *there exists a constant $\lambda_0 \in \mathbb{R}$ such that $(\lambda_0, \lambda_1(s), \lambda_2(s), \lambda_3(s))$ never vanishes on $[0, L]$ and the following transversality conditions hold:*

$$\mu(L) = 2\lambda_0(x(L) - x_0), \qquad (4.6)$$
$$\Lambda(L) = 0. \qquad (4.7)$$

Corollary 4.2.2 *This problem is normal ($\lambda_0 \neq 0$) since otherwise also $\mu(L) = 0$ because of (4.6) and $\Lambda(L) = 0$ because of (4.7) which is impossible.*

Lemma 4.2.3 *Let $\hat{h} := (H_1, H_2, H_3)^T$ and $\hat{H} := (H_4, H_5, H_6)^T$. Then*

1. *μ is constant,*

2. *$\hat{h} = (\mu^T a_1, \mu^T a_2, \mu^T a_3)^T = R^T \mu$,*

3. *$\hat{h}' = -S(u)\hat{h}$,*

4. *$\hat{H}' = -S(u)\hat{H} + \hat{h} \times e_1$,*

5. *$R\hat{H} - \mu \times x = b = $ constant,*

6. *$||\hat{h}||^2 = ||\mu||^2 = $ constant,*

7. *$H_1 H_4 + H_2 H_5 + H_3 H_6 \equiv 0$,*

8. *$\mu \neq 0$ whenever $x_0 \notin W$.*

Proof   1. is obvious, since H does not depend on x.

2. is obvious.

3. Since μ is constant by 1. we have

$$\hat{h}' = (R^T)'\mu = -S(u)R^T\hat{h} = -S(u)\hat{h}.$$

4. This can be calculated in a straightforward manner with Theorem 4.2.1

$$
\begin{aligned}
H_4' &= (\lambda_2^T a_3 - \lambda_3^T a_2)' = (\lambda_2^T)' a_3 - (\lambda_3^T)' a_2 + \lambda_2^T a_3' - \lambda_3^T a_2' = \\
&= (u_1 \lambda_3^T - u_3 \lambda_1^T) a_3 - (u_1 \lambda_2^T - u_2 \lambda_1^T) a_2 + \lambda_2^T (u_1 a_2 - u_2 a_1) - \\
&\quad - \lambda_3^T (u_1 a_3 - u_3 a_1) = u_3 H_5 - u_2 H_6, \\
H_5' &= (\lambda_3^T a_1 - \lambda_1^T a_3)' = (\lambda_3^T)' a_1 - (\lambda_1^T)' a_3 + \lambda_3^T a_1' - \lambda_1^T a_3' = \\
&= (u_1 \lambda_2^T - u_2 \lambda_1^T) a_1 - (u_3 \lambda_2^T - u_2 \lambda_3^T - \mu^T) a_3 + \lambda_3^T (u_2 a_2 - u_2 a_3) - \\
&\quad - \lambda_1^T (u_1 a_2 - u_2 a_1) = -u_3 H_4 + u_1 H_6 + H_3, \\
H_6' &= (\lambda_1^T a_2 - \lambda_2^T a_1)' = (\lambda_1^T)' a_2 - (\lambda_2^T)' a_1 + \lambda_1^T a_2' - \lambda_2^T a_1' = \\
&= (u_3 \lambda_2^T - u_2 \lambda_3^T - \mu^T) a_2 - (u_1 \lambda_3^T - u_3 \lambda_1^T) a_1 + \lambda_1^T (u_1 a_3 - u_3 a_1) - \\
&\quad - \lambda_2^T (u_3 a_2 - u_2 a_3) = u_2 H_4 - u_1 H_5 - H_2,
\end{aligned}
$$

and the claim follows.

5. Using 2. and 4. we get

$$
\begin{aligned}
(R\hat{H} - \mu \times x)' &= R'\hat{H} + R\hat{H}' - \mu \times x' = \\
&= RS\hat{H} + R(-S\hat{H} + \hat{h} \times e_1) - R\hat{h} \times a_1 = \\
&= R\hat{h} \times a_1 - R\hat{h} \times a_1 = 0.
\end{aligned}
$$

6. $||\hat{h}||^2 = ||R^T \mu||^2 = ||\mu||^2$ since R is orthonormal.

7. After differentiation, we get

$$
\begin{aligned}
(H_1 H_4 + H_2 H_5 + H_3 H_6)' &= (\hat{h}')^T \hat{H} + \hat{h}^T \hat{H}' = \\
&= \hat{h}^T S(u) \hat{H} + \hat{h}^T (-S(u)\hat{H} + \hat{h} \times e_1) = \\
&= \hat{h}^T (\hat{h} \times e_1) = 0
\end{aligned}
$$

and $H_1 H_4 + H_2 H_5 + H_3 H_6$ is constant. The constant is 0 since $H_4(L) = H_5(L) = H_6(L)$ because of the transversaltiy condition (4.7) in Theorem 4.2.1.

8. is obvious from Corollary 4.2.2.

∎

Remark 4.2.4 If $x_0 \in W$, then obviously $J_{x_0} = 0$. From (4.6) it follows that $\mu = 0$ and from Lemma 4.2.3 (2.) then $H_1 \equiv H_2 \equiv H_3 \equiv 0$. Since $(H_4(L), H_5(L), H_6(L)) = (0, 0, 0)$ by (4.7), from Lemma 4.2.3 (4.) follows that $H_4 \equiv H_5 \equiv H_6 \equiv 0$ and Theorem 4.2.1 gives no direct information about the optimal controls. □

Since the derivatives of the functions $H_1, \ldots, H_6$ can easily be computed by using Poisson brackets, we will determine all Lie brackets between the vector fields $A_1, \ldots, A_6$ and the Poisson brackets of the corresponding Hamiltonians $H_1, \ldots, H_6$. The vector fields $A_1, \ldots, A_6$ are left invariant and we only need to compute the Lie brackets for the vector fields $A_1(g), \ldots, A_6(g)$ at $g = I_4$, which is just the matrix commutator $[A_i, A_j] = A_i A_j - A_j A_i$ here. The table of Lie brackets looks as follows:

$$
\begin{array}{c||c|c|c|c|c|c}
[\,,\,] & A_1 & A_2 & A_3 & A_4 & A_5 & A_6 \\
\hline\hline
A_1 & 0 & 0 & 0 & 0 & -A_3 & A_2 \\
\hline
A_2 & 0 & 0 & 0 & A_3 & 0 & -A_1 \\
\hline
A_3 & 0 & 0 & 0 & -A_2 & A_1 & 0 \\
\hline
A_4 & 0 & -A_3 & A_2 & 0 & A_6 & -A_5 \\
\hline
A_5 & A_3 & 0 & -A_1 & -A_6 & 0 & A_4 \\
\hline
A_6 & -A_2 & A_1 & 0 & A_5 & -A_4 & 0
\end{array}
\tag{4.8}
$$

The manifolds T^*M and $T^*\mathbb{R}^{12}$ are symplectic with the standard symplectic form and thus the standard Poisson bracket on $T^*\mathbb{R}^{12}$. Here, the equivalent table holds for the Hamiltonians $H_1, \ldots, H_6$ corresponding to the vector fields $A_1, \ldots, A_6$:

$$
\begin{array}{c||c|c|c|c|c|c}
\{\,,\,\} & H_1 & H_2 & H_3 & H_4 & H_5 & H_6 \\
\hline\hline
H_1 & 0 & 0 & 0 & 0 & -H_3 & H_2 \\
\hline
H_2 & 0 & 0 & 0 & H_3 & 0 & -H_1 \\
\hline
H_3 & 0 & 0 & 0 & -H_2 & H_1 & 0 \\
\hline
H_4 & 0 & -H_3 & H_2 & 0 & H_6 & -H_5 \\
\hline
H_5 & H_3 & 0 & -H_1 & -H_6 & 0 & H_4 \\
\hline
H_6 & -H_2 & H_1 & 0 & H_5 & -H_4 & 0
\end{array}
\tag{4.9}
$$

4.2.2 Adapted basis in T_gM and T_g^*M

We follow a slightly different approach here. Since we already know that everything takes place on a manifold isomorphic to the 6-dimensional manifold M, we do not need to consider the 12-dimensional manifold $\mathbb{R}^{12}$. One might follow the ideas of [22], but some results are achieved more transparently using an appropiate choice of basis in T_gM and T_g^*M as persued similarly in [39].

At any $g \in M$, the simpliest basis of $T_g M$ is already given in Section 4.2.1, namely by the left-invariant vector fields $X_{(i)} :$ $X_{(i)}(g) := gA_i$, $i = 1, \ldots, 6$. The basis of $T_g^* M$ dual to the basis of $T_g M$ introduced above is given by

$$
\begin{aligned}
\omega^{(i)} &:= A_i^T g^T, \quad i = 1, 2, 3, \\
\omega^{(j)} &:= \frac{1}{2} A_j^T g^T, \quad j = 4, 5, 6.
\end{aligned}
$$

Definition 4.2.5 *If there exists a system of coordinates $q^{(i)}$ such that $X_{(i)} = \frac{\partial}{\partial q^{(i)}}$ (equivalently, if the $\omega^{(i)}$ are exact, i.e., $\omega^{(i)} = dq^{(i)}$), the field of frames $\{X_{(1)}, \ldots, X_{(6)}\}$ is called* holonomic, *else* anholonomic.

Definition 4.2.6 *The* object of anholonomy *is given by*

$$
A_{(i)(j)}^{(k)} := d\omega^{(k)}([X_{(i)}, X_{(j)}]) = -\langle \omega^{(k)}, [X_{(i)}, X_{(k)}] \rangle
$$

There should be no problem distinguishing the object of anholonomy $A_{(i)(j)}^{(k)}$ from the vector fields A_i.

Lemma 4.2.7 *The following basic properties of the object of anholonomy hold.*

a) *Skew-symmetry* $A_{(i)(j)}^{(k)} = -A_{(j)(i)}^{(k)}$, $i, j, k = 1, \ldots, 6$,

b) *The field of frames $\{X_{(1)}, \ldots, X_{(6)}\}$ is holonomic if and only if $A_{(i)(j)}^{(k)} = 0$, $i, j, k = 1, \ldots, 6$,*

c) $[X_{(i)}, X_{(j)}] = -\sum_{k=1}^{6} A_{(i)(j)}^{(k)} X_{(k)}$, $i, j = 1, \ldots, 6$.

Proof   See [39] and further references therein.   ∎

The object of anholonomy then follows from (4.8) and is given as follows (mind the skew-symmetry):

$$
\begin{aligned}
A_{(1)(5)}^{(3)} &= 1, & A_{(1)(6)}^{(2)} &= -1 \\
A_{(2)(4)}^{(3)} &= -1, & A_{(2)(6)}^{(1)} &= 1 \\
A_{(3)(4)}^{(2)} &= 1, & A_{(3)(5)}^{(1)} &= -1 \\
A_{(4)(5)}^{(6)} &= 1, & A_{(4)(6)}^{(5)} &= -1 \\
A_{(5)(6)}^{(4)} &= 1.
\end{aligned}
\qquad (4.10)
$$

All other $A_{(i)(j)}^{(k)}$ are equal to 0.

Now an arbitrary element $\omega \in T_g^* M$ can be represented by

$$\omega = \sum_{j=1}^{6} \mu_{(j)} \omega^{(j)} = \sum_{j=1}^{3} \mu_{(j)} A_j^T g^T + \frac{1}{2} \sum_{j=4}^{6} \mu_{(j)} A_j^T g^T.$$

We introduce $H_i := \langle \omega, X_{(i)} \rangle$ and get

$$\begin{aligned}
H_i &= \left\langle \sum_{j=1}^{6} \mu_{(j)} \omega^{(j)} = \sum_{j=1}^{3} \mu_{(j)} A_i^T g^T + \frac{1}{2} \sum_{j=4}^{6} \mu_{(j)} A_j^T g^T, g A_i \right\rangle = \\
&= \operatorname{tr}\left(\sum_{j=1}^{3} \mu_{(j)} A_j^T g^T g A_i \right) + \frac{1}{2} \operatorname{tr}\left(\sum_{j=4}^{6} \mu_{(j)} A_j^T g^T g A_i \right) = \mu_{(i)}
\end{aligned}$$

regarding $g^T g = I$ and the fact that the A_j and $A_i^T, \frac{1}{2} A_j^T$ form dual bases in $T_e M$ and $T_e^* M$, respectively. Then the Hamiltonian writes as

$$\begin{aligned}
H &:= \langle \omega, X_{(1)} + \sum_{i=4}^{6} u_{i-3} X_{(i)} \rangle = \mu_{(1)} + \mu_{(4)} u_1 + \mu_{(5)} u_2 + \mu_{(6)} u_3 = \\
&= H_1 + \sum_{i=4}^{6} u_{i-3} H_i.
\end{aligned}$$

This structure of the Hamiltonian is very simple but has its price. The natural Poisson structure is no longer as simple as $\frac{\partial}{\partial \mu_{(i)}} \wedge \frac{\partial}{\partial \mu_{(j)}}$ but

$$\begin{aligned}
\Omega &= -\sum_{i=1}^{6} \frac{\partial}{\mu_{(i)}} \wedge X_{(i)} + \frac{1}{2} \sum_{i,j,k=1}^{6} \mu_{(k)} A_{(i)(j)}^{(k)} \frac{\partial}{\partial \mu_{(i)}} \wedge \frac{\partial}{\partial \mu_{(j)}} = \\
&= \frac{1}{2} \sum_{i,j,k=1}^{6} \mu_{(k)} A_{(i)(j)}^{(k)} \frac{\partial}{\partial \mu_{(i)}} \wedge \frac{\partial}{\partial \mu_{(j)}}
\end{aligned}$$

since $\sum_{i=1}^{6} \frac{\partial}{\mu_{(i)}} \wedge X_{(i)} = 0$ for all functions $H_1, \dots, H_6$ which only depend on $\mu_{(1)}, \dots, \mu_{(6)}$ (Ω is the double contravariant tensor such that $\Omega(\cdot, dH) = X_H$). With this structure the Poisson bracket is given by

$$\{F, G\} = \Omega(F, G).$$

The table of Poisson brackets between the functions $H_1, \dots, H_6$ can be easily computed and looks exactly as in (4.9). Lemma 4.2.3 can be shown equivalently. This result could be expected, but it is, nevertheless, another natural approach to this problem and the proof is straightforward.

Lemma 4.2.8 *Let $\hat{h} := (H_1, H_2, H_3)^T$ and $\hat{H} := (H_4, H_5, H_6)^T$. Then*

1. $\hat{h}' = -S(u)\hat{h}$,

2. $\hat{H}' = -S(u)\hat{H} + \hat{h} \times e_1$,

3. $||\hat{h}||$ *is constant,*

4. $H_1 H_4 + H_2 H_5 + H_3 H_6 \equiv 0$,

Proof   1. This works a little different from the $\mathbb{R}^{12}$ considerations. We use the fact that $H_i' = \{H_i, H\}$ and get

$$
\begin{aligned}
H_1' &= \{H_1, H\} = u_2\{H_1, H_5\} + u_3\{H_1, H_6\} = -u_2 H_3 + u_3 H_2, \\
H_2' &= \{H_2, H\} = u_1\{H_2, H_4\} + u_3\{H_2, H_6\} = u_1 H_3 - u_3 H_1, \\
H_3' &= \{H_3, H\} = u_1\{H_3, H_4\} + u_2\{H_3, H_5\} = -u_1 H_2 + u_2 H_1.
\end{aligned}
$$

2. Again, we use $H_i' = \{H_i, H\}$ and get

$$
\begin{aligned}
H_4' &= \{H_4, H\} = u_2\{H_4, H_5\} + u_3\{H_4, H_6\} = -u_2 H_6 + u_3 H_5, \\
H_5' &= \{H_5, H\} = u_1\{H_5, H_4\} + u_3\{H_5, H_6\} = u_1 H_6 - u_3 H_4 + H_3, \\
H_6' &= \{H_6, H\} = u_1\{H_6, H_4\} + u_2\{H_6, H_5\} = -u_1 H_5 + u_2 H_4 - H_2.
\end{aligned}
$$

3. With 1. we get

$$
\begin{aligned}
\frac{1}{2}(||\hat{h}||^2)' &= H_1 H_1' + H_2 H_2' + H_3 H_3' = -u_2 H_1 H_3 + u_3 H_1 H_2 + \\
&\quad + u_1 H_2 H_3 - u_3 H_1 H_2 - u_1 H_2 H_3 + u_2 H_1 H_3 = 0
\end{aligned}
$$

4. After differentiation, we get

$$
\begin{aligned}
(H_1 H_4 + H_2 H_5 + H_3 H_6)' &= (\hat{h}')^T \hat{H} + \hat{h}^T \hat{H}' = \\
&= \hat{h}^T S(u)\hat{H} + \hat{h}^T(-S(u)\hat{H} + \hat{h} \times e_1) = \\
&= \hat{h}^T(\hat{h} \times e_1) = 0
\end{aligned}
$$

and $H_1 H_4 + H_2 H_5 + H_3 H_6$ is constant. The constant is 0 because of the transversaltiy conditions.

∎

4.3 Consequences of the necessary conditions of Pontryagin's Maximum Principle

We investigate the optimal control problems with $x_0 \notin W$ only. As in the 2D case the Hamiltonian (derived as in Section 4.2.1 or as in Section 4.2.2) is linear in the controls and an immediate consequence of Pontryagin's Maximum principle is

$$u_i = -\text{sign } H_{i+3}, \quad i = 1, 2, 3, \quad \text{whenever } H_{i+3} \neq 0. \tag{4.11}$$

Thus the functions H_4, H_5 and H_6 are switching functions here.

In the 2D case it was rather easy to determine further properties of the switching function. We could conclude that there are only finitely many switchings and that the control vanishes whenever the switching function vanishes on an interval. To show this is a lot more complicated here and we need to consider different cases.

Lemma 4.3.1 *Let $I \subset [0, L]$ be an open, non-empty interval. Then the following properties hold.*

(A) *If $H_4|_I = H_5|_I = H_6|_I = 0$, then $H_2|_I = H_3|_I = u_2|_I = u_3|_I = 0$, $u_1|_I$ is an arbitrary admissible control function, $x|_I$ is a straight line segment and the coordinate frame R is rotating with angular velocity u_1 around the constant a_1-axis.*

(B) *If $H_4|_I = H_5|_I = 0$ and $H_6|_I \neq 0$, then $H_3|_I = u_1|_I = u_2|_I = 0$ and $x|_I$ is an arc of a circle of radius 1 rotating around the constant a_3-axis.*

(C) *If $H_4|_I = H_6|_I = 0$ and $H_5|_I \neq 0$, then $H_2|_I = u_1|_I = u_3|_I = 0$ and $x|_I$ is an arc of a circle of radius 1 rotating around the constant a_2-axis.*

(D) *$H_5|_I = H_6|_I = 0$ and $H_4|_I \neq 0$ is either impossible or also $H_1|_I = 0$, $H'_4|_I = 0$, $u_3(s) = \frac{1}{H_4} \cos(s + s_0)$ and $u_2(s) = \frac{1}{H_4} \sin(s + s_0)$ hold for some $s_0 \in [0, 2\pi)$.*

(E) *$H_4|_I = 0$ and $(H_5 H_6)|_I \neq 0$ is impossible.*

(F) *$H_5|_I = 0$ and $(H_4 H_6)|_I \neq 0$ is impossible.*

(G) *$H_6|_I = 0$ and $(H_4 H_5)|_I \neq 0$ is impossible.*

Proof   (A) $0 = H'_5 = \{H_5, H\} = H_3$ and $0 = H'_6 = \{H_6, H\} = H_2$. Therefore $0 = H'_3 = \{H_3, H\} = u_2 H_1$ and $0 = H'_2 = \{H_2, H\} = -u_3 H_1$. Since the vector (H_1, H_2, H_3) never vanishes by Lemma 4.2.3 (2. and 8.) we get $u_2 = u_3 = 0$. Thus a_1 is constant and $x|_I$ is a straight line segment.

(B) $0 = H_4' = \{H_4, H\} = -u_2 H_6$, thus $u_2 = 0$. Furthermore, $0 = H_5' = \{H_5, H\} = -u_1 H_6 + H_3 = -u_1 H_6$ since $H_3 = 0$ by Lemma 4.2.3 (7.) and thus $u_1 = 0$. Then $u_3 = \pm 1$ and the body fixed coordinate frame (a_1, a_2, a_3) rotates around the a_3-axis with constant angular velocity 1 which results in $x|_I$ being an arc of a circle of radius 1.

(C) This works just as case (B).

(D) If this case is possible at all, then from Lemma 4.2.3 (7.) follows $H_1 = 0$ and we have $H_4' = \{H_4, H\} = 0$ here. Furthermore,

$$
\begin{aligned}
H_5' &= \{H_5, H\} = H_3 - u_3 H_4 = 0, & (4.12)\\
H_6' &= \{H_6, H\} = -H_2 + u_2 H_4 = 0 \quad \text{and} & (4.13)\\
u_2^2 + u_3^2 &= \frac{1}{H_4^2}(H_3^2 + H_2^2 + H_1^2) = \text{const.} > 0 & (4.14)
\end{aligned}
$$

since $H_1 = 0$ and $(H_1, H_2, H_3) \neq (0,0,0)$ by using Lemma 4.2.3 (2. and 8.). Additionally,

$$
\begin{aligned}
H_3' &= \{H_3, H\} = -u_1 H_2 \quad \text{and}\\
H_2' &= \{H_2, H\} = u_1 H_3,
\end{aligned}
$$

thus $H_3(s) = \cos(s + s_0)$ and $H_2(s) = \sin(s + s_0)$ and u_2 and u_3 are as claimed by (4.12) and (4.13).

(E) Since $H_2 H_5 + H_3 H_6 = 0$ by Lemma 4.2.3 we have

$$
\begin{aligned}
H_1 &= \{H_3, H_5\} = \{H_2 \frac{H_5}{H_6}, H_5\} = -H_2 H_5 \{\frac{1}{H_6}, H_5\} =\\
&= \frac{H_2 H_5}{H_6^2}\{H_6, H_5\} = \frac{H_2 H_5}{H_6^2} H_4 = 0.
\end{aligned}
$$

Thus $H_1' = \{H_1, H\} = -u_2 H_3 + u_3 H_2 = 0$ and together with $H_2 H_5 + H_3 H_6 = 0$ this leads to $H_1 = H_2 = H_3 = 0$ since $u_3 H_3 + u_2 H_2 \neq 0$. But this contradicts Lemma 4.2.3 (2. and 8.) and we are done in this case.

(F) This works as (E).

(G) This works as (E).   ■

Corollary 4.3.2 *In the regular case, from now on denoted by (R), if $H_4 H_5 H_6 \neq 0$ on an open interval $I \subset [0, L]$, then the curve $x|_I$ is a helix with curvature $\kappa = \sqrt{2}$ and torsion $\tau = \pm 1$.*

Corollary 4.3.3 *Optimal solutions are concatenations of straight line segments (case (A)), arcs of circles of radius 1 (cases (B) and (C)), arcs of helices with curvature $\kappa = \sqrt{2}$ and torsion $\tau = \pm 1$ (case (R)) or described by case (D).*

At this stage, all possible control configurations are well described. Piecewise constant controls seem to suffice, only case (D) differs and we guess in Conjecture 4.3.4 that case (D) is not possible for optimal solutions. In the 2D case we were able to show that optimal controls are finite concatenations of constant (single) controls, whereas we are not even able to show that the number of concatenations of different (multiple) control strategies (cases (A) through (D) and regular case) is finite. Piecewise, the switching functions are determined by the system of differential equations derived in Lemma 4.2.3 (3. and 4.) and at this stage we are not able to characterize all possible concatenations of the solutions. Nevertheless, since strategies with two switchings describe parametrized (by the two switching parameters) planes in $\mathbb{R}^3$, we conjecture the following.

Conjecture 4.3.4 *The optimal solution to (4.3) is a concatenation of at most 3 parts each of which is described by one of the cases (A),(B),(C) or the regular case (R).*

In order to discuss the conjecture, we investigate two slightly more simple problems, namely the cases $u_2 = 0$ ($u_3 = 0$ would give similar results) on the entire interval $[0, L]$ and $u_1 = 0$ on $[0, L]$ in the following sections. These two problems are also of great interest themselves since two controls suffice to reach non-empty subsets of $\mathbb{R}^3$.

4.3.1 The case $u_2 \equiv 0$

In this case we assume that the control u_2 is inactive, i.e., $u_2|_{[0,L]} = 0$. The equations of motion of the coordinate frame (a_1, a_2, a_3) is the same as the Frenet equations up to differentiability. The Hamiltonian reduces to $H = H_1 + u_1 H_4 + u_3 H_6$. The properties of Lemma 4.3.1 still hold and we get further information for case (D).

Lemma 4.3.5 *If $u_2 = 0$ on $[0, L]$ and $I \subset [0, L]$ is an open interval then $H_5|_I = H_6|_I = 0$ and $H_4|_I \neq 0$ (case (D)) is impossible for an optimal solution.*

Proof From Lemma 4.2.3 (7.) follows that $H_1|_I = 0$. Furthermore,

$$
\begin{aligned}
H_6' &= \{H_6, H\} = -H_2 = 0 \quad \text{and thus} \\
H_2' &= \{H_2, H\} = u_1 H_3 = 0.
\end{aligned}
$$

Since $u_1 = \pm 1$ it follows that $H_3 = 0$ and therefore $(H_1, H_2, H_3)|_I = 0$ in contradiction to Lemma 4.2.3 (2. and 8.). Thus this case cannot occur and we are done. $\blacksquare$

This helps us to believe that case (D) might also be impossible for optimal solutions in the general setup.

In the regular case, the curve x is an arc of a helix with curvature $\kappa = 1$ and torsion $\tau = \pm 1$ (this follows from Corollary 4.3.2). Cases (A) and (B) are as in the general setup, case (C) degenerates to a straight line segment with constant coordinate frame and we summarize as follows.

Corollary 4.3.6 *If $u_2 = 0$ on $[0, L]$, then optimal solutions to (4.3) are (possibly infinite) concatenations of straight line segments, arcs of circles of radius 1 or arcs of helices with curvature $\kappa = 1$ and torsion $\tau = \pm 1$.*

Because of the possible arbitrary rotations around the a_1-axis in case (A) we are, in this simple setup, not able to determine the boundary of the workspace even assuming that Conjecture 4.3.4 is true. But we can give at least a few facts about possible switchings.

Lemma 4.3.7 *Switchings between the cases (C) and (A) and switchings between the cases (C) and (B) are impossible.*

Proof Assume that we have a switching from case (C) to case (A) or (B). Then in case (C) we have

$$
\begin{aligned}
H_3' &= \{H_3, H\} = -u_1 H_2 = 0 \quad \text{and} \\
H_5' &= \{H_5, H\} = H_3.
\end{aligned}
$$

Since in case (A) as well as in case (B) we have $H_3 = 0$ and because of continuity it follows that $H_3 = 0$ also in case (C). Thus, for the same reason, it follows that $H_5 = 0$ in case (C) which leads to a contradiction. ∎

Corollary 4.3.8 *(i) Optimal solutions contain at most three consecutive parts that are not regular. they are of the types (C), (B)(B)(B), (B)(A)(B) and subtypes thereof (concatenations of the type (B)(R)(B)(A)(B)(R) and similar ones are still possible).*
(ii) If an optimal solution does not contain any regular part, then it is a concatenation of one of the types (C), (B)(B), (B)(A) or subtypes thereof.

Proof Analogously to the proofs of Theorem 3.2.11 and Theorem 3.2.17 it can be shown that, if no regular part (R) is involved, between the switching from a straight line segment (A) and an arc of a circle (B) and the next/previous switching there can be only full circles which can be neglected for optimal solutions (for the same reasons as in the proofs of the mentioned theorems). Claim (i) then follows from Theorem 3.2.17 and claim (ii) from Theorem 3.2.11. ∎

4.3.2 The case $u_1 \equiv 0$

In this case, we assume that the control u_1 is inactive, i.e., $u_1|_{[0,L]} = 0$, and that Conjecture 4.3.4 is true, i.e., we have at most two switchings. The Hamiltonian reduces to $H = H_1 + u_2 H_5 + u_3 H_6$. The properties of Lemma 4.3.1 still hold and we get further information for case (D). In the regular case, the curve x is an arc of a circle of radius $1/\sqrt{2}$ since the torsion vanishes on $[0, L]$.

Lemma 4.3.9 *If $L < \frac{\pi}{2}$, $u_1 = 0$ on $[0, L]$ and $I \subset [0, L]$ is an open interval then $H_5|_I = H_6|_I = 0$ and $H_4|_I \neq 0$ (case (D)) is impossible for an optimal solution.*

Proof Assume that $H_5|_I = H_6|_I = 0$ and $H_4|_I \neq 0$. By Lemma 4.2.3 (7.) we have $H_1|_I = 0$, thus $H \equiv 0$, $H_1(L) = 0$ and on the interval I

$$
\begin{aligned}
H_2' &= \{H_2, H\} = -u_3 H_1 = 0, \\
H_3' &= \{H_3, H\} = u_2 H_1 = 0 \quad \text{and} \\
H_4' &= \{H_4, H\} = u_2 H_6 - u_3 H_5 = 0.
\end{aligned}
$$

Furthermore,

$$
\begin{aligned}
H_5' &= \{H_5, H\} = -u_3 H_4 + H_3 = 0 \quad \text{and} \\
H_6' &= \{H_6, H\} = u_2 H_4 - H_2 = 0.
\end{aligned}
$$

Now we show the following.

(i) Case (A) cannot appear at all.

(ii) Case (D) cannot appear at the last interval, i.e., $I \neq (a, L)$ for all $a \in [0, L)$. Switchings between (D) and (B) or (C) are impossible.

(iii) If we have the regular case (R) on the last interval J, i.e., $J = (a, L)$ for some $a \in [0, L)$, then $a = 0$ and no switchings (in particular to case (D)) appear at all.

(iv) If we have case (B) (or case (C)) on the last interval J_2, i.e., $J_2 = (s_2, L)$ for some $s_2 \in [0, L)$, then either $s_2 = 0$ or we have the regular case (R) on $J_1 = (s_1, s_2)$ for some $s_1 \in [0, s_2)$. Furthermore, if $s_1 \neq 0$, a switching from case (D) to case (R) in s_1 is impossible.

From that obviously follows that case (D) cannot occur at all in this setup.
(i) $H \equiv 0$ implies $H_1 = 0$ in case (A). Since $H_2 = H_3 = 0$ anyhow in this case this contradicts $(H_1, H_2, H_3) \neq 0$, see Lemma 4.2.3 (2. and 8.).
(ii) We have $0 \neq H_4|_I = $ constant and $H_4(L) = 0$ by transversality condition (4.7). Since H_4 is continuous we get the first claim. Because of the same reason switchings between case (D) and the cases (B) or (C) are impossible (at the switching parameter H_4 would have to be 0).

(iii) Assume that, without loss of generality, $u_2|_J = u_3|_J = 1$. Since $H_1(L) = 0$, we can normalize the Hamiltonian (since $\lambda_0 \neq 0$) such that

$$(H_1(L), \ldots, H_6(L)) = (0, \cos\varphi, \sin\varphi, 0, 0, 0)$$

with some fixed $\varphi \in [0, 2\pi)$. By Lemma 4.2.3 (3. and 4.) we get on J by integration:

$$H_4(s) = \frac{\sqrt{2}}{2} \sin\left(\frac{\pi}{4} + \varphi\right) \left[1 - \cos(\sqrt{2}(s - L))\right],$$

$$H_5(s) = \frac{\sqrt{2}}{2} \sin\varphi \sin(\sqrt{2}(s - L)),$$

$$H_6(s) = -\frac{\sqrt{2}}{2} \cos\varphi \sin(\sqrt{2}(s - L)).$$

The function H_5 and H_6 have no zeros on $[0, L)$ since $\sin(\sqrt{2}(s - L))|_{[0,L)} \neq 0$ for $L < \frac{\pi}{\sqrt{2}}$ ($\sin\varphi \neq 0$ and $\cos\varphi \neq 0$ since H_5 and H_6 do not vanish on J). Thus switchings are impossible and we have the claim.

(iv) Assume that $u_3|_{J_2} = 1$ (without loss of generality). Since $H_1(L) = 0$ and $H_3|_{J_2} = 0$, we can normalize the Hamiltonian such that

$$(H_1(L), \ldots, H_6(L)) = (0, 1, 0, 0, 0, 0).$$

By Lemma 4.2.3 (3. and 4.) we get on J_2:

$$H_1(s) = \sin(s - L),$$
$$H_2(s) = \cos(s - L),$$
$$H_6(s) = -\sin(s - L).$$

Since there are no zeros of H_6 on $[0, L)$ for $L < \pi$, we only need to consider switchings at s_2 from the regular case to case (B). At this switching parameter we have

$$(H_1(s_2), \ldots, H_6(s_2)) = (\sin(s_2 - 1), \cos(s_2 - 1), 0, 0, 0, -\sin(s_2 - 1)) =$$
$$= (\sin\vartheta, \cos\vartheta, 0, 0, 0, -\sin\vartheta)$$

with $\vartheta = s_2 - L \in (-\frac{\pi}{2}, 0)$. Now on the interval J_1 we get by Lemma 4.2.3 (3. and 4.)

$$H_6(s) = -H_1(s) = -\sin\vartheta \cos\left(\sqrt{2}(s - s_2)\right) - \frac{\sqrt{2}}{2} \cos\vartheta \sin\left(\sqrt{2}(s - s_2)\right)$$

and for all $\vartheta \in (-\frac{\pi}{2}, 0)$ and all $s \in [0, s_2)$ there are no further zeros of H_6 since

$$\frac{\sqrt{2}}{2} \tan\left(\sqrt{2}(s - s_2)\right) < 0 \leq -\tan\vartheta.$$

Thus a switching to case (D) at s_1 is impossible in this case.
Case (C) on the interval (s_2, L) works as case (B) and we are done. ∎

Corollary 4.3.10 *If $L < \frac{\pi}{2}$, $u_1|_{[0,L]} = 0$ and Conjecture 4.3.4 is true, then optimal solutions are concatenations of at most three parts each of which is either a straight line segment (case (A)), an arc of a circle (different planes possible) of radius 1 (cases (B) and (C)) or an arc of a circle of radius $\frac{1}{\sqrt{2}}$ (case (R)).*

But even then many different strategies that can be optimal. Using the necessary conditions derived from PMP we can exclude quite a few of the strategies.

Lemma 4.3.11 *The following strategies can be excluded (* denotes any of the cases (A), (B), (C) or (R)):*

1. **(A)(A) and (A)(A)*,*

2. *All strategies with only (A) and (B) or only (A) and (C) as well as all strategies with only (A) and (R) with at least one (A) part,*

3. **(B)(C) and (B)(C)(A) (and *(C)(B) and (C)(B)(A)),*

4. **(B)(R) (and *(C)(R))*

5. *(A)(R)* (and *(R)(A)),*

6. *(B)(R)(B) (and (C)(R)(C))*

Proof   1. is obvious since concatenations of different straight line segments cannot be continuously differentiable.

2. The strategies that involve only (A) and (B) or (A) and (C) all lie in one plane and cannot be optimal by Theorem 3.2.11. Analogously, if only the cases (A) and (R) are involved, between a straight line segment (A) and a switching point or the terminal point can only be full circles of type (R) which can be neglected.

3. From Lemma 4.2.3 (3. and 4.) and Lemma 4.3.1 follows that the (C) part (or the (B) part) would have to be of length 2π which is not optimal.

4. At the switching from the (B) part to the (R) part, denoted by s_2, we have, after suitable normalization (recall $\lambda_0 \neq 0$), $(H_1(s_2), \ldots, H_6(s_2)) = (\cos\varphi, \sin\varphi, 0, 0, 0, k)$ with $\varphi \in [0, 2\pi)$ and $k \in \mathbb{R}$. Then, on the interval (s_2, L), we assume without loss of generality that $u_2 = u_3 = 1$ and get by Lemma 4.2.3 (3. and 4.) that $H_5(s) = \frac{1}{2}(\cos\varphi + k)\left[1 - \cos(\sqrt{2}(s - s_2))\right]$ and $H_5(L) \neq 0$ which is a contradiction to (4.7). The other case works the same way.

5. Denote the switching parameter between the (A) part and the (R) part with s_1. After normailization we have $(H_1(s_1), \ldots, H_6(s_1)) = (1, 0, 0, 0, 0, 0)$. Then, for $s > s_1$, we assume without loss of generality that $u_2 = u_3 = 1$ and have by Lemma 4.2.3 (3. and 4.) $H_5(s) = H_6(s) = \frac{1}{2}\left[1 - \cos(\sqrt{2}(s - s_1))\right]$ and there are no further zeros between s_1 and L which leads to a contradiction. The other case works the same way.

6. At the switching parameter s_1 from (B) to (R) we have, after normalization, $(H_1(s_1), \ldots, H_6(s_1)) = (\cos\varphi, \sin\varphi, 0, 0, 0, k)$ for some $\varphi \in [0, 2\pi)$ and $k \in \mathbb{R}$. For $s > s_1$ we assume without loss of generality that $u_2 = u_3 = 1$ and have by by Lemma 4.2.3 (3. and 4.) $H_5(s) = \frac{1}{2}(\cos\varphi + k)\left[1 - \cos(\sqrt{2}(s - s_1))\right]$. Since $H_5 \not\equiv 0$ the first factor does not vanish, but the second factor has no zeros in $(s_1, L]$ and we arrive again at a contradiction. The other case works the same way.

■

Obviously there are many possible strategies left that might be optimal, namely

(R)(B)(A)	(R)(C)(A)	(B)(R)(C)	(C)(R)(B)
(B)(R)(R)	(C)(R)(R)	(R)(B)(B)	(R)(C)(C)
(R)(R)(B)	(R)(R)(C)	(R)(R)(R)	

All these strategies can be realized with various control combinations, e.g., in each case (R) both controls u_2 and u_3 can take the two values ± 1 which gives four possibilities. Plugging all these strategies into the control system (4.2) with variable switching times $0 \le s_1 \le s_2 \le L$ gives many surfaces (parametrized by the switching times s_1 and s_2) that contain the optimal solutions.
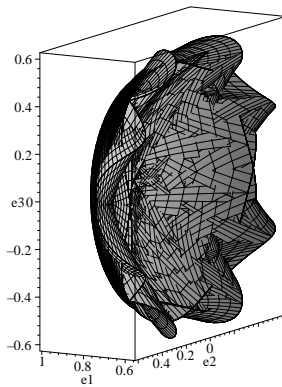

Figure 4.2: Outside boundary of the workspace, $L = 1$

Unfortunately, we are not even able to describe the workspace completely under

the given restriction. Nevertheless, we plot the surfaces to all strategies which are left after the considerations above. Their union contains the boundary of the workspace and for $L = 1$ (still assuming that Conjecture 4.3.4 is true) it is depicted in Figure 4.2.

In Figure 4.3 we show the workspace from different angles in order to give an idea how it looks like form different sides.
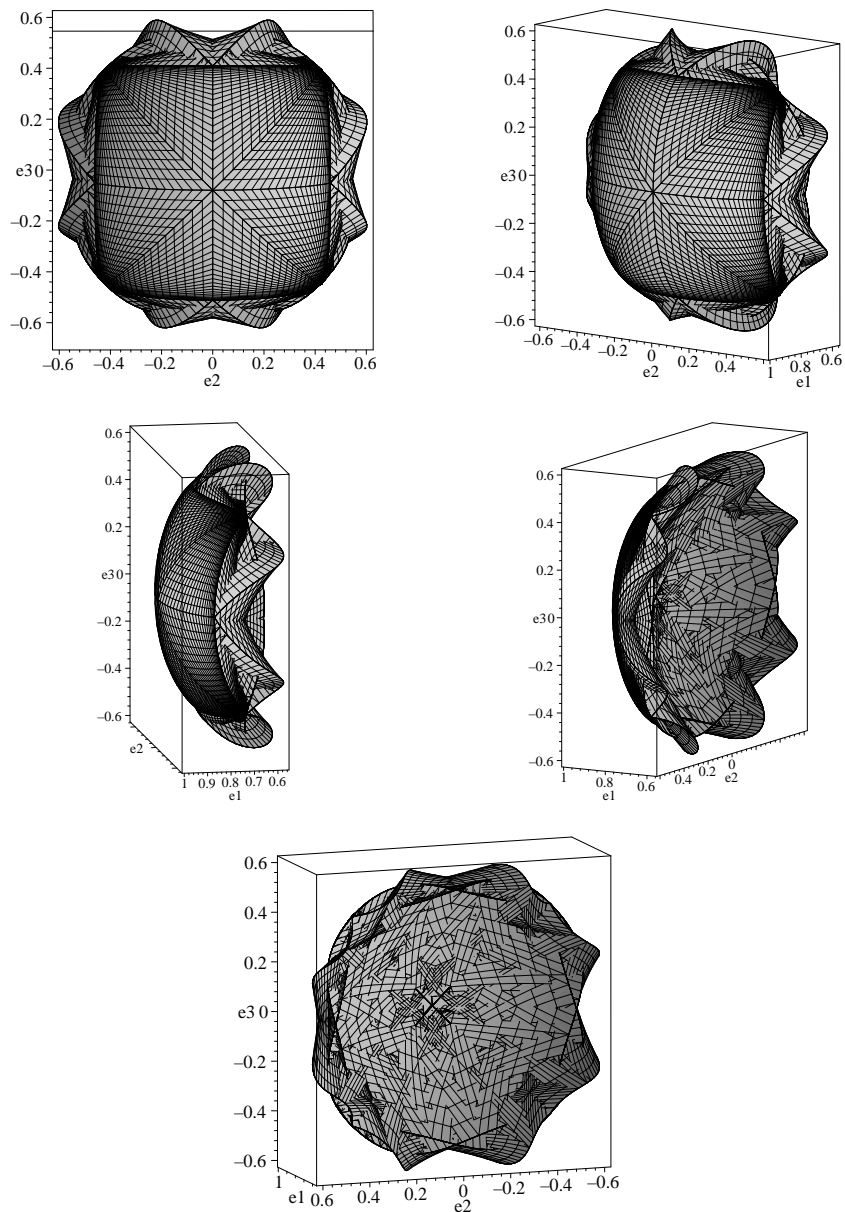

Figure 4.3: Figure 4.2 for angles $0^o, 40^o, \ldots, 160^o$

Since it is not easy to get an idea of the topology of the workspace from these pictures, we present a few coss-sections of Figure 4.2 from the bottom to the top (with respect to the e_3-coordinate) in Figure 4.4. The cross-sections all have
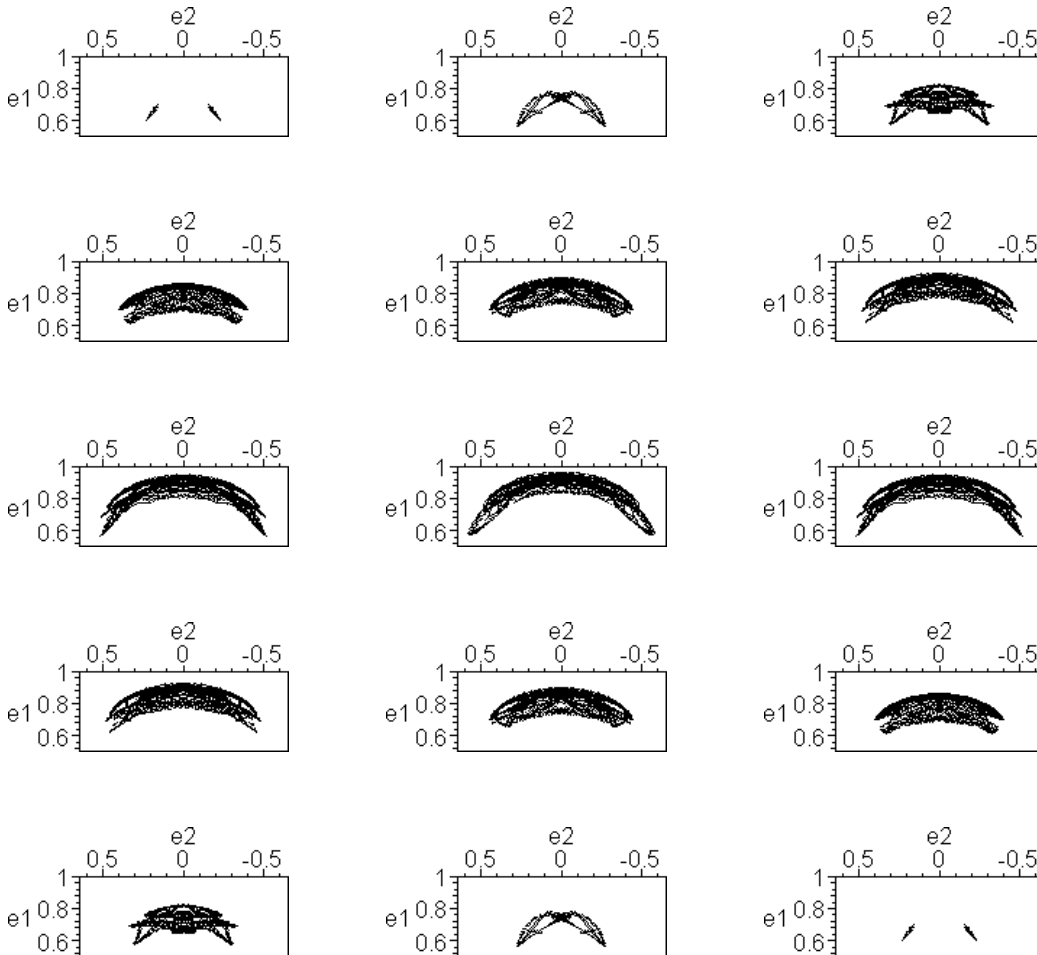

Figure 4.4: Horizontal cross-sections of the workspace at $L = 1$

the same thickness (which is greater than zero, otherwise it would be almost impossible to see anything at all) and range from -0.7 to 0.7 in steps of 0.1. These give further insight particularly of the interior of the workspace. Here, at $L = 1$, they give the impression that no holes appear in the interior of the workspace and that it is simply connected.

If we consider manipulators of different lengths and still assume that Conjecture 4.3.4 is true and that Lemma 4.3.11 also holds for lengths $L \geq \frac{\pi}{2}$, then we get the following, topologically more interesting workspaces. For varying lengths we expect that effects show up which are similar to those in the 2D case.

For $L = \frac{\pi}{\sqrt{2}}$ the ouside of the workspace looks like in Figure 4.5. From different
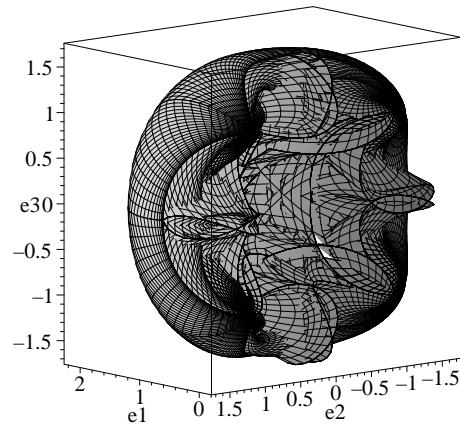
Figure 4.5: Outside boundary of the workspace, $L = \frac{\pi}{\sqrt{2}}$

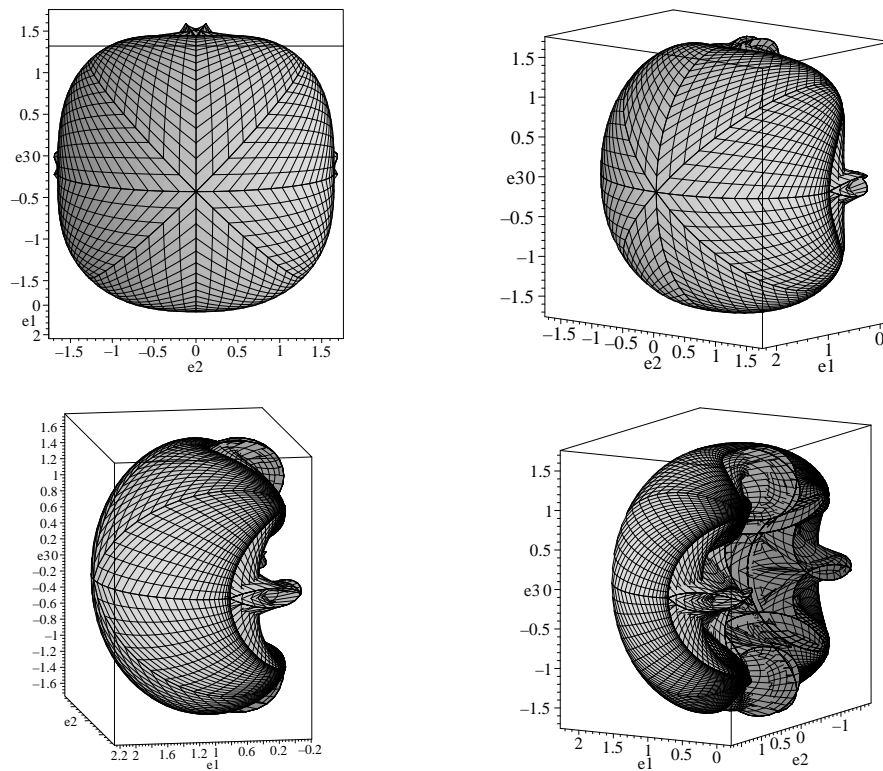angles it can be seen in Figures 4.6 and 4.7.

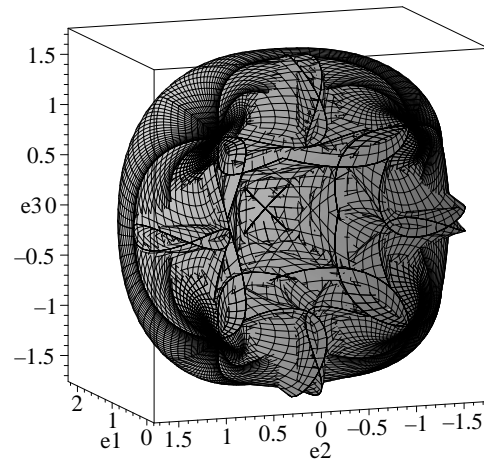Figure 4.6: Outside boundary of the workspace with $L = \frac{\pi}{\sqrt{2}}$ for angles 0°, $40^o, \ldots, 140^o$

Figure 4.7: Outside boundary of the workspace with $L = \frac{\pi}{\sqrt{2}}$ for angle 160°

Again, we present a few coss-sections of Figure 4.5 ranging from -1.7 to 0 in 0.1 steps in the e_3-coordinate in Figure 4.13. Because of the symmetry with respect to the e_1-e_2-plane the pictures in the range from 0 to 1.7 look the same. At this length, still no holes seem to appear in the interior of the workspace.
As in the 2D case, the workspace changes continuously with growing length L. At $L = \frac{1.5\pi+1}{\sqrt{2}}$ a hole in the middle of the workspace seems to appear. For values slightly smaller than that the workspace looks as depicted in Figure 4.8.
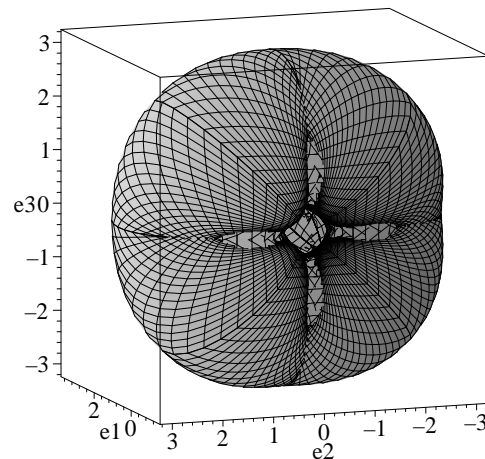

Figure 4.8: Outside boundary of the workspace at L slightly smaller than $\frac{1.5\pi+1}{\sqrt{2}}$

In order to get an idea of the interior, we cut off the upper half (with respect to the e_3-coordinate) and get Figure 4.9.
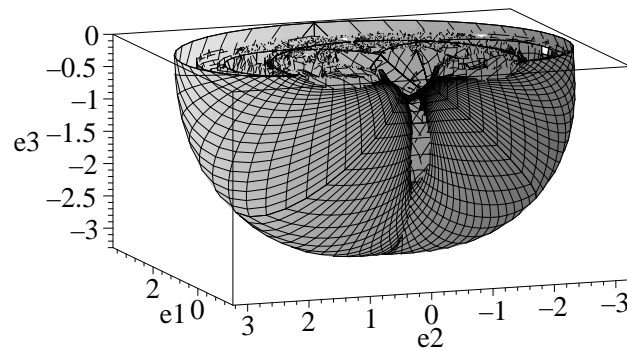

Figure 4.9: Lower half of Figure 4.8

There still seems to be no holes in the interior, but from these figures one can imagine that one hole appears for growing values of L.
For $L = \frac{1.5\pi + 1}{\sqrt{2}}$ the workspace looks as in Figure 4.10.

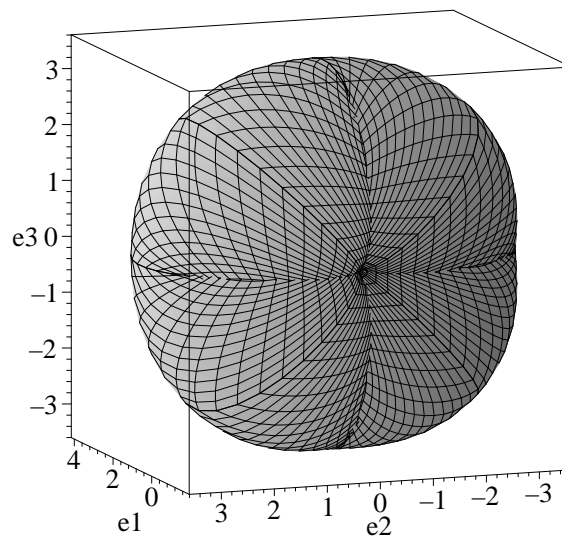Figure 4.10: Outside boundary of the workspace with $L = \frac{1.5\pi + 1}{\sqrt{2}}$

Again, we present a few coss-sections of Figure 4.10 in Figure 4.14. From these and Figures 4.8 and 4.9 we see that the workspace is simply connected but a hole in the interior occurs. Up to the normalizing factor $\frac{1}{\sqrt{2}}$ this is exactly the value when a hole occured in the 2D case. To confirm this result numerically,

we descretesize the possible (constant) control values and the possible switching parameters, i.e., $u_2, u_3 \in \{-1, -\frac{1}{2}, 0, \frac{1}{2}, 1\}$ and $s_1, s_2 \in \{0, \frac{1}{4}, \frac{1}{2}, \frac{3}{4}, 1\}$ with $s_1 \leq s_2$. The lower half of points that the manipulator can reach then looks as depicted in Figure 4.11.
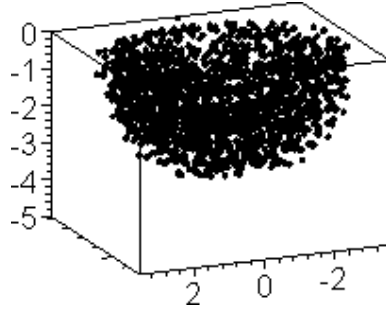
Figure 4.11: Lower half of discretesized workspace at $L = \frac{1.5\pi + 1}{\sqrt{2}}$

The cross-section of Figure 4.11 around $e_3 = 0$ combined with the corresponding cross-section of Figure 4.10 looks as in Figure 4.12.

Figure 4.12: Combination of Figure 4.11 and Figure 4.10

This strengthens the believe that a hole appears. For large values of L we believe that the workspace has no holes in the interior as in the 2D case.

Figure 4.13: Horizontal cross-sections of the workspace with $L = \frac{\pi}{\sqrt{2}}$

Figure 4.14: Horizontal cross-sections of the workspace with $L = \frac{1.5\pi+1}{\sqrt{2}}$

Chapter 5

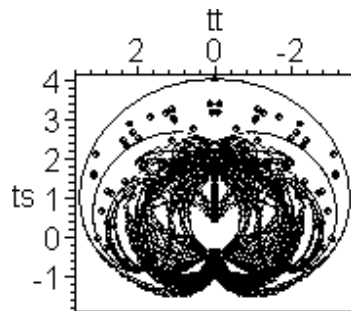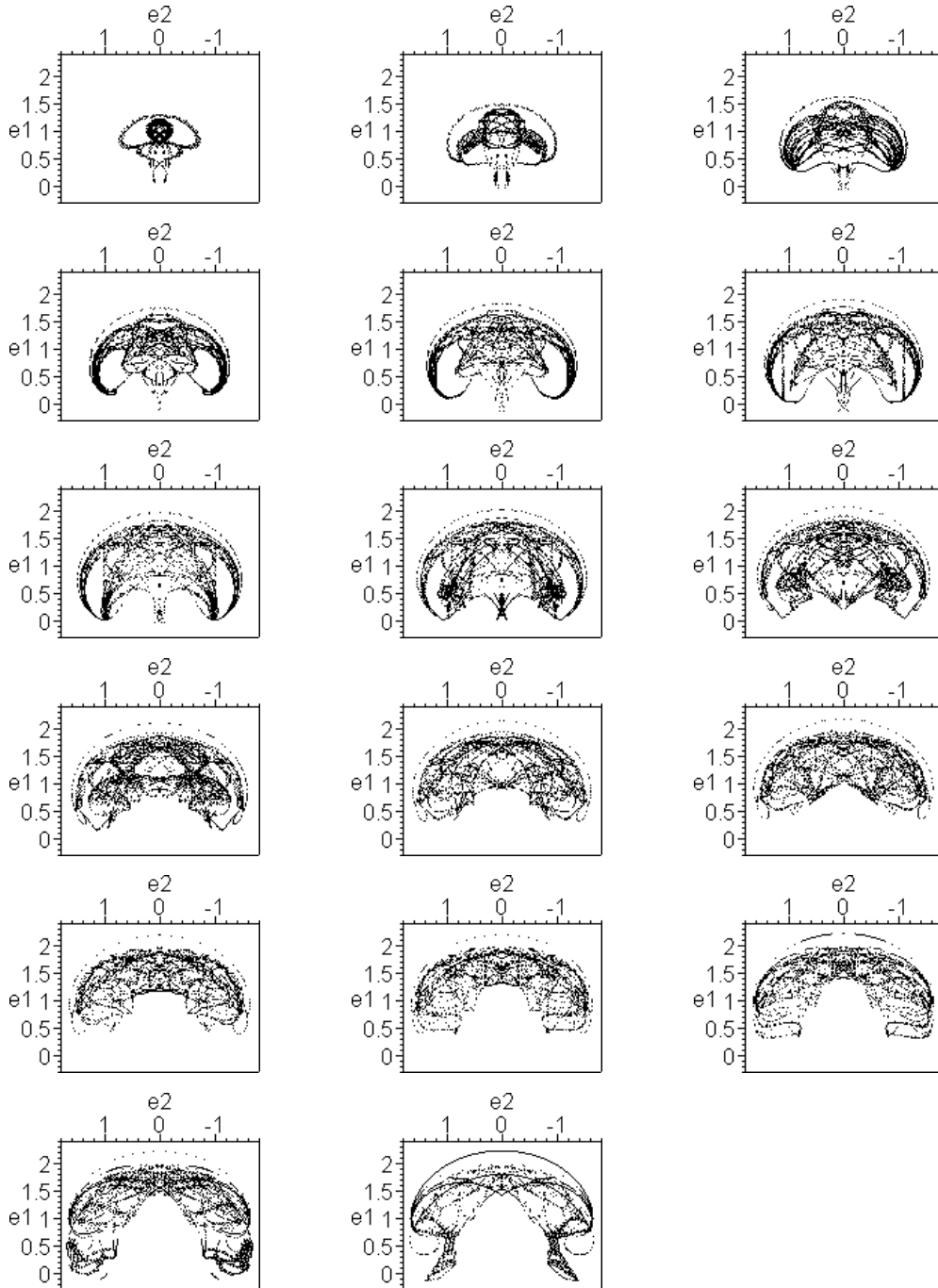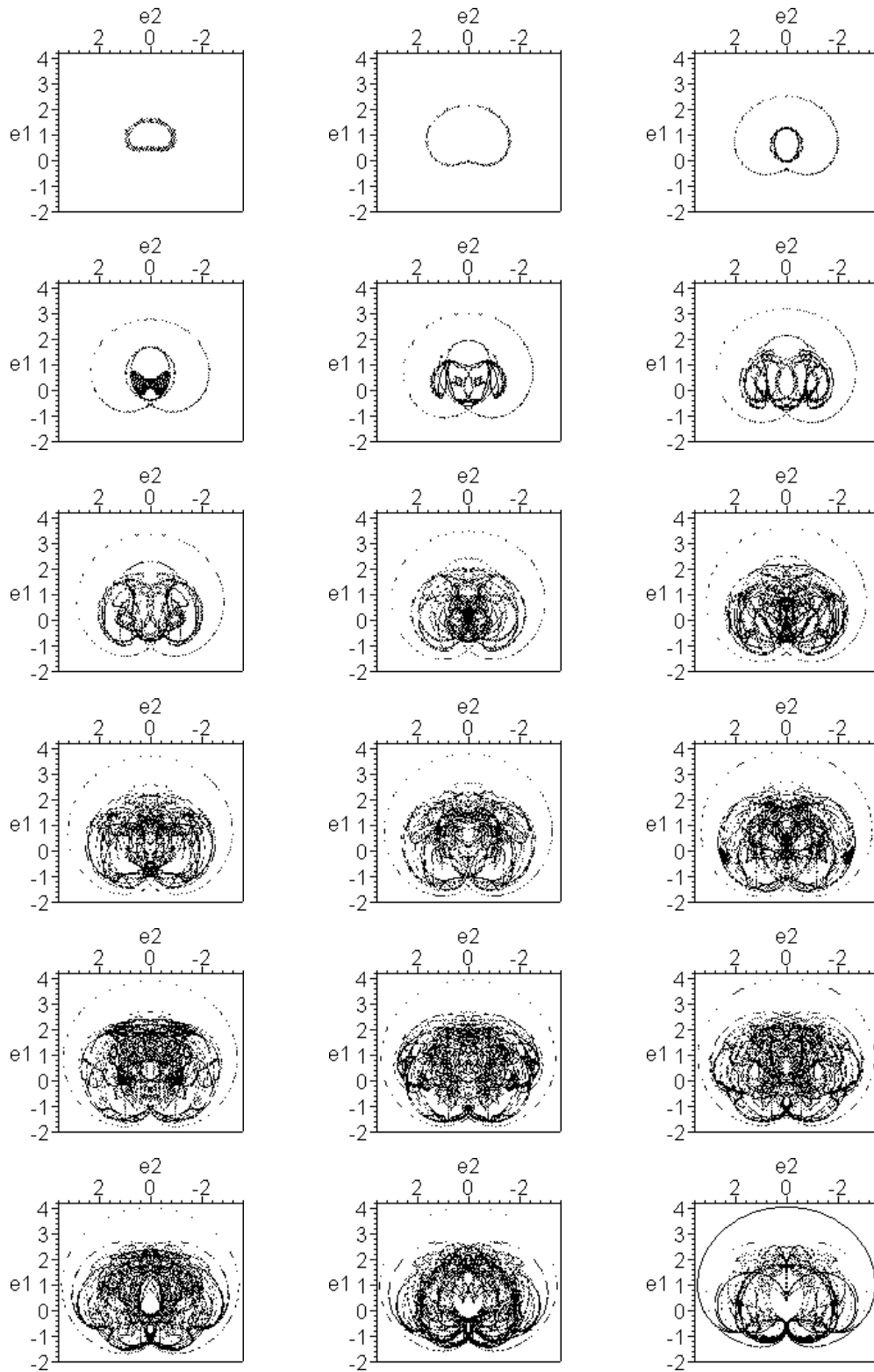# Conclusions

Since there is an increasing need for very flexible robotic manipulators it is quite natural to investigate 2D and 3D hyper-redundant robotic manipulators. Many authors have already introduced various models for discrete robots of that type and described their workspaces and possible (optimal) control. It is quite natural to extend these ideas to manipulators with distributed bending moments in order to describe an 'ideal' setup.

In this work simple models for continuous robotic manipulators were introduced, even though it might be impossible to construct these today. The main goal of the thesis was to determine their workspaces. Basic properties of the workspaces as compactness or symmetries were shown by elementary functional analytical and geometric methods.

In the 2D case (Chapter 3) it was possible to completely describe the workspaces with and withput prescription of the terminal orientation. By applying optimal control techniques, mainly Pontryagin's Maximum Principle, it was possible to determine a 'small' family of manipulator configurations that contains the configurations when the manipulator reaches the boundary of its workspace. Further geometric considerations completed the approach. The methods applied were very similar to those used for the solution of Dubins' problem and in this context it was helpful to solve Dubins' problem for free terminal direction (Chapter 2).

The 3D case (Chapter 4) was much more complicated since we were no longer in the single input setup of the 2D case. Unfortunately, the methods used for the solution of the 2D case did not suffice to completely determine the workspaces. Only in a simplified version with strict hypotheses the possible workspaces could be illustrated. Nevertheless, quite a few necessary conditions for manipulators reaching the boundary of its workspace were derived from Pontryagin's Maximum Principle. Furthermore, many useful conclusions concerning possible switching strategies were drawn.

This thesis leaves open many interesting questions for future research. Some of them are listed below.

1. The 3D workspaces of the model used in this work still have to be determined completely. Optimal control techniques seem not to suffice and one should consider other methods additionally.

2. Other models that are closer to real manipulators should be investigated. The results can then be compared with the workspaces derived here. Futhermore, a detailed comparison with descrete models could be carried out.

3. Dynamics: We only determined (static) workspaces here. Thus there is still the need to determine the controls (forces) that take one manipulator configuration into another. This also affords the use of suitable models. Since the manipulator is described by a continuous curve, this will involve control theory for partial differential equations which affords completely different methods.

4. 3D Dubins' problem: The model of the 3D manipulators could also be used as a model for 3D Dubins' problem. The main question, that arises, is: How do shortest paths in $\mathbb{R}^3$ look like then? The same difficulties as in the determination of the 3D workspaces should appear. Note that this model is different than those used in [31] and [41].

Bibliography

[1] J. D. Boissonnat, A. Cerezo and J. Leblond, *Shortest paths of bounded curvature constraints,* J. Intell. Robot. Syst. 11, No. 1-2, 5-20 (1994)

[2] W. G. Boltjanski, *Mathematische Methoden der optimalen Steuerung,* Akademische Verlagsgesellschaft Geest & Portig K.-G., Leipzig (1971)

[3] X.-N. Bui, P. Souères, J.-D. Boissonnat and J.-P. Laumond, *Shortest path synthesis for non-holonomic robots moving forwards,* Research report 2153, INRIA, Sophia Antipolis, France (1994)

[4] X.-N. Bui, P. Souères, J.-D. Boissonnat and J.-P. Laumond, *Shortest path synthesis for Dubins' non-holonomic robot,* IEEE Int. Conf. on Robotics and Automation, San Diego (1994)

[5] J. Burdick, J. Radford and G. S. Chirikjian, *A Sidewinding Locomotion Gait for Hyper-Redundant Robots,* Advanced Robotics, vol. 9, No. 3, pp. 195-216 (1995)

[6] L. Cesari, *Optimization-Theory and Applications,* Springer Verlag, New York, (1983)

[7] G. S. Chirikjian and J. Burdick, *The Kinematics of Hyper-Redundant Robotic Locomotion,* IEEE Trans. on Robotics and Automation, vol. 11, no. 6, pp. 781-793 (1995)

[8] G. S. Chirikjian and J. Burdick, *A Modal Approach to Hyper-Redundant Manipulator Kinematics,* IEEE Trans. on Robotics and Automation , vol. 10, no. 3, pp. 343-354 (1994)

[9] G. S. Chirikjian and J. Burdick, *Kinematically Optimal Hyper-Redundant Manipulator Configurations,* IEEE Trans. on Robotics and Automation, vol. 11, no. 6, pp. 794-806 (1995)

[10] G. S. Chirikjian and J. Burdick, *A Hyper-Redundant Manipulator,* IEEE Robotics and Automation Magazine, pp. 22-29 (1994)

[11] G. S. CHIRIKJIAN AND J. BURDICK, *Design and experiments with a 30 degree-of-freedom robot,* Proc. IEEE Int. Conf. Robotics and Automation, Atlanta, GA, May 2-5, vol. 3, pp. 113-119 (1993)

[12] G. S. CHIRIKJIAN AND J. BURDICK, *A Geometric Approach to Hyper-Redundant Manipulator Obstacle Avoidance,* ASME J. of Mechanical Design, vol. 114, no. 4, pp. 580-585 (1992)

[13] G. S. CHIRIKJIAN, *Hyper-redundant manipulator dynamics: a continuum approximation,* Advanced Robotics, Vol. 9, No. 3, pp. 217-243 (1995).

[14] G. S. CHIRIKJIAN AND I. EBERT-UPHOFF, *Numerical convolution on the euclidean group with applications to workspace generation,* IEEE Transactions on Robotics and Automation, Vol. 14, No. 1, pp. 123-136 (1998).

[15] I. EBERT-UPHOFF AND G. S. CHIRIKJIAN, *Efficient workspace generation for binary manipulators with many actuators,* Journal of Robotic Systems, Vol. 12, No. 6, pp. 383-400 (1995).

[16] E. J. COCKAYNE AND G. W. C. HALL, *Plane motion of a particle subject to curvature constraints,* SIAM J. Control, Vol. 13, No. 1, pp. 197-220 (1975)

[17] L. E. DUBINS, *On curves of minimal length with a constraint on average curvature, and with prescribed initial and terminal positions and tangents,* Amer. J. Math. 79, pp. 497-516 (1957)

[18] S. HIROSE S AND A. MORISHIMA, *Kinematic control of active cord mechanism with tactile sensors,* Proc. 2nd Int. CISM-IFT Symp. Theory and Practice of Robots and Manipulators, pp. 241-252 (1976)

[19] S. HIROSE, *Biologically inspired robots, snake-like locomotors and manipulators,* Oxford Science Publications, Oxford (1993)

[20] H. HUIJBERTS, *Dynamic feedback in nonlinear synthesis problems,* PhD thesis at the Twente University, Enschede (1991)

[21] A. ISIDORI, *Nonlinear control systems,* Springer Verlag, 3rd edition, New York Berlin Heidelberg Tokyo (1996)

[22] V. JURDJEVIC, *Geometric Control Theory,* Cambridge Studies in Advanced Mathematics, Cambridge University Press (1997)

[23] B. KLAASSEN AND K.-L. PAAP, *GMD-SNAKE2: A Snake-Like Robot Driven by Wheels and a Method for Motion Control,* Proc. 1999 IEEE Int. Conf. on Robotics and Automation, Detroit, Michigan, pp. 3014-3019 (1999)

[24] J.-P. LAUMOND AND P. SOUÈRES, *Metric induced by the shortest paths for a nonholonomic car-like mobile robot,* Proc. Int. Conf. Intelligent Robots and Systems (IROS), Yokohama (1993)

[25] R. LINNEMANN, K.-L. PAAP AND B. KLAASSEN, *Motion Control of a Snake-Like Robot,* IEEE Procedings of the EUROBOT99, pp. 1-10 (1999)

[26] A. A. MARKOV, *Some examples of the solution of a special kind of problem in greatest and least quantities,* Soobshch Karkovsk. Mat. Obshch. 1, pp. 250-276 (1887)

[27] F. MUNERATO, D. MIHALACHI AND C. LAURENT, *Flexible Mini-Robot with Autonomous Motion,* Proc. ICRAM 99, Istanbul (1999)

[28] I. P. NATANSON, *Theorie der Funktionen einer Veränderlichen,* Verlag Harri Deutsch, Thun - Frankfurt/Main, (1981)

[29] H. NIJMEIJER AND A. VAN DER SCHAFT, *Nonlinear dynamical control systems,* Springer Verlag, 2nd printing, New York Berlin Heidelberg Tokyo (1991)

[30] P. J. OLVER, *Applications of Lie groups to differential equations,* Springer Verlag, New York Berlin Heidelberg Tokyo (1986)

[31] R. F. M. PÉREZ, *Non-Euclidean Dubins' problem: A control theoretic approach,* PhD thesis at the University of Toronto (1995)

[32] L. S. PONTRYAGIN, V. G. BOLTYANSKY, R. V. GAMKRELIDZE AND E. F. MISCHENKO, *The mathematical theory of optimal processes,* Wiley, New York (1962)

[33] J. A. REEDS AND R. A. SHEPP, *Optimal paths for a car that goes both forward and backward,* Pacific J. Math., Vol. 145, No. 2 (1990)

[34] A. B. SLATKIN AND J. BURDICK, *The development of a Robotic Endoscope,* Proc. 1995 IROS Conf., Pittsburg, PA. (1995)

[35] E. D. SONTAG, *Mathematical control theory,* Texts in Applied Mathematics, Springer Verlag, Berlin Heidelberg New York (1990)

[36] P. SOUÈRES AND J.-P. LAUMOND, *Shortest path synthesis for a car-like robot,* IEEE Transactions on Automatic Control, Vol. 41, No. 5, (1996)

[37] P. SOUÈRES AND J.-D. BOISSONNAT, *Optimal Trajectories for Nonholonomic Mobile Robots,* Robot motion planning and control, J.-P. Laumond (ed.), Lecture Notes in Control and Information Sciences 229, pp. 93-170 (1998)

[38] P. Souères, J.-Y. Fourquet and J.-P. Laumond, *Set of reachable positions for a car,* IEEE Trans. Aut. Control, Vol. 39, No. 8 (1994)

[39] J. Steigenberger, *Classical framework for nonholonomic mechanical control systems,* Rep. SYCON-91-10, Rutgers Univ. (1991)

[40] H. J. Sussmann and W. Tang, *Shortest paths for the Reeds-Shepp car: A worked out example of the use of geometric techniques in nonlinear optimal control,* Rep. SYCON-91-10, Rutgers Univ. (1991)

[41] H. J. Sussmann, *Shortest 3-dimensional paths with a prescribed curvature bound,* Proc. 34th CDC, New Orleans, LA (1995)

[42] F. A. Valentine, *Konvexe Mengen,* Bibliographisches Institut Mannheim, Hochschultaschenbücher-Verlag, Mannheim (1968)

Zusammenfassung der Arbeit

In diesem Kapitel wird eine Zusammenfassung in deutscher Sprache gegeben. Entsprechende Abbildungen sind vorne im Text nachzulesen. Die einzelnen Abschnitte sind wie die Kapitel in der Arbeit numeriert.

Einleitung

Manipulatoren und Industrieroboter spielen eine wichtige Rolle sowohl in der Produktion und Konstruktion als auch in der Medizin. Üblicherweise ist deren Freiheitsgrad nicht sonderlich hoch, d.h., sie bestehen aus wenigen Gliedern, die durch translatorische oder rotatorische Gelenke verbunden sind. Daher sind sie relativ einfach zu steuern und auch nach vielen Wiederholungen sind einzelne Konfigurationen sehr präzise zu erreichen. Dafür treten aufgrund ihrer recht starren Struktur allerdings Schwierigkeiten bei der Vermeidung von Kollisionen mit Hindernissen in ihrem Arbeitsbereich auf. Dies will man insbesondere bei medizinischen Anwendungen vermeiden, und daher ist die Erforschung flexiblerer Manipulatoren sehr interessant.

Ein Meilenstein war die Einführung des 'Active Cord Mechanism' durch Hirose im Jahre 1976. Seitdem sind 'hyper-redundante' Roboter von großem Interesse für Ingenieure und Mathematiker, die sowohl sich schlangenförmige fortbewegende Fahrzeuge als auch elefantenrüsselartige Manipulatoren verschiedenster Art untersuchen.

Viele Ansätze mit diskreten Modellen wurden bereits bearbeitet. In dieser Arbeit werden zwei- und dreidimensionale Modelle kontinuierlicher Manipulatoren eingeführt und die Erreichbarkeitsmengen dieser beschrieben. Da die Gleichungen, die die zweidimensionalen Manipulatoren beschreiben, dieselben wie die Bewegungsgleichungen von Dubins' Problem sind, wird auch diese Fragestellung hier nochmals aufgegriffen.

Dubins' Problem

Im 2. Kapitel der Arbeit wird Dubins' Problem mit freier Endrichtung gelöst, welches das folgende ist:

Finde den kürzesten stetig differenzierbaren Weg zwischen einem Anfangs- und einem Endpunkt mit vorgeschriebener Tangentenrichtung am Anfangspunkt und der Krümmungsbeschränkung $|\kappa| \leq 1$ fast überall.

Bei Dubins' ursprünglichem Problem war zusätzlich die Tangentenrichtung am Endpunkt vorgeschrieben. Die Bewegungsgleichungen lauten folgendermaßen, wenn der Weg durch die Bogenlänge parametrisiert wird:

$$\begin{aligned}
\dot{x}(t) &= \cos\theta(t), & x(0) &= 0, \\
\dot{y}(t) &= \sin\theta(t), & y(0) &= 0, \\
\dot{\theta}(t) &= u(t), & \theta(0) &= 0,
\end{aligned} \tag{Z.1}$$

Nun wird zu jedem $(x_T, y_T) \in \mathbb{R}^2$ die minimale Bogenlänge $T \geq 0$ gesucht, so daß der Endpunkt von $(x(\cdot), y(\cdot))$ genau $(x(T), y(T)) = (x_T, y_T)$ ist und $\theta(T)$ beliebig ist. Formal stellt man das folgende Optimalsteuerproblem:

$$\begin{aligned}
&\text{Minimiere } T \geq 0 \text{ unter der Nebenbedingung } (Z.1) \\
&\text{mit } (x(T), y(T)) = (x_T, y_T) \text{ und } |u(t)| \leq 1 \; \forall \, t \in [0, T].
\end{aligned} \tag{Z.2}$$

Dubins' Problem mit freier Endrichtung

Zunächst wird gezeigt, daß stets eine optimale (nicht notwendigerweise eindeutige) Lösung existiert. Mit Hilfe des Maximumprinzips von Pontryagin werden notwendige Bedingungen für optimale Lösungen hergeleitet, mit deren Hilfe gezeigt werden kann, daß die Lösungen Aneinanderreihungen von endlich vielen Kreisbögen mit Radius 1 (C) und Geradenstücken (L) sind. Weiterhin kann die Anzahl der Umschaltungen auf höchstens eine Umschaltung eingeschränkt werden, und schließlich wird bewiesen, daß alle optimalen Lösungen der Form CC, CL, C oder L sind. Zudem wird angegeben, für welche Endpunkte $(x_T, y_T) \in \mathbb{R}^2$ die einzelnen Strategien angewandt werden müssen.

Dubins' ursprüngliches Problem

Am Ende des Kapitels wird zudem ein neuer, kurzer Beweis von Dubins' ursprünglichem Resultat präsentiert. Insbesondere wird ein neuer Weg aufgezeigt, wie man beweisen kann, daß Aneinanderreihungen von vier oder mehr Kreisbögen nicht optimal sein können.

Erreichbarkeitsmengen zweidimensionaler kontinuierlicher Manipulatoren

Anschließend wird in die Thematik der kontinuierlichen Manipulatoren eingeführt und folgendes Modell zugrundegelegt: Die Mittellinie eines Manipulators der

Länge $L = 1$ wird als zweidimensionale, stetig differenzierbare Kurve der Länge $L = 1$ aufgefasst und durch die Bogenlänge parametrisiert. Die Gleichungen lauten dann analog zu (Z.1):

$$\begin{array}{rclrcl}
x'(s) & = & \cos\theta(s), & x(0) & = & 0, \\
y'(s) & = & \sin\theta(s), & y(0) & = & 0, \\
\theta'(s) & = & \kappa(s), & \theta(0) & = & 0,
\end{array} \qquad \text{(Z.3)}$$

mit $s \in [0,1]$ und Krümmung κ mit $|\kappa| \leq M$. Führt man nun

$$\mathcal{F} := \{(x(\cdot), y(\cdot), \theta(\cdot)\}$$

als die Menge von Lösungsfunktionen von (Z.3) für alle zulässigen κ ein und für $\Omega \subset \mathcal{F}$

$$P_\Omega := \{(x_1, y_1) \in \mathbb{R}^2 \,:\, (x(1), y(1)) = (x_1, y_1) \text{ für ein } (x(\cdot), y(\cdot), \theta(\cdot)) \in \Omega\},$$

so ist die Erreichbarkeitsmenge des Manipulators definiert durch

$$W := P_\mathcal{F} \quad \text{oder} \quad W_{\theta_1} := \{(x_1, y_1) \in W \,|\, \theta(1) = \theta_1 \bmod 2\pi\}$$

für eine vorgegebene Endrichtung $\theta_1 \in [0, 2\pi)$.

Manipulatoren mit freier Endrichtung

Zunächst wird nur W untersucht. Es wird gezeigt, daß die Erreichbarkeitsmenge W symmetrisch zur x-Achse, wegzusammenhängend und kompakt ist. Um den Rand der Erreichbarkeitsmenge zu charakterisieren, wird die folgende 2-parametrige ($(x_0, y_0) \in \mathbb{R}^2$) Familie von Optimalsteuerproblemen mit Nebenbedingung (Z.3) betrachtet

$$J_{x_0, y_0} = (x(1) - x_0)^2 + (y(1) - y_0)^2 \to \min, \qquad \text{(Z.4)}$$

wobei über alle $(x(\cdot), y(\cdot), \theta(\cdot)) \in \mathcal{F}$ (also $(x(1), y(1)) \in W$) minimiert wird. Die Menge der optimalen Lösungen wird mit $\mathcal{G}$ bezeichnet, und offensichtlich gilt $\mathcal{G} \subset \mathcal{F}$. Da gezeigt wird, daß $\mathrm{cl}P_\mathcal{G} = \partial W$ gilt, ist dieses Optimalsteuerproblem zur Bestimmung des Randes ∂W der Erreichbarkeitsmenge sehr gut geeignet. Im Folgenden wird das Optimalsteuerproblem zwar nicht vollständig gelöst, aber mit Hilfe des Maximumprinzips von Pontryagin wird eine hinreichend kleine Familie von Funktionen $\mathcal{B}$ bestimmt, die die optimalen Lösungen enthält und eine Beschreibung des Randes ∂W ermöglicht. Folgende Abbildung dient zur Erläuterung:

$$\begin{array}{ccccc}
\mathcal{F} & \supset & \mathcal{B} & \supset & \mathcal{G} \\
P \downarrow & & P \downarrow & & P \downarrow \\
W = P_\mathcal{F} & \supset & P_\mathcal{B} & \supset & P_\mathcal{G}
\end{array}$$

Die dem Problem zugehörige Hamilton-Funktion lautet mit $\lambda = (\lambda_1, \lambda_2, \lambda_3)^T$

$$H : \mathbb{R}^3 \times \mathbb{R}^3 \times [-M, M] \rightarrow \mathbb{R},$$
$$((x, y, \theta), \lambda, \kappa) \mapsto \lambda_1 \cos\theta + \lambda_2 \sin\theta + \lambda_3 \kappa.$$

Die Funktion $\lambda_3(\cdot)$ ist entscheidend für das Verhalten von $\kappa(\cdot)$, und das Maximumprinzip liefert

$$\kappa(s) = -M \operatorname{sign} \lambda_3(s), \text{ falls } \lambda_3(s) \neq 0,$$

und $\kappa|_I = 0$, falls $\lambda_3|_I = 0$ auf einem Intervall I gilt. Weiterhin folgt, daß $\lambda_3(\cdot)$ stetig differenzierbar ist, und zwischen je zwei Nullstellen von $\lambda_3(\cdot)$ (Umschaltpunkte) gilt die folgende Differentialgleichung

$$\lambda_3''(s) = -M^2 \lambda_3(s) + c M \kappa(s)$$

für ein $c \in \mathbb{R}$. Es folgt direkt, daß optimale Lösungen Aneinaderreihungen von Geradenstücken (L) und Kreisbögen (C) mit Radius $\frac{1}{M}$ sind. Weitere Überlegungen führen dazu, daß es höchstens einen Umschaltpunkt geben kann, und daß optimale Lösungen notwendigerweise der Form CC, CL, C oder L sein müssen (vgl. optimale Lösungen im vorigen Kapitel). Daraufhin werden die Erreichbarkeitsmengen skizziert.

Manipulatoren mit vorgeschriebener Endrichtung

Die Erreichbarkeitsmenge W_{θ_1} für eine vorgeschriebene Endrichtung θ_1 ist ebenfalls kompakt. Mit den gleichen Methoden wie oben wird gezeigt, daß optimale Lösungen des zugehörigen Optimalstuerproblems der Form CCC, CLC, CC, CL, LC, C oder L sind, und die entsprechenden Erreichbarkeitsmengen werden skizziert.

Erreichbarkeitsmengen dreidimensionaler kontinuierlicher Manipulatoren

In diesem Kapitel werden die Erreichbarkeitsmengen von kontinuierlichen, dreidimensionalen Manipulatoren der Länge L untersucht. Analog zum zweidimensionalen Fall wird die Mittellinie durch die Bogenlänge parametrisiert. Es wird angenommen, daß im ausgestreckten Zustand an jedem Punkt der Mittellinie das kanonische Dreibein (mit e_1, e_2 und e_3 bezeichnet) angeheftet wird. Unter Deformationen wird dies zu einer kontinuierlichen, körpereigenen Dreibeinfunktion (mit $a_1(\cdot)$, $a_2(\cdot)$ und $a_3(\cdot)$ bezeichnet). Es werden Rotationen um die Achsen a_i

mit Geschwindigkeiten u_i mit $|u_i| \leq 1$, $i = 1, 2, 3$, zugelassen. Die Gleichungen lauten dann folgendermaßen:

$$
\begin{aligned}
x' &= a_1 \\
a_1' &= u_3 a_2 - u_2 a_3 \\
a_2' &= u_1 a_3 - u_3 a_1 \\
a_3' &= u_2 a_1 - u_1 a_2 \\
x(0) &= 0 \\
a_i(0) &= e_i, \; i = 1, 2, 3
\end{aligned}
\tag{Z.5}
$$

Setzt man $R := (a_1, a_2, a_3) \in \mathbb{R}^{3 \times 3}$ und

$$
S(u) := \begin{pmatrix} 0 & -u_3 & u_2 \\ u_3 & 0 & -u_1 \\ -u_2 & u_1 & 0 \end{pmatrix},
$$

so kann das Kontrollsystem (Z.5) geschrieben werden als

$$
x' = Re_1, \quad R' = RS(u), \quad x(0) = 0, \quad R(0) = I_3.
$$

Analog zum zweidimensionalen Fall wird wieder mit

$$
\mathcal{F} := \{(x(\cdot), R(\cdot)\}
$$

die Menge von Lösungsfunktionen von (Z.5) für alle zulässigen u_1, u_2 und u_3 bezeichnet und für $\Omega \subset \mathcal{F}$

$$
P_\Omega := \{x_1 \in \mathbb{R}^3 \, : \, x(L) = x_1 \text{ für ein } (x(\cdot), R(\cdot)) \in \Omega\}
$$

definiert. Die Erreichbarkeitsmenge des Manipulators ist dann definiert durch $W := P_\mathcal{F}$.

Einige Grundeigenschaften

Es läßt sich zeigen, daß die Erreichbarkeitsmenge W symmetrisch zu der e_1-e_2- und der e_1-e_3-Ebene ist. Außerdem ist W wegzusammenhängend und kompakt. Um den Rand der Erreichbarkeitsmenge zu charakterisieren, wird hier die 3-parametrige ($x_0 \in \mathbb{R}^3$) Familie von Optimalsteuerproblemen mit Nebenbedingung (Z.5) betrachtet:

$$
J_{x_0} = \|x(L) - x_0\|^2 \to \min, \tag{Z.6}
$$

wobei über alle $(x(\cdot), R(\cdot)) \in \mathcal{F}$ (also $x(L) \in W$) minimiert wird. Die optimalen Lösungen existieren und werden mit $\mathcal{G}$ bezeichnet. Ebenso gilt wieder

$\mathcal{G} \subset \mathcal{F}$ sowie $\mathrm{cl} P_{\mathcal{G}} = \partial W$. Mit der Hilfe des Maximumprinzips erhält man einige notwendige Bedingungen, die alle $(x(\cdot), R(\cdot)) \in \mathcal{G}$ erfüllen müssen. Diese Menge wird mit $\mathcal{B}$ bezeichnet. In einer Vermutung wird eine Familie $\mathcal{B}_1 \subset \mathcal{B}$ beschrieben, die $\mathcal{G}$ enthalten könnte, und das folgende Diagramm veranschaulicht diese Zusammenhänge:

$$
\begin{array}{ccccccc}
\mathcal{F} & \supset & \mathcal{B} & \supset & \mathcal{B}_1 & \supset & \mathcal{G} \\[2mm]
P \downarrow & & P \downarrow & & P \downarrow & & P \downarrow \\[2mm]
W = P_{\mathcal{F}} & \supset & P_{\mathcal{B}} & \supset & P_{\mathcal{B}_1} & \supset & P_{\mathcal{G}}
\end{array}
$$

Die Mannigfaltigkeit, auf der sich die Dynamik abspielt, kann wie folgt gewählt werden

$$
M := \left\{ g = \left(\begin{array}{c|c} 1 & 0 \\ \hline x & R \end{array} \right), x \in \mathbb{R}^3, R \in \mathrm{SO}_3(\mathbb{R}) \right\}.
$$

Sie ist isomorph zu $\mathrm{SE}_3(\mathbb{R}) = \mathbb{R}^3 \times \mathrm{SO}_3(\mathbb{R})$. Setzt man

$$
\tilde{A}_4 := \begin{pmatrix} 0 & 0 & 0 \\ 0 & 0 & -1 \\ 0 & 1 & 0 \end{pmatrix}, \quad \tilde{A}_5 := \begin{pmatrix} 0 & 0 & 1 \\ 0 & 0 & 0 \\ -1 & 0 & 0 \end{pmatrix}, \quad \tilde{A}_6 := \begin{pmatrix} 0 & -1 & 0 \\ 1 & 0 & 0 \\ 0 & 0 & 0 \end{pmatrix},
$$

$$
A_j := \left(\begin{array}{c|c} 0 & 0 \\ \hline 0 & \tilde{A}_j \end{array} \right), \qquad A_i := \left(\begin{array}{c|c} 0 & 0 \\ \hline e_i & 0 \end{array} \right),
$$

für $i = 1, 2, 3$ und $j = 4, 5, 6$, so wird der Tangentialraum $T_g M$ in $g \in M$ durch die linksinvarianten Vektorfelder $g A_k$, $k = 1, \ldots, 6$, aufgespannt. Die Anfangsbedingung lautet dann $g(0) = I_4$ und die Differentialgleichung

$$
\dot{g} = \left(\begin{array}{c|c} 0 & 0 \\ \hline a_1 & R S(u) \end{array} \right) = g \left(A_1 + \sum_{i=1}^{3} u_i A_{3+i} \right).
$$

Differentialgeometrische Beschreibung

Im Weiteren werden nun zwei Wege verfolgt. Zunächst wird die Mannigfaltig M durch folgende Identifikationen als Untermannigfaltigkeit des $\mathbb{R}^{12}$ aufgefaßt:

$$\mathbb{R}^{12} \approx \left\{ r = \left(\begin{array}{c|c} 1 & 0 \\ \hline y & B \end{array} \right), y \in \mathbb{R}^3, B \in \mathbb{R}^{3\times3} \right\},$$

$$T_g \mathbb{R}^{12} \approx \left\{ Y = \left(\begin{array}{c|c} 0 & 0 \\ \hline v & F \end{array} \right), v \in \mathbb{R}^3, F \in \mathbb{R}^{3\times3} \right\},$$

$$T_g^* \mathbb{R}^{12} \approx \left\{ \beta = \left(\begin{array}{c|c} 0 & \mu^T, \\ \hline 0 & \Lambda^T \end{array} \right), \mu \in \mathbb{R}^3, \Lambda \in \mathbb{R}^{3\times3} \right\}.$$

Zudem wird eine geeignete 1-Form eingeführt

$$\langle \beta, \alpha \rangle = \operatorname{tr}(\beta\alpha) = \mu^T v + \operatorname{tr}(\Lambda^T F)$$

und weiterhin ist

$$T_g M = \left\{ X = \left(\begin{array}{c|c} 0 & 0 \\ \hline Rv & RS \end{array} \right), v \in \mathbb{R}^3, S \in \operatorname{so}_3(\mathbb{R}) \right\}$$

$$T_g^* M = \left\{ \omega = \left(\begin{array}{c|c} 0 & \mu^T R^T \\ \hline 0 & \tilde{S}^T R^T \end{array} \right), \mu \in \mathbb{R}^3, \tilde{S} \in \operatorname{so}_3(\mathbb{R}) \right\}$$

Mittels obiger 1-Form werden auf $T^*\mathbb{R}^{12}$ die Funktionen

$$H_i := \langle \beta, g A_i \rangle, \quad i = 1, \dots, 6$$

und die Hamilton-Funktion

$$H := \left\langle \beta, g \left(A_1 + \sum_{i=1}^{3} u_i A_{3+i} \right) \right\rangle = H_1 + \sum_{i=1}^{3} u_i H_{3+i} \tag{Z.7}$$

definiert. Mit Hilfe des Maximumprinzips von Pontyagin kann gezeigt werden, daß für $\hat{h} := (H_1, H_2, H_3)^T$ und $\hat{H} := (H_4, H_5, H_6)^T$ gilt:

$$\begin{aligned}
\mu' &= 0, \\
\hat{h} &= R^T \mu, \\
\hat{h}' &= -S(u)\hat{h}, \\
\hat{H}' &= -S(u)\hat{H} + \hat{h} \times e_1, \\
0 &\equiv H_1 H_4 + H_2 H_5 + H_3 H_6, \\
\mu &\neq 0.
\end{aligned}$$

Ein anderer Ansatz ist eine geeignete Wahl der Basen des Tangential- und des Kotangentialraumes an jedem Punkt $g \in M$. Mit dem Einsatz von Mitteln der Differentialgeometrie kann durch diese Methode die unnötige Erhöhung der Dimension von 6 auf 12 vermieden werden. Die Ergebnisse stimmen selbstverständlich mit den oben gewonnenen Resultaten überein.

Folgerungen aus dem Maximumprinzip

Nun werden Konsequenzen aus den Eigenschaften gezogen, die aus dem Maximumprinzip gewonnen wurden. Im Wesentlichen wird gezeigt, daß optimale Lösungen stückweise aus Geradenstücken, Kreisbögen und Spiralenstücken bestehen, lediglich ein Fall (mit (D) bezeichnet) kann nicht vollständig beschrieben werden. Doch wie viele Umschaltungen nötig sind, kann hier nicht gesagt werden. Allerdings wird vermutet, daß der Fall (D) gar nicht optimal sein kann und höchstens zwei Umschaltungen ausreichen, da dadurch bereits Flächen (potentiell Randflächen der Erreichbarkeitsmenge) im $\mathbb{R}^3$ beschrieben werden können. Um diese Vermutung zu bekräftigen, werden die Fälle untersucht, daß a priori die Steuerungen u_2 bzw. u_1 nicht einwirken. Man gewinnt hier weitere Struktureinsichten. Für $u_2 = 0$ fällt der Fall (D) komplett weg und für $u_1 = 0$ kann er für kleine Längen L nicht auftreten. Hier werden auch weitere Umschaltungen ausgeschlossen und die Erreichbarkeitsmengen unter Annahme obiger Vermutung skizziert.

Index

abnormal, 18, 19
anholonomic, 70

cotangent space, 7
covector field, 7
curvature, 3, 4, 13–17, 31–33, 48, 58,
74, 76

double contravariant tensor, 10, 71
Dubins' problem, 4, 13, 15, 90

elastic rod, 57

free initial direction, 41
Frenet equations, 58, 59

Hamiltonian function, 10, 16, 17, 65,
66, 69, 71
Hamiltonian vector field, 10
holonomic, 70

left-invariant, 8, 65
Lie bracket, 8, 69
Lie group, 8, 65

manifold, 7, 64, 69
manipulator, 1–4, 13–14, 32, 39–43,
57–59, 89–90

necessary conditions, 6, 14, 27, 63,
65, 79
no side-slip condition, 14
normal, 18, 19, 67

object of anholonomy, 70
one-form, 7, 65, 66

phase portrait, 18, 37
Poisson bracket, 9, 65, 69

Poisson structure, 9
Pontryagin's Maximum Principle, 4,
6, 14, 16, 35, 63, 65, 66, 89

reachable, 6, 13, 15, 32, 59
rigid body, 58

submanifold, 7
sufficient conditions, 6, 20
switching function, 18
switching parameter, 18
switching point, 18
switching time, 18
symplectic form, 10, 65
symplectic manifold, 10

tangent space, 7
terminal direction, 3, 13, 31, 33, 41–
43, 52, 55
terminal point, 4, 6, 13, 14, 18–26,
39–44
torsion, 58, 74, 76, 77

vector field, 7, 65, 69

workspace, 3–4, 13–14, 33, 39–43, 59–
60, 80